

# PHYSICO-CHEMICAL APPLICATIONS OF PULSATING SENSORS

By

**R. ANANTHANARAYANAN**

**CHEM02200804012**

**Indira Gandhi Centre for Atomic Research, Kalpakkam**

**A thesis submitted to the  
Board of Studies in Chemical Sciences**

*In partial fulfillment of requirements*

*for the Degree of*

**DOCTOR OF PHILOSOPHY**

*Of*

**HOMI BHABHA NATIONAL INSTITUTE**



**August, 2014**

**Homi Bhabha National Institute**

**Recommendations of the Viva Voce Committee**

As members of the viva voce committee, we certify that we have read the dissertation prepared by R.Ananthanarayanan entitled “Physico-chemical applications of pulsating sensors” and recommend that it may be accepted as fulfilling the thesis requirement for the award of degree of Doctor of Philosophy.

---

Chairman- Dr. V.Ganesan

Date:

---

Guide/Convener- Dr.R.Baskaran

Date:

---

Technical Advisor- Dr.P.Sahoo

Date:

---

Examiner- Dr.A.K.Mishra

Date:

---

Member 1- Dr. Amarendra

Date:

---

Member 2- Dr.C. Mallika

Date:

---

Member 3- Dr. T.G.Srinivasan

Date:

---

Final approval and acceptance of this thesis is contingent upon the candidate’s submission of the final copies of the thesis to HBNI.

I/We hereby certify that I/We have read this thesis prepared under my/our direction and recommended that it may be accepted as fulfilling the thesis requirement.

Date:

Place:

## **STATEMENT BY AUTHOR**

This dissertation has been submitted in partial fulfillment of requirements for an advanced degree at Homi Bhabha National Institute (HBNI) and is deposited in the Library to be made available to borrowers under rules of the HBNI.

Brief quotations from this dissertation are allowable without special permission, provided that accurate acknowledgement of source is made. Requests for permission for extended quotation from or reproduction of this manuscript in whole or in part may be granted by the Competent Authority of HBNI when in his or her judgment the proposed use of the material is in the interests of scholarship. In all other instances, however, permission must be obtained from the author.

R. Ananthanarayanan

## **DECLARATION**

I, hereby declare that the investigation presented in the thesis has been carried out by me. The work is original and has not been submitted earlier as a whole or in part for a degree/diploma at this or any other Institution/University.

R. Ananthanarayanan

## List of publications arising from the thesis

### Journal

1. "Pulsating potentiometric titration technique for assay of dissolved oxygen in water at trace level", Sahoo, P., **Ananthanarayanan, R.**, Malathi, N., Rajiniganth, M.P., Murali, N., Swaminathan, P., *Analytica Chemical Acta*, **2010**, 669, 17-24.
2. "Digital conductometry for determination of boron in light water and heavy water at trace levels", **Ananthanarayanan, R.**, Sahoo, P., Murali, N., *Indian Journal of Chemical Technology*, **2012**, 19, 278-288
3. "High resolution conductometry for isotopic assay of deuterium in mixtures of heavy water and light water", **Ananthanarayanan, R.**, Sahoo, P., Murali, N., *Journal of radioanalytical and nuclear chemistry*, **2014**, 299, 293-301
4. "Experimental investigation on carbonation of sodium aerosol generated from sodium fire in the context of fast reactor safety", **Ananthanarayanan, R.**, Subramanian, V., Sahoo, P., Jitendra Mishra., Amit Kumar., Baskaran, R., Venkatraman, B., Murali, N., *Annals of Nuclear Energy*, **2015**, 80, 188-194

R. Ananthanarayanan

**DEDICATED TO MY BELOVED PARENTS**

## ACKNOWLEDGEMENTS

I sincerely thank **Dr.R.Baskaran**, Head, Radiological Impact Assessment Section for his constant guidance and encouragement throughout this work. I am obliged to his meticulous planning, wholehearted support and constructive suggestions. I thank **Dr.P.Sahoo**, Head Innovative Instrumentation Section (IIS), for helping me to solve the problems presented in this work. I thank him for his constant guidance, valuable advice, patience and active support. I thank **Shri B.Saha**, former Head IIS, who introduced me to pulsating sensors and encouraged me to undertake this work.

I thank **Shri S.A.V. Satya Murty**, Director Electronics Instrumentation and Radiological Safety Group (EIRSG) and **Shri N.Murali**, former associate director EIRSG, for their constant encouragement and for providing all the required facilities to carry out this work.

I take this opportunity to thank my colleagues **Smt. N.Malathi**, **Dr.V.Subramanian**, **Shri M.P.Rajiniganth**, **Shri Jitendra Mishra**, **Smt. Jeena Pradeep**, **Shri A. Suriyanarayanan** and **Shri M.Manogaran** for providing their support in various ways during the course of this work.

Finally I thank my **parents** and **sisters** for showering their unbound love, care and affection throughout my life.

## CONTENTS

	<b>Page no</b>
<b>SYNOPSIS</b>	I
<b>LIST OF FIGURES</b>	X
<b>LIST OF TABLES</b>	XIII
 <b>CHAPTER 1 INTRODUCTION</b>	
1.1. India's fast reactor program	1
1.2. Sensor program at IGCAR	1
1.3. Literature review	3
1.3.1. A brief survey of applications of pulsating sensors in nuclear facilities	3
1.3.1.1. Applications of conductivity based sensors	4
1.3.1.2. Applications of dielectric based sensors	7
1.3.1.3. Applications of inductance based sensors	9
1.3.1.4. Applications of EMF based sensors	9
1.4. Review of major analytical instruments used in quality control laboratories attached to reactors	10
1.5. Objective of the current work	13
1.6. Scope of the current work	14
 <b>CHAPTER 2 INSTRUMENTATION AND TECHNIQUES</b>	
2.1. Introduction	15
2.2. Pulsating Sensors	16
2.3. Pulsating type conductivity meters	19
2.3.1. Sensing methodology	20

2.3.2.	Calibration	21
2.3.3.	Instrumentation	23
2.3.4.	Salient Features	23
2.4.	EMF based measurements	25
2.5.	Graphical user interface for recording titrations	25
2.5.1	Salient features of GUI	29
2.6.	Reagent volume dispenser	29
2.7.	Conductometric titration facility	32
2.8.	Potentiometric titration facility	34
2.9.	Commercial instruments used in the thesis	36
2.9.1.	UV-Visible spectrophotometer	36
2.9.2.	Infrared spectrophotometer	37
2.9.3.	Ion chromatograph	39
2.9.4.	Refractometer	40

### **CHAPTER 3 DEVELOPMENT OF ANALYTICAL TECHNIQUE FOR TRACE ASSAY OF DISSOLVED OXYGEN BY REDOX TITRATION**

3.1.	Introduction	42
3.2.	Experimental	44
3.2.1.	Materials and reagents	44
3.2.1.1.	Alkaline potassium iodide (~8M sodium hydroxide/~4M potassium iodide)	44
3.2.1.2.	Manganese sulphate solution (3M MnSO <sub>4</sub> .H <sub>2</sub> O)	44
3.2.1.3.	5M Sulphuric acid	45
3.2.1.4.	Standard Sodium thiosulphate solution	45

3.2.1.5.	0.05M Iodine solution prepared in 2% (w/v) KI solution	45
3.2.1.6.	Potentiometric titration facility	45
3.2.1.7.	DO sampler	45
3.3.	Methodology	46
3.4.	Results and discussion	47
3.4.1.	Principle	47
3.4.2.	Advantages of current technique over classical Winkler's titration	48
3.4.3.	Initial studies on potentiometric based Winkler's titration technique	49
3.4.4.	Potentiometric titrations at trace levels	51
3.4.5.	Kinetic investigations	60
3.5.	Conclusion	60

#### **CHAPTER 4 DETERMINATION OF TRACE BORON IN LIGHT WATER AND HEAVY WATER**

4.1.	Introduction	61
4.2.	Experimental	64
4.2.1.	Materials and reagents	64
4.2.1.1.	Preparation of boric acid solution	64
4.2.1.2.	Preparation of mannitol solution	64
4.2.1.3.	Preparation of standard NaOH solution	65
4.2.1.4.	Reagents for interference study	65
4.2.1.5.	Heavy water	65
4.2.1.6.	Conductometric titration facility	65
4.3.	Methodology	65
4.4.	Result and discussion	67

4.4.1.	Principle	67
4.4.1.1.	Conductometric titration technique	67
4.4.1.2.	Direct conductivity approach	68
4.4.2.	Conductometric titration approach for the assay of boron	69
4.4.2.1.	Titration plots in light water matrix	69
4.4.2.2.	Titration plots in heavy water matrix	70
4.4.2.3.	Performance evaluation of titration approach	71
4.4.2.4.	Effect of non reacting impurities on titration plots	73
4.4.2.5.	Effect of reacting impurities on titration plots	74
4.4.3.	Direct conductivity approach for the assay of boron	76
4.4.3.1.	Performance evaluation of direct conductivity approach	79
4.5.	Analysis of MAPS moderator samples	79
4.6.	Conclusion	81

## **CHAPTER 5 DETERMINATION OF ISOTOPIC PURITY OF HEAVY WATER IN MIXTURES OF LIGHT WATER AND HEAVY WATER BY CONDUCTIVITY APPROACH**

5.1.	Introduction	83
5.2.	Experimental	85
5.2.1.	Materials and reagents	85
5.2.1.1.	Boron stock solution	85
5.2.1.2.	Heavy water	85
5.2.1.3.	20% w/v mannitol solution	86
5.2.1.4.	Constant temperature bath	86
5.2.1.5.	Pulsating conductivity meters	86

5.3.	Graphical user interface	87
5.4.	Methodology	88
5.5.	Results and discussion	89
5.5.1.	Principle	89
5.5.2.	Choice of reaction	90
5.5.3.	Scoping study on the feasibility of conductivity approach	90
5.5.4.	Effect of temperature on conductivity measurement	92
5.5.5.	Miniaturization of conductivity probe	93
5.5.6.	Further miniaturization of conductivity probe	96
5.5.7.	Validation of technique	100
5.6.	Conclusion	101

## **CHAPTER 6 PARAMETRIC STUDY ON THE RATE OF CARBONATION OF SODIUM AEROSOLS**

6.1.	Introduction	102
6.2.	Experimental	105
6.2.1.	Aerosol Test Facility	105
6.2.2.	Dual filter paper sampling system	106
6.2.3.	Humidity adjustment system	107
6.2.4.	Nitrogen flow setup	108
6.2.5.	Conductometric titration facility	108
6.3.	Methodology	109
6.3.1.	Combustion of sodium and sampling of sodium aerosol	109
6.3.2.	Analysis of aerosol sample	110
6.4.	Results and discussion	110

6.4.1.	Calculation of various aerosol species from conductometric titration plot	110
6.4.2.	Influence of RH% and CO <sub>2</sub> content in the carbonation of sodium aerosols	113
6.5.	Conclusion	118
<b>CHAPTER 7 CONCLUSION</b>		119
<b>REFERENCES</b>		124

## **SYNOPSIS**

### **1. Introduction**

A new class of sensors called pulsating sensors has been developed at Innovative Instrumentation Section (IIS) of Indira Gandhi Centre for Atomic Research (IGCAR), Kalpakkam, India. Such sensors got evolved due to the continuous look out for simpler, more flexible and more dependable devices with improved performance. Conventional instrumentation with commonly available sensors involve handling of analog signals in the crucial stages right from extraction of primary electronic responses as small voltage or current signals, their pre-amplification, signal conditioning to further amplification. Usually digital systems take over only after these stages with addition of analog-to-digital conversion devices. In comparison, pulsating sensors produce their first electronic response directly in digital domain and thus greatly simplify the associated instrumentation. Pulsating sensors are simple yet powerful devices that require reduced electric, electronic and mechanical hardware. They are not dependent on any special mechanical or electronic hardware and they are quick to assemble and implement in an imaginative and highly flexible manner.

### **2. Objective of the current research**

From the exhaustive literature survey on the application of pulsating sensors it was found that these sensors offer a large scope for developing analytical techniques at trace level. The objective of the current research work was to develop inexpensive and reliable analytical techniques using pulsating sensors that addresses the problems encountered in nuclear facilities. Generally sophisticated instruments with trained operators are required to carry out analysis at trace level. Such instruments are not only costly but also take a long time to get it serviced once

the instrument develops some problem. This is due to the fact that most of the instruments are procured from abroad and there is an associated delay in rectifying the problems. Therefore it is always desirable to have reliable in-house developed instruments in plant monitoring, surveillance and quality control laboratories as the instruments can be repaired and put back to service in minimum time. Moreover it avoids long waiting periods that are generally associated with procuring such costly instruments. Towards this objective some physico-chemical techniques have been developed with the deployment of pulsating sensor based instrumentation. These have been presented in separate chapters of the thesis and each of these techniques find excellent application in nuclear program.

### **3. Organization of the thesis**

The details of the research work carried out to meet these objectives will be submitted as a Ph.D. thesis and the organization of the thesis is outlined below

#### **Chapter 1: Introduction**

This chapter gives a detailed literature review on the various types of pulsating sensors and their applications. The chapter also details the scope and objective of the current work.

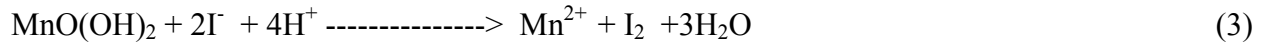
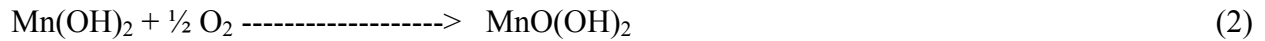
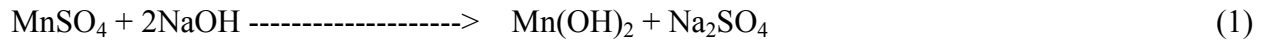
#### **Chapter 2: Instrumentation and techniques**

This chapter gives the detailed instrumentation including the in-house developed instruments used in this work.

#### **Chapter 3: Development of analytical technique for trace assay of dissolved oxygen by redox titration**

The chapter describes the development of a simple but high performing PC based potentiometric titration approach for the determination of dissolved oxygen (DO) in water samples. Though the

technique adopted involves the well known Winkler's chemistry [1], probably for the first time DO was assayed down to 8 ppb using a titration approach. Winkler's titration is basically an iodometric titration [2] with the first step involving the in-situ generation of Mn(OH)<sub>2</sub> in the water sample. The DO present in the sample reacts with Mn(OH)<sub>2</sub> to form a brown MnO(OH)<sub>2</sub> precipitate. Under acidic condition iodide reduces MnO(OH)<sub>2</sub> to Mn<sup>2+</sup> while itself getting oxidized to I<sub>2</sub>. The liberated iodine which is equivalent to DO present in the sample is titrated against sodium thiosulphate using starch as the indicator. The corresponding equations involved in the Winkler's chemistry is given below



Although the traditional Winkler's technique using starch as indicator is considered as the most suitable technique for assay of DO at ppm levels, it has certain limitations such as (i) difficulty to apply the technique below 0.5 ppm of DO (ii) uncertainty in the end point determination which depends on the analyst's skill and (iii) poor precision at lower detection limits. In order to overcome these limitations a PC based potentiometric titration facility using pulsating sensor was developed in this work which could work down to 8 ppb level of DO [3]. Such low levels of DO detection was made possible because of high resolution in potential measurement (less than 0.1mv) offered by the potentiometric titration facility.

In this work a special type of DO sampler was successfully designed to collect water samples without the ingress of any air bubble. After applying this modified Winkler's technique to many processed samples at sub ppm DO levels in a series of experiments, the technique was successfully deployed in analyzing DO in the steam generator waters of Fast Breeder Test Reactor (FBTR) and Madras Atomic Power Station (MAPS). It was found that DO can be assayed down to 8 ppb with a precision of 1.75% RSD. From kinetic studies it was observed that there is no loss of iodine if the titration is carried out within 2 hours from acidification whereas there is a 20% loss of iodine if the titration is carried out after 3 hours. Further it was found that even if the sample is preserved overnight after fixing the DO, there is no change in DO content from the fresh sample.

#### **Chapter 4: Determination of trace boron in light water and heavy water**

This chapter deals with the determination of trace boron in both light water matrix as well as heavy water matrix using a conductivity based approach. Estimation of boron is essential in the heavy water moderator of Pressurized Heavy Water Reactor's (PHWR) during reactor startup and also during reactor operation. Boron is usually monitored by curcumin [4] or carminic acid [5] spectrophotometric techniques when the concentration is in ppm range and by ion chromatography [6] when it is in ppb range. In this work two conductivity based approaches were evolved in order to estimate boron in both light water and in heavy water matrices. A PC based conductometric titration approach was followed to quantify boron at ppm and sub ppm levels and a direct conductivity based approach was followed to quantify boron at a few ppb levels [7]. In the titration approach a fixed quantity of mannitol is added to the sample before titrating it against sodium hydroxide solution. The addition of mannitol converts the weak boric acid to a relatively stronger acid through the formation of a boron mannitol complex. Although

this principle is widely followed in volumetric titration using phenolphthalein indicator and by potentiometric titration approaches, it is done either at percentage or at several ppm levels. Consequently the present study was undertaken to extend the detection of boron to sub ppm and ppb levels using conductivity based approach. From the study it was found that while the titration plot obtained in light water matrix consisted of three regions the plot obtained in heavy water matrix consisted of two regions only. The precision of the technique was found to be 2.2% at 100 ppb level and the technique was validated using curcumin spectrophotometric method. The technique was successfully applied to estimate boron in heavy water moderator samples collected from MAPS during reactor startup.

In order to lower the detection limit in both light water as well as heavy water matrix a direct conductivity approach was followed. As boric acid is an extremely weak acid the conductivity of the sample does not change appreciably with increasing concentration of boric acid in the sample. However the addition of a fixed quantity of mannitol to the sample raises the solution conductivity depending on the amount of boron present in the sample. This principle was exploited to detect boron at ppb levels using calibration curves generated separately in both light water as well as heavy water matrices. From the study it was observed that for the same concentration of boron the shift in conductivity in light water matrix is almost five times higher as compared to heavy water matrix. The precision of the method was found to be 4.1% RSD at 20 ppb level and the method was validated by the standard ion chromatographic technique. Further the method was successfully applied to determine the concentration of boron in the heavy water moderator samples of MAPS collected during reactor operation.

## **Chapter 5: Determination of isotopic purity of heavy water in mixtures of light water and heavy water by conductivity approach**

The chapter describes in detail a conductivity based approach to determine the isotopic purity of heavy water in mixtures of light water and heavy water. Generally infra red [8], refractive index [9], density measurement [10] and mass spectrometry [11] techniques are used to determine the isotopic purity of heavy water. Probably for the first time a conductivity based approach has been followed to determine the isotopic purity of heavy water. In the present work the shift in conductivity of a sample before and after the generation of a fixed concentration of boron mannitol complex is monitored. It was observed that the shift in conductivity is maximum in pure light water while it is minimum in pure heavy water. Further the conductivity of a mixture of light water and heavy water decreases as the percentage composition of heavy water in the mixture increases. This property was successfully exploited to find a correlation between shift in conductivity of the sample before and after the generation of boron mannitol complex and the percentage composition of heavy water. As heavy water is extremely costly and also as the present technique is destructive in nature, a mini conductivity cell was designed and used for the analysis using about 1mL of sample volume. Since this technique is purely dependent on shift in conductivity measurement and as conductivity is highly influenced by temperature, all measurements were carried out in a thermostat at a constant solution temperature. The technique was examined in the entire range from 0% to 100% with a precision of  $\leq 1.5\%$  RSD and an accuracy of  $\leq 1.75\%$  [12]. The current technique was validated using refractive index as well as infra red techniques.

## Chapter 6: Parametric study on the rate of carbonation of sodium aerosols

Information on chemical speciation of sodium aerosol is important in the context of fast reactor safety as well as potential environmental health impacts. In this direction the effect of % relative humidity (RH) and carbon dioxide (CO<sub>2</sub>) content on the rate of carbonation of sodium aerosol was investigated in detail [13]. The study was carried out at two different CO<sub>2</sub> levels namely 280 ppm and 390 ppm and varying the %RH from 20% to 90%. All experiments were carried out in the Aerosol Test Facility [14] by burning ~10g of sodium which produced an aerosol mass concentration of 4g/m<sup>3</sup>. The sodium was burnt in a combustion cell and the resulting sodium aerosol was released into a 1000 liter chamber maintained at the required CO<sub>2</sub> level and %RH. Aerosols were collected onto filter papers at different time intervals from the onset of sodium fire. The various aerosol species deposited on each filter paper was quantified by following in-house developed PC based conductometric titration technique. From the study it is found that the aerosol samples collected after 1 minute of sodium fire under 90% RH and 390 ppm CO<sub>2</sub> level contained a higher percentage of sodium hydroxide (~0.8 mole fraction). Further it was found that sodium hydroxide undergoes complete carbonation after 20 minutes from the start of sodium fire. The reactions governing the conversion are presented below



When the same experiment was carried out at 90% RH and 280 ppm CO<sub>2</sub>, the rate of carbonation of NaOH was slightly delayed though the initial concentration of NaOH collected after 1 minute of sodium fire remained almost same as observed in the case of 90% RH and 390 ppm CO<sub>2</sub>. The

delay in conversion is attributed to the reduced  $\text{CO}_2$  content in the chamber. A similar behavior in carbonation was exhibited when experiments were carried out at 50% RH and 280 ppm  $\text{CO}_2$ . In the experiments conducted at 20%RH and 390 ppm  $\text{CO}_2$ , it was found that the mole fraction of NaOH in samples collected after 1 minute of sodium fire was 0.55 and that it takes about one hour for complete carbonation. A similar trend in the carbonation behavior was observed at 20%RH and 280 ppm  $\text{CO}_2$ . In the case of experiments carried out at 50% RH and 390 ppm  $\text{CO}_2$  level both NaOH and  $\text{Na}_2\text{CO}_3$  were found to be equally distributed for the first 13 minutes from the start of sodium fire. About 85% of carbonation of NaOH occurred after half an hour whereas it took about one hour for complete carbonation.

## **Chapter 7 Conclusion and future work**

This chapter describes the conclusion of the thesis and scope of future work.

### **4. Conclusion**

Simple but high performing physico-analytical techniques have been developed using pulsating sensors. It is demonstrated that trace analysis can be achieved without using costly and sophisticated instruments that are generally associated with such analysis. All these activities presented in the thesis are targeted towards crucial applications in nuclear facilities. These sensors offer a lot of scope for developing many physico-chemical techniques. Besides high resolution titration facilities and their deployment to evaluate many novel analytical techniques, work is in progress towards development of a homemade ion chromatography instrument using pulsating type conductivity detector.

## References

1. Labasque, T., Chaumery, C., Aminot, A., Kergoat, G., *Mar. Chem.*, **88** (2004) 53
2. Helm, I., Jalukse, L., Vilbaste, L., Leito, I., *Anal. Chim. Acta*, **648** (2009) 167
3. Sahoo, P., Ananthanarayanan, R., Malathi, N., Rajiniganth, M.P., Murali, N., Swaminathan, P., *Anal. Chim. Acta*, **669** (2010) 17
4. Standard test method for boron in water, D 3082-09, ASTM
5. Callicoat, D.L., Wolszon, J.D., *Anal. Chem.*, **31** (1959) 1434
6. Tapparo, A., Pastore, P., Bombi, G., *Analyst*, **123** (1998) 1771
7. Ananthanarayanan, R., Sahoo, P., and Murali, N., *Indian J. Chem. Techn.*, **19** (2012) 278
8. Skjoldebrand, .R., *Appl. Sci. Res. B-Elec.*, **5** (1956) 401
9. G.P.Baxter, G.P., L.L.Bargess, L.L., H.W.Daudt, H.W., *J. Am. Chem. Soc.*, **33** (1911) 893
10. Inoue, Y., Tanaka, K., Kasida, Y., *Analyst*, **106** (1981) 609
11. WM Thurston, W.M., MWD James, M.W.D., *Anal. Chem.*, **56** (1984) 386
12. Ananthanarayanan, R., Sahoo, P., and Murali, N., *J. Radioanal. Nucl. Ch.*, **299** (2014) 293
13. Ananthanarayanan, R., Subramanian, V., Sahoo, P., Jitendra Mishra., Amit Kumar., Baskaran, R., Venkatraman, B., Murali, N., “Experimental investigation on carbonation of sodium aerosol generated from sodium fire in the context of fast reactor safety”., communicated to *Ann. Nucl. Energ.*. Manuscript number ANUCENE-D-14-00408
14. Baskaran, R., .Selvakumaran, T.S., Subramanian, V., *Indian J. Pure Appl. Phys.*, **42** (2004) 873

## LIST OF FIGURES

<b>Figure no</b>	<b>Title of the figure</b>	<b>Page no</b>
II.1a.	LGO circuit for conductance based measurements.	18
II.1b.	LGO circuit for dielectric based measurements.	18
II.1c.	LGO circuit for inductance based measurements.	18
II.1d.	LGO circuit for EMF monitoring.	19
II.2.	A typical second degree calibration plot between frequency and conductivity for a lab made conductivity sensor.	22
II.3.	Block diagram of instrumentation for PC based conductivity monitoring instrument.	23
II.4	Flowchart of the graphical user interface.	26
II.5.	Screen capture view of a PC based conductometric titration plot.	27
II.6.	Screen capture view of a PC based potentiometric titration plot.	28
II.7a.	Schematic representation of a complete conductometric titration facility using the reagent volume dispenser.	31
II.7b.	Schematic representation of the reagent volume dispenser.	31
II.8.	A typical potentiometric titration plot obtained using the reagent volume dispenser.	32
II.9.	Photograph of the rapid conductometric titration facility.	33
II.10a.	Block diagram of potentiometric titration facility.	35
II.10b.	Photograph of the rapid potentiometric titration facility.	35
III.1.	The schematic of the DO sampler used in collecting water samples.	46
III.2.	Titration of 50 mL of $2.47 \times 10^{-3}$ mM iodine in 0.5%(w/v) KI (equivalent to 39.5 ppb DO) against 0.00103M sodium thiosulphate using the automated dispenser. The DO corresponding to end point (0.242 mL) is 39.8 ppb as against 39.5 ppb. The sampling time is 0.3 seconds while each peak in the second channel represents 15 $\mu$ L.	51
III.3.	Titration of 25 mL of $6 \times 10^{-4}$ mM iodine in 0.5%( w/v) KI (equivalent to 9.6	52

ppb DO) against 0.001M sodium thiosulphate using manual addition of reagent. (Sampling time = 2 seconds, steps of titrant addition = 2.5 $\mu$ L). The sample contains 9.6 ppb DO (end point: 0.03mL).

- III.4. Titration of 25mL of 0.116 mM iodine in 0.5% (w/v) KI (equivalent to 1.86 ppm DO) against 0.0257M sodium thiosulphate using the automated volume dispenser. Sampling time is 0.3 seconds while each peak in the second channel represents 15  $\mu$ L of titrant. DO corresponding to the end point (0.227 mL) is 1.87ppm. 53
- III.5. Online titration plot of standard iodine solution (equivalent to 16 ppb O<sub>2</sub>) against 0.001M sodium thiosulphate using 'shorting electrodes approach', 10th step of addition (corresponding to 50  $\mu$ L volume) is the end point. 54
- III.6. 100mL tap water sample collected in DO sampler, added small aliquot of 1% (w/v) Na<sub>2</sub>SO<sub>3</sub> to bring down DO to ppb level. Added MnSO<sub>4</sub>, NaOH/KI and 5M sulphuric acid as recommended in Winkler technique. 25mL of sample titrated against 0.001M sodium thiosulphate in 10  $\mu$ L steps by manual addition The sample contains 77 ppb of DO (end point: 0.24 mL). 55
- III.7. Titration of 25 mL of sample collected from steam generator feed water of MAPS against 0.001M sodium thiosulphate by manual addition of reagent. Sampling time is 2 seconds, end point 0.027 mL and the volume corresponding to each aliquot of reagent addition is 2.5 $\mu$ L. The DO present in the sample is 8.64 ppb. 57
- IV.1. Titration plot of 50mL of 0.1 ppm boron in light water against sodium hydroxide. To 50mL sample 1g of mannitol was added and titrated against 0.005N NaOH in 10 micro liter steps. Argon was flushed to avoid interference from dissolved carbon dioxide. The end point occurs at 0.08 mL which corresponds to a boron concentration of 0.086 ppm. 69
- IV.2. Titration plot of 50mL of 0.2 ppm boron in heavy water against NaOH. To 50mL sample 1g of mannitol was added and titrated against 0.005N NaOH in 20 micro liter steps. Argon was flushed to avoid interference from dissolved carbon dioxide. The end point (0.177 mL) corresponds to a boron concentration of 0.19 ppm. 71
- IV.3. Titration plot of 25mL of 1 ppm boron in light water containing trace hydrochloric acid against sodium hydroxide. To 25mL sample 0.5g of mannitol was added and titrated against 0.005N NaOH in 50 micro liter steps. Argon was flushed to avoid interference from dissolved carbon dioxide. The titration end points are 0.36 mL and 0.86 mL. The boron content in the sample is 1.08 ppm as against 1ppm. 75
- IV.4. Calibration plot between shift in frequency and concentration of boron in light 78

	water matrix.	
IV.5.	Calibration plot between shift in frequency and concentration of boron in heavy water matrix.	78
V.1.	Flow chart of the graphical user interface developed in C language.	87
V.2.	Schematic diagram of the experimental set up used for the assay of isotopic purity of heavy water.	89
V.3.	Shift in specific conductance on complexation as a function of D <sub>2</sub> O content in H <sub>2</sub> O-D <sub>2</sub> O mixture.	92
V.4.	Relationship between shift in specific conductance and volume percent heavy water.	95
V.5a.	Relationship between shift in conductivity and concentration of D <sub>2</sub> O in lower range (0-40% concentration of D <sub>2</sub> O).	97
V.5b.	Relationship between shift in conductivity and concentration of D <sub>2</sub> O in higher range (40-100% concentration of D <sub>2</sub> O).	98
VI.1.	Schematic diagram of ATF facility.	106
VI.2.	Photograph of the dual filter paper sampling system.	107
VI.3.	A typical conductometric titration plot obtained by titrating an aerosol sample in water medium against HCl solution.	111
VI.4.	Real time change in concentration of NaOH as a function of different %RH and CO <sub>2</sub> concentrations.	114

## LIST OF TABLES

<b>Table no</b>	<b>Title of table</b>	<b>Page no</b>
III.1.	Assay of dissolved oxygen in tap water samples by potentiometric titration technique.	50
III.2.	Comparison of pulsating potentiometric titration technique with classical Winkler's titration method.	50
III.3.	Comparison of pulsating potentiometric titration technique with electrochemical DO meter for assay of dissolved oxygen.	56
III.4.	Comparison of analytical results obtained using potentiometric titration technique with electrochemical DO meter.	58
III.5.	Precision in measurement of DO down to 10 ppb levels by potentiometric titration technique.	59
IV.1.	Recovery of boron by conductometric titration approach and by spectrophotometric approach.	72
IV.2.	Recovery of boron in the presence of non interfering impurities.	73
IV.3.	Shift in pulse frequency in heavy water – mannitol and light water – mannitol mixtures with step-wise addition of boric acid at ppb levels.	77
IV.4.	Assay of boron in synthetic samples by direct conductivity approach and by ion chromatography.	79
IV.5.	Assay of boron in heavy water samples collected from the moderator system of a PHWR.	81
V.1.	Shift in conductivity due to the formation of boron mannitol complex with increasing concentration of D <sub>2</sub> O in the sample.	91
V.2.	Summary of results obtained from three independent campaigns.	94
V.3.	Assay of isotopic purity of heavy water in synthetic mixtures of light water and heavy water.	96
V.4.	Summary of results obtained from four independent measurement campaigns.	99

V.5.	Precision and accuracy of the present technique in the assay of heavy water content.	100
V.6.	Comparison of the present technique against refractometry and IR spectroscopy.	100
VI.1	Summary of results obtained on the carbonation of sodium aerosols under different RH% and CO <sub>2</sub> levels.	117

---

## 1. INTRODUCTION

---

### 1.1. India's fast reactor program

Indira Gandhi Centre for Atomic Research (IGCAR) is a multi-disciplinary research centre located at Kalpakkam, Tamilnadu, India. The centre was established in 1971 for developing fast breeder technology as electricity production through fast breeder reactors forms the second stage of India's nuclear program [1]. In this direction a Fast Breeder Test Reactor (FBTR) was constructed at IGCAR, Kalpakkam. FBTR is a loop type 13.2 MWe sodium cooled research reactor that became operational in 1985 [2]. Based on the experience gained from operating the reactor a 500MWe Prototype Fast Breeder reactor (PFBR) is being built at Kalpakkam. PFBR is a sodium cooled,  $\text{PuO}_2\text{-UO}_2$  fuelled, pool type reactor [3,4] which is under advanced stage of construction. As nuclear reactor technology is complex and interdisciplinary in nature the centre has various science and engineering disciplines that are involved in reactor technology oriented research. Further, in this centre research activities have been pursued towards development of a variety of sensors for multi-disciplinary applications in nuclear program. Some of the specific sensors which are successfully developed and deployed in many miscellaneous applications are briefly brought out as follows.

### 1.2. Sensor program at IGCAR

In sodium cooled fast reactors it is important to monitor the levels of hydrogen, oxygen and carbon in liquid sodium. In such reactors the primary sodium transfers the heat removed from the reactor core to the secondary sodium at the intermediate heat exchanger. The secondary sodium in turn transports the heat to the steam generator where steam is produced to drive the

turbines [4]. Any crack in the wall separating the sodium and steam causes the ingress of steam inside the sodium loop which may lead to violent explosion. Hence prompt detection of hydrogen spike is important for taking corrective action at the earliest and therefore it necessitates the use of hydrogen sensor. Oxygen sensors are required to detect early ingress of air or moisture inside the sodium loop as oxygen in sodium results in enhanced corrosion and activity transport. Similarly sensors are required to monitor the level of carbon in sodium in order to avoid carburization or decarburization of the structural material. Carburization is the process in which the material takes up carbon while decarburization is the process in which the material loses carbon [5]. As both these processes affect the structural integrity it becomes necessary to monitor the carbon activity as well. In order to monitor these above mentioned impurities in liquid sodium IGCAR has developed electrochemical based sensors [5, 6, 7, 8]. The oxygen sensor works in the range of 1 ppm to 20 ppm while the carbon sensor works in the range of 5ppb to 5ppm. The hydrogen sensor shows a linear response in the range of 60-250 ppb and is capable of detecting a change of 10ppb of hydrogen in a background of 60 ppb [7].

Superconducting quantum interface devices (SQUID) based sensors have been developed for non destructive evaluation of structural materials. SQUID sensors are highly sensitive to minor changes in magnetic fluxes and this property is exploited for the surface evaluation of materials [9]. Non destructive methods are attractive as they do not affect the continuous usability of the material.

Temperature monitoring of hot sodium loops is a crucial requirement in a fast breeder reactor. For this purpose thermocouples are used at many selected locations. In order to expand the number of monitoring locations feasibility of fiber optics based sensors is being explored [10].

For this purpose a distributed temperature monitoring system based on Raman scattering in fiber optics is being developed and tested in simulated test facility loop.

All of the above mentioned sensors are used in specific applications and they have their own limitations. Each type of sensor is confined to a specific instrumentation device. Although a lot of development has been pursued towards characterization of sensing materials, attention should be focused towards simplification of instrumentation, development of common instrument for a variety of sensing devices and development of cost effective yet high performance instrumentation. Towards this a new class of sensors called pulsating sensors has been developed at Innovative Instrumentation Section (IIS) of IGCAR. Unlike conventional sensors available in the market these sensors produce their first electronic response directly in digital domain [11, 12] and thereby achieving a significant amount of simplification in the instrumentation. Moreover these sensors offer flexibility in probe design, miniaturization of instrument, long distance communication, low power consumption (mostly 5V), ease of servicing and maintenance as all the components are available in the local market (India) etc. An elaborate discussion on these pulsating sensors is presented in chapter 2.

### **1.3. Literature review**

#### **1.3.1. A brief survey of applications of pulsating sensors in nuclear facilities**

Pulsating sensors are broadly classified into four different categories depending on the primary electrical parameter being sensed. They are (i) conductivity based, (ii) dielectric based, (iii) inductance based, and (iv) EMF based [13].

These four different classes of sensors individually or in combination offer an extensive scope for monitoring diverse parameters. Any parameter that causes either of the above property to

change, directly or indirectly, becomes measurable. The output from all the sensors is a train of rectangular pulses of 5V amplitude. Counting the pulses for fixed duration gives the pulse frequency and the pulse frequency carries information on the parameter being sensed. Finally through appropriate calibration the relationship between frequency and the sensed parameter is established. In the following sections applications from each class of sensor is described briefly.

#### **1.3.1.1. Applications of conductivity based sensors**

Pulsating type conductivity meters have been deployed in many applications. In the case of conductivity measurement a suitable conductivity probe with of a pair of sensing electrodes forms the resistance component of an RC logic gate oscillator circuit [13]. The resistance component is made variable while the capacitance component remains fixed and hence the frequency output from such a circuit depends on the prevailing conductivity of the sensing medium. A brief overview of the applications of these unconventional conductivity meters are discussed below.

A pulsating type high resolution online conductivity monitoring unit is currently being used round the clock in FBTR [14]. The device monitors the conductivity of steam generator water entering the condensate polishing unit (CPU). The steam after rotating the turbine is cooled by raw water in the condenser. A crack in the pipe line carrying the raw water will contaminate the steam generator water and thus increasing its conductivity. In order to detect the leak at the earliest and also to protect the CPU from raw water contamination, the conductivity of steam generator water is monitored continuously. Apart from FBTR such an instrument is being used at separation technology section of IGCAR for monitoring the conductivity of high purity water emerging from the mixed ion exchange resin bed. Besides online conductivity meters offline bench top conductivity meters are also being used in the quality control laboratories of FBTR

[14,15], Reprocessing group in IGCAR [16] and Kakrapar Atomic Power Station [17] for general purpose applications. Some of the novel features of such conductivity monitoring instruments are (i) high precision in measurement, (ii) high resolution, (iii) fast response (iv) ease of signal transmission to long distances and (v) low cost of maintenance.

A conductivity based technique was successfully developed for the determination of carbon in uranium carbide pellets as well as in solutions of uranyl nitrate [18]. FBTR uses 70% PuC and 30% UC as its fuel and extraction of Pu and U from the irradiated fuel is achieved through solvent extraction based reprocessing technique. In this technique the fuel is dissolved in nitric acid and then extracted into 30% TBP in n-dodecane for the separation of U and Pu. During dissolution a part of carbon from the fuel gets converted to a host of soluble organic compounds in the solution. These carbon compounds have to be completely destroyed before proceeding with the solvent extraction step as the presence of these compounds leads to a loss of plutonium due to the formation of complexes with the organic ligands. Generally chemical and electrochemical techniques are utilized to destroy the organic species. In order to test the efficacy of these chemical and electrochemical methods an analytical technique based on conductivity approach was developed. The technique is currently being followed in fuel reprocessing facility for the routine assay of carbon in nuclear dissolver solutions. The method involves the conversion of organic species to carbon dioxide and its subsequent absorption in barium hydroxide solution. The shift in conductivity of the barium hydroxide solution is monitored online and from the resulting shift in conductivity the amount of carbon in the sample is quantified.

One of the important applications of pulsating type conductivity monitoring unit was towards the chemical characterization of sodium aerosols resulting from controlled sodium fire experiments

[19]. Such studies are important in the context of safety analysis of fast reactors. Fast reactors such as FBTR and PFBR use liquid sodium as coolant and a leak in the secondary heat transfer loop inside the steam generator building results in a sodium fire. The resulting sodium fire generates a lot of sodium aerosols in the form of sodium hydroxide, sodium carbonate and sodium bicarbonate depending on the prevailing ambient conditions. From safety point of view it is important to know the time period over which the sodium hydroxide aerosol gets completely converted to sodium bicarbonate aerosol. In order to characterize and quantify the various sodium aerosols species present at different time intervals from the start of sodium fire, a PC based high resolution conductometric titration approach was developed and standardized [19].

A pulsating type conductance based sensor was used in the investigation of free level fluctuations occurring in a simulated model of PFBR [11]. Argon will act as cover gas above the hot liquid sodium pool of PFBR and free level fluctuations of sodium results in the entrapment of argon inside the sodium pool. Argon entrapment causes a change in reactivity and also reduces the heat removal capability of the coolant in the core. Apart from argon entrapment, free level oscillations results in thermal fluctuation of the components at the sodium – cover gas interface which are at two different temperatures, i.e., 530 °C and 325 °C respectively. Such sudden temperature variations can cause high thermal fatigue to the reactor components at the sodium argon interface and hence there arises a necessity to minimize the free level fluctuations. Simulation studies towards the reduction of free level fluctuations were carried out in a ¼ model of PFBR in the thermal hydraulics section of IGCAR. In this facility water was used as the coolant in place of liquid sodium which is the actual coolant that will be employed in PFBR. The fluctuations occurring inside the pool were captured using a conductance based level probe and a lab made graphical user interface (GUI). The GUI was used to record data and to display all the

statistical parameters relevant to water oscillation after recording the data. Data was sampled at 20 milli seconds time duration in order to effectively capture the rapid fluctuations occurring inside the pool. Such small sampling times could be achieved due to the fast response of the conductance based level probe.

Apart from the above mentioned applications conductivity sensor has been used in the following areas, (i) acid leak detection system in nitric acid loop at reprocessing group of IGCAR [20], (ii) development of an intelligent titrator for chemical assay of process solutions [21], (iii) characterization of aqueous flowing systems through conductivity monitoring [22] and (iv) development of a pumpless flow injection analyzer using conductivity detector [23].

#### **1.3.1.2. Applications of dielectric based sensors**

In dielectric based measurements the probe forms the capacitive part of an RC logic gate oscillator circuit. The resistive component of the circuit is fixed whereas the capacitive component is made variable and hence the frequency output from such a probe varies as a function of capacitance of the sensing medium. The most important applications of capacitance based sensors are towards differential pressure monitoring and oil height monitoring.

An indigenously made differential pressure (DP) monitoring system which works on the dielectric based principle finds a direct application in PFBR [24]. DP units working in the range of 0-25 mbar and 0-60 mbar will be deployed to monitor the DP existing between main vessel and safety vessel and between safety vessel and reactor vault of PFBR. The main vessel houses the reactor core and the primary coolant and the surface above the primary coolant is surrounded by argon. A vessel similar in shape of main vessel, called the safety vessel, surrounds the main vessel and is filled with nitrogen. The distance of separation between the main vessel and the

safety vessel is 30 cm. The load from main vessel and safety vessel is transferred to the surrounding cylindrical concrete structure known as the reactor vault. The DP between argon in the main vessel and nitrogen in the safety vessel is maintained above 20 mbars while the DP between safety vessel and reactor vault is maintained at 25mbars. The DP existing between the different components of the reactor (main vessel and safety vessel and safety vessel and reactor vault) should not fall below the specified levels and hence reliable and precise DP monitoring is required. Towards this pulsating type dielectric based sensors will be deployed in PFBR. The devices are made of stainless steel and can operate in temperatures up to 60 °C. They show excellent precision in measurement and have a resolution of 0.1 mbar. Further these devices have passed the prerequisite electromagnetic interference, electromagnetic compatibility, seismic and environmental tests and are ready for deployment in the reactor.

Another crucial application of dielectric based sensors is towards the continuous monitoring of oil level in the dashpots of control and safety rod drive mechanism (CSRDM) of PFBR [25]. CSRDM is used for shutting down the reactor safely by scram action. During scram action the control and safety rod falls under the influence of gravity and at the end of free fall the mobile assembly of CSRDM is decelerated by an oil dashpot [26]. The subsequent rise in oil height resulting from the deceleration of mobile assembly is captured by the oil level sensors mounted on the oil dashpot. Thus the rise in oil height as sensed by the level probes provides an indication regarding the scram action. The oil level sensors are designed to work in the range of 0-60 mm and have a resolution of 0.1mm. Like the differential pressure monitoring devices these oil level sensors too have passed the necessary qualification tests and are ready for deployment in the reactor.

### **1.3.1.3. Applications of inductance based sensors**

In this class of sensors a suitable coil acts as the sensing element in a RCL type logic gate oscillator circuit. The resistive and capacitive components are fixed whereas the inductive component is made variable. Inductance based sensors are mainly used for position sensing. One such example involves the measurement of water film thickness profiles over the weir crest at structural mechanics laboratory, IGCAR. The detailed description of the laboratory made experimental arrangement can be found elsewhere [27]. Similarly using the concept of position sensing a novel reagent dispenser for automated titration has been reported [28].

### **1.3.1.4 Applications of EMF based sensors**

Unlike oscillator based signal generation technique discussed above, EMF measurement follows a different principle. EMF measurements involve the direct conversion of potential of the medium as sensed by an appropriate electrode to digital pulse frequency using a voltage to frequency converter. Such novel sensing methodology allows carrying out potentiometric titrations in much simpler way. Some of the applications of EMF based sensors are discussed briefly below.

EMF based sensors find extensive use in nuclear reprocessing applications. Hydrazine and uranium have been successfully estimated during PUREX (Plutonium Uranium recovery by extraction) process using an in-house developed PC based miniaturized potentiometric titration facility. PUREX is a solvent extraction based reprocessing technique applied for the separation of plutonium and uranium (and finally plutonium from uranium) from other fission products using tri butyl phosphate as solvent [29]. As uranium and plutonium are of strategic importance their estimation and bookkeeping helps in effective management of these precious resources. Similarly estimation of hydrazine during PUREX process is important as it helps in keeping U

and Pu in their respective stable oxidizing states (IV and III respectively) [30]. It acts as a scavenger of nitrite ion which is responsible for the conversion of U(IV) and Pu (III) to U(VI) and Pu(IV) respectively [31]. Hence controlled addition of hydrazine to fuel dissolver solution and its estimation becomes important.

Compared to analysis involving non radioactive samples analysis of radioactive samples pose many restrictions such as (i) the total waste generated after each analysis should be minimum, (ii) the instrument should be simple and robust (iii) the instrument should fit inside a glove box and (iv) the instrument should be easily handled inside the glove box. The PC based miniaturized potentiometric titration facility meets the above requirements. A glass vial of 3mL capacity with a pair of tungsten platinum bimetallic electrodes embedded inside the vial acts as the titration vessel. Each titration requires a sample volume ranging from 50-200  $\mu$ L while the total volume of solution taken for titration after adding all the reagents is about 2.5 mL [32, 33]. This in turn restricts the waste generated after each titration to well within 3mL. Further the unit is robust and can be easily operated inside a glove box. Using this facility uranium was determined by the Davis Gray method [34] while hydrazine was determined by titrating against potassium iodate solution [32].

#### **1.4. Review of major analytical instruments used in quality control laboratories attached to reactors**

After an exhaustive literature survey on the pulsating sensors it was found that there is a major scope of applying these sensors for the development of analytical techniques which are suitable for quality control of water and heavy water samples used in reactor. Hence a further literature survey was carried out on the analytical techniques and the instruments used in the quality control laboratories attached to Fast Breeder Reactors (FBR) and Pressurized Heavy Water

Reactors (PHWRs). The choice of analytical instruments used in such labs was found to be based on the following criteria (i) quantity of analyte to be detected, (ii) reliability of data, (iii) speed of analysis, (iv) ease of analysis (v) and sample volume to be handled. Many of the instruments available in these laboratories are used to determine the water (including heavy water) quality round the clock. Maintaining proper water chemistry is very important from the view point of preventing corrosion. The consequences of corrosion are manifold [35]; (i) it results in the loss of construction material, (ii) transport of radioactive materials in the heat transfer system, (iii) loss of heat transfer efficiency in heat exchangers, (iv) loss of productivity due to plant shutdown and (v) loss of money. Considering these above factors the quality of water used in the various units of the reactor is maintained such that it avoids corrosion and bio-fouling. For instance the steam generator feed water of FBTR should have the following specifications; pH between 8.8-9.2, dissolved oxygen < 10 ppb, hydrazine 20-30 ppb, Iron < 10 ppb, silica < 20ppb, copper < 2ppb, chloride < 20ppb, conductivity < 0.5  $\mu\text{Scm}^{-1}$ . Similarly the specification of water varies depending on its use in the reactor. Although corrosion cannot be completely avoided it can be minimized by choosing appropriate material of construction and maintaining proper water chemistry. In order to periodically evaluate the water quality suitable analytical instruments and techniques are being used in the quality control laboratories attached to FBRs and PHWRs. A brief review of analytical techniques and instruments used in these laboratories is given below.

Some of the most important instruments that are routinely used in the quality control labs are Ion Chromatograph (IC), Gas Chromatograph (GC), UV-VIS spectrophotometer, Atomic Absorption Spectrometer (AAS), gamma spectrometer, refractometer, infrared spectrometer etc. IC is routinely used to detect analytes at ppb levels. The instrument is used in the detection of cations and anions in the feed water of steam generator unit. It is also used for the detection of boron in

the heavy water moderators of PHWR when the reactor is under operation. During reactor operation the concentration of boron in the moderator is maintained at a few ppb levels (20-30 ppb) and IC is used to detect such low levels of boron using a few micro liters of sample. UV-Visible spectrophotometer is a versatile instrument that is used to detect a variety of analytes at both ppm and ppb levels. It is used in the analysis of iron [36], silica [37] and hydrazine [38] in the steam generator feed waters. It is also used for the analysis of boron [39,40] in the moderators of PHWR during reactor startup when the boron concentration is maintained at around 4-5 ppm. Compared to IC UV-Visible spectrophotometer is not only cheaper but can also be used in the detection of many analytes at ppb levels. However the instrument has the following limitations; (i) unlike IC it can't detect multiple ions in a single run and thus save analysis time and (ii) the sample volume required for each analysis is quite larger as compared to that of IC.

GC is used extensively for the analysis of various gases. In PHWR nitrogen is used as the cover gas in primary heat transport (PHT) system whereas helium is used as the cover gas over the moderator. GC is used to analyze  $D_2$ ,  $O_2$  and  $N_2$  in the moderator cover gas while it is used to analyze  $D_2$  and  $O_2$  in PHT cover gas. In FBTR 100% argon acts as cover gas when the reactor is in shutdown condition while a mixture of helium and argon (80% and 20% respectively) acts as cover gas during reactor operation. Here too GC is used to analyze the composition of cover gas both during reactor operation and also during reactor shutdown. AAS is a spectroanalytical technique which is suitable for certain analytes which show high sensitivity towards this method. In PHWR the steam generator feed water takes the heat from the heavy water coolant and goes to rotate the turbine. In this process the quality of water (now called the boiler water) deteriorates slightly as compared to the feed water and AAS is used to detect iron [36], copper [41] and

nickel [42] in the boiler water. Another important parameter that is constantly monitored in a PHWR is the isotopic purity of heavy water. In a PHWR heavy water is used as both moderator and coolant and their isotopic purity should not fall below the specified levels. Besides many recommended techniques for the determination of isotopic purity of heavy water, IR [43,44,45,46] and refractometer [47,48,49] techniques are widely used in many quality control laboratories. IR is generally used for analysis of heavy water in the entire range but it is mostly used in nuclear facilities when the isotopic purity of heavy water is above 88% (w/w) or when it is below 9% (w/w) because of better precision and accuracy in measurement. Refractometer is used in the entire range to get the concentration of heavy water rapidly with reasonable precision. It provides a firsthand information to the analyst regarding the further technique to be adopted for the assay of heavy water with reasonable accuracy and reliability. Apart from the instruments described above for the analysis of samples in the laboratory, there are a number of instruments for online analysis such as dissolved oxygen meters, pH meters, conductivity meters etc.

### **1.5. Objective of the current work**

The objective of the current work was to develop inexpensive and reliable analytical techniques using pulsating sensors for the application in nuclear industries. Normally sophisticated and expensive instruments are used to carry out trace analysis and such instruments are beyond the reach of most laboratories and educational institutions. Moreover a trained person is required to operate the instrument smoothly. In order to minimize the dependence on such instruments there is a need to develop low cost but powerful analytical techniques. In this direction pulsating sensors show immense potential and in the current research work these sensors are used in developing analytical techniques that have direct application in nuclear facilities besides general applications in many quality control laboratories.

## **1.6. Scope of the current work**

After a critical analysis of analytical techniques used in the quality control laboratories attached to nuclear reactors and also the various applications of pulsating sensors in the nuclear industry and its associated facilities, it was found that there is a lot of potential in developing newer and simpler trace analytical techniques using these pulsating sensors. The analytical techniques developed and validated in this work are based on either conductivity or potentiometry principle. The second chapter deals with the various kinds of pulsating instruments and also the commercial instruments used in this present research work. Commercial instruments were used to validate the techniques developed using pulsating sensors. The third chapter deals with the potentiometric determination of dissolved oxygen at trace level. Using this approach dissolved oxygen down to 8 ppb was analyzed. The fourth chapter deals with determination of boron in light water as well as in heavy water using conductivity based approach. The fifth chapter deals with the determination of isotopic purity of heavy water using a conductivity based approach. Chapter six deals with the investigation of humidity and carbon dioxide content on the rate of carbonation of sodium aerosols resulting from controlled sodium fire. Finally the seventh chapter describes the conclusion of the thesis and scope of future work.

---

## 2. INSTRUMENTATION AND TECHNIQUES

---

### 2.1. Introduction

This chapter covers the detailed instrumentation including the in-house developed instruments used in this work. The chapter elaborately describes about a new type of sensor called pulsating sensors, their classification, working principle and their unique features. Generally sophisticated and costly instruments are used for the trace assay of analytical species at sub  $\text{mgL}^{-1}$  and  $\mu\text{gL}^{-1}$  levels. These instruments are not only expensive but also require a trained operator to run the instrument smoothly. Seldom such instruments are within the reach of a large number of laboratories and therefore evolving analytical techniques with simple and cost effective instruments becomes attractive. In view of this analytical techniques were developed using in-house built sensors for trace assay of various species of interest to nuclear industry. The analytical techniques developed and validated in this work are based on either conductivity or potentiometry principle. The conductometric and potentiometric units used in this work have been designed and developed in-house and their instrumentation is entirely different from that of commercially available conductivity and potentiometric units. This chapter brings out the detailed working principles and instrumentation of both conductometric and potentiometric units based on pulsating instrumentation.

Besides conductivity and EMF measurements, PC based rapid conductometric and potentiometric titration facilities for carrying out trace analysis has been developed in our laboratory. The details of both the titration setups are presented in sections 2.7 and 2.8 of this chapter. A graphical user interface (GUI) in C language was developed to follow titrations

through a PC. A brief description of the GUI, the flowchart, salient features, and some typical titration plots obtained using the GUI are given in section 2.5. Apart from in-house built instruments many commercial instruments were also used to validate the various analytical techniques developed using pulsating sensors. Section 2.9 brings out the list of commercial instruments used in this work along with their working principle.

## **2.2. Pulsating Sensors**

Pulsating sensors are designed to generate the first electronic response directly in digital domain and thus avoiding the intermediate signal processing step which is normally used in conventional devices. Pulsating sensors are constructed to respond very sensitively to shifts in one of the four properties namely, (i) resistivity (or conductivity), (ii) dielectric permeability, (iii) inductance and (iv) EMF of the physical or physico-chemical system being probed. These four different classes of sensors individually or in combination offer an extensive scope for monitoring diverse parameters. Any parameter that causes either of the above property to change, directly or indirectly, becomes measureable. The basic sensing element in the first three class of sensors are a pair of electrodes or set of electrodes or a coil as the probe in a desired medium and is placed directly in the timing circuit of a R-C or R-C-L type appropriately designed miniature logic gate oscillator circuit (LGO) whose output is a train of rectangular pulses of 5V amplitude at a frequency determined by the prevailing time constant. The output from such a sensor thus alternates between logic states 0 and 1. Any parameter, which has direct or indirect effect on the conductive (R), capacitive (C) or inductive property (L) of the static or dynamic physical or physico-chemical system, is measureable as it manifests through its influence on the time constant by either R or C or L, and hence, on the digital pulse frequency. In the case of EMF based measurements the EMF of the medium as sensed by the electrode is directly converted to

frequency using a lab made Voltage to frequency (V to f) converter. Since the signal output from all the four classes of sensors is in the form of digital pulse frequency these sensors are named as pulsating sensors. Schematic diagrams as shown in Figures II.1a, II.1b, II.1c and II.1d demonstrates the working principle of each class of sensors.

Measurements with pulsating sensors involve counting of pulses for fixed duration for the determination of frequency by an appropriate device (standalone embedded system or through a PC). Pulse frequency carries information with respect to the parameter being made to sense and the relationship between frequency and the parameter of interest is determined by appropriate calibration. The calibration co-efficients are then loaded in a PC or in an embedded system to convert the frequency to the parameter of interest. These sensors consume very low power and require only 5 V DC in most of the cases and 12 V DC in a few cases. Even they can be operated by battery. Hence they are handy and are suitable for field measurements.

In comparison conventional instrumentation with commonly available sensors involve handling of analog signals in the crucial stages right from extraction of primary electronic responses as small voltage or current signals, their pre amplification, signal conditioning to further amplification. Usually digital systems take over only after these stages with addition of analog-to-digital conversion devices.

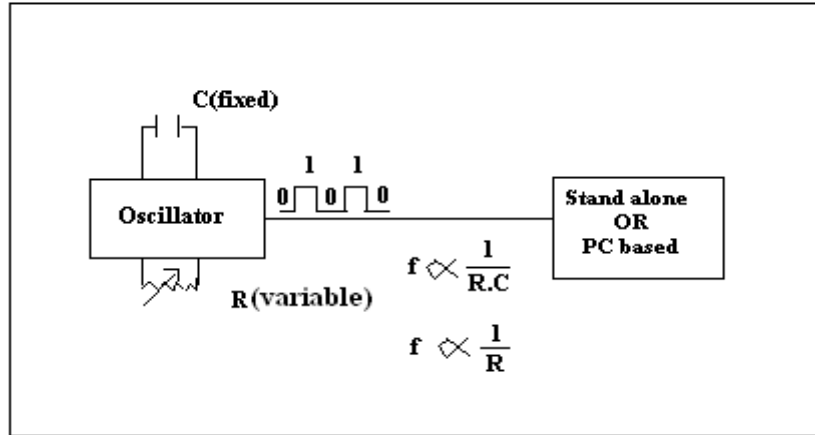


**Fig.II.1a.** LGO circuit for conductance based measurements.

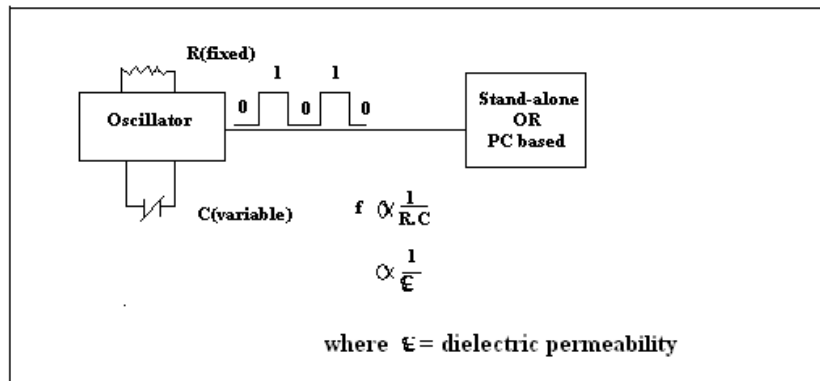


**Fig.II.1b.** LGO circuit for dielectric based measurements.

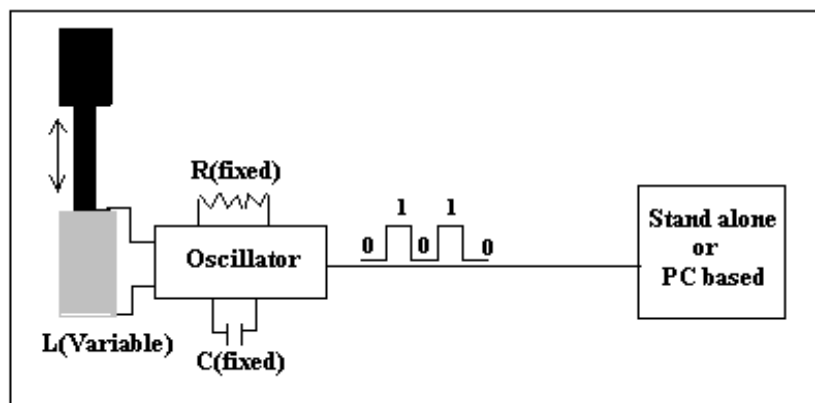


**Fig.II.1c.** LGO circuit for inductance based measurements.

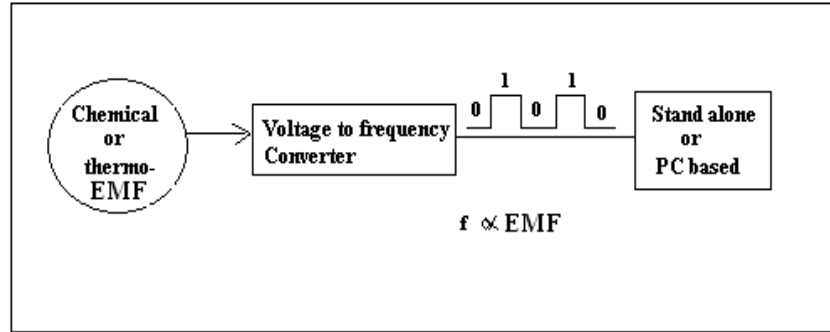


**Fig.II.1d.** LGO circuit for EMF monitoring.

### 2.3. Pulsating type conductivity meters

Conventional conductivity monitoring instruments available in the market work on the principle of alternating current bridge circuit. The use of alternating current avoids problems associated with polarization and electrolysis. Recently four electrode systems [50] have been introduced to measure highly conducting solutions. The use of four electrode system avoids polarization and fouling of electrodes. A low cost high performance conductivity meter composed of a triangular wave generator, a current-to voltage converter, and a precision half-wave rectifier implemented with only one integrated circuit (TL084) has been reported [51]. This instrument was designed for measuring solution conductivities ranging from  $<0.1 \mu\text{Scm}^{-1}$  to  $20 \text{ mS cm}^{-1}$ . In another approach an electronic conditioning circuit which converts electrical conductivity of solution to voltage has been reported in order to get reliable readings without the effect of polarization [52]. However in our laboratory an entirely novel sensing and measurement system has been developed for rapid monitoring of shifts in conductance with high precision and sensitivity [13]. These devices operate entirely in digital domain with time dependent monitoring facilities in single channel or in multichannel modes. The advantage of such unconventional systems is that

it not only simplifies the instrumentation but also makes the system less expensive and readily compatible for PC based measurements.

### 2.3.1. Sensing methodology

Figure II.1a shows the schematic representation of a typical RC LGO circuit used for the measurement of solution conductance. A conductivity probe with a pair of platinum electrodes forms the variable R component while a fixed capacitor forms the C component. When powered by a 5V DC the LGO circuit oscillates between the logic gates 0 and 1. Thus the signal generated by the LGO circuit is a train of rectangular pulses of 5V amplitude. Pulse frequency is determined by counting the pulses for fixed duration either using a standalone embedded system or using a PC loaded with a customized GUI. However during the course of this work all the conductivity measurements (refer chapters 4, 5 and 6) were carried out using a PC. The relationship between frequency and conductance is given by the following equation

$$f \propto 1/RC \quad (1)$$

where f= frequency, R= resistance and C=capacitance.

As  $1/R$  is conductance (K) and also as conductance is related to conductivity (k) by the following equation

$$K = k/x \quad (2)$$

where x is the cell constant of the conductivity probe

Equation 1 becomes

$$f \propto k \quad (3)$$

It has been observed that a linear relationship exists between the two variables in a narrow range of calibration while a higher degree polynomial fit becomes more appropriate when covering a wider range. Hence in order to avoid error in measurement a multipoint calibration technique has been adopted.

### **2.3.2. Calibration**

The technique adopted to calibrate a pulsating type conductivity probe is entirely different from the technique adopted to calibrate a commercially available probe. Commercially available conductivity probes make use of a single point calibration approach for the determination of cell constant. Depending upon the range the resistance of a suitable KCl standard is measured. The corresponding conductivity value of the KCl solution is obtained from the literature. Using the resistance (R) and conductivity (k) data the cell constant (l/a) is determined using the following formula [53] given below

$$k = (1/R) * (l/a) \quad (4)$$

With the knowledge of cell constant the unknown conductivity of a solution is determined by measuring the solution resistance and multiplying its value with the predetermined cell constant.

However in the case of pulsating type conductivity meters a multipoint calibration technique is adopted. Here a series of standard KCl solutions are generated in situ such that the resulting solution conductivities cover the entire application range. After generating each KCl standard the corresponding stable frequency value is noted. In order to evaluate the conductivity of KCl standards the following technique is adopted. Using the equivalent conductance and concentration data available in the literature [54] a polynomial relationship between equivalent conductance and square root of concentration is established. With the help of this relationship the

equivalent conductance of KCl standards are determined. Finally by knowing the equivalent conductance and concentration the solution conductivity of each KCl standard is found out by the formula as given below.

$$\Lambda_{\text{KCl}} = k / C \quad (5)$$

where  $\Lambda$  is the equivalent conductance and  $C$  is the concentration

From the frequency and conductivity data as generated by the above described procedure a suitable polynomial relationship is established. The resulting polynomial coefficients are then loaded to a GUI in order to convert the measured frequency to conductivity. Figure II.2 shows a typical calibration plot between frequency and conductivity along with the second degree polynomial relationship.

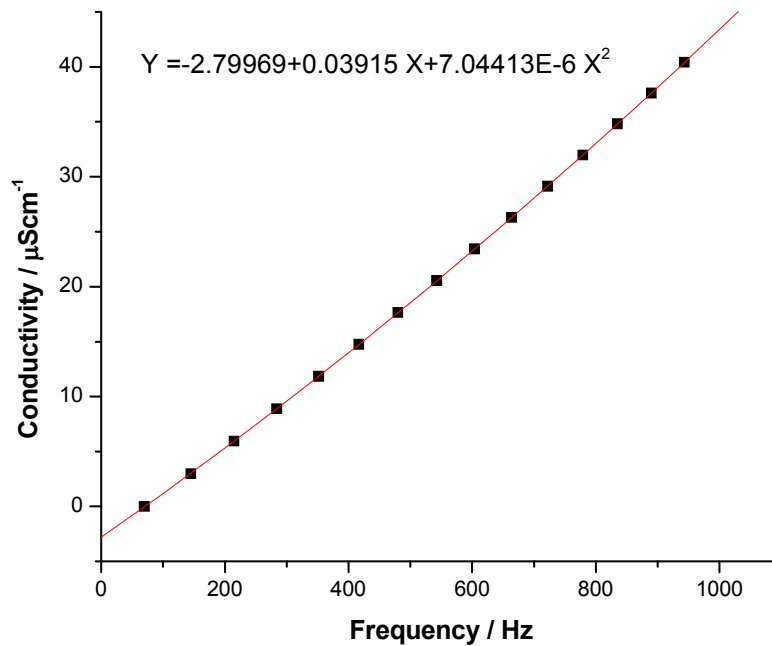


**Fig.II.2** A typical second degree calibration plot between frequency and conductivity for a lab made conductivity sensor.

### 2.3.3. Instrumentation

An appropriate conductivity probe depending on the application is connected to a signal routing cum power supply unit which in turn is connected to the PC via its parallel port. The train of digital pulses generated from the sensor head is sent to the PC through the signal routing unit. A custom made GUI (refer section 2.5) loaded in the PC determines the frequency and converts it to the corresponding conductivity value using the preloaded polynomial coefficients established through the calibration procedure described in section 2.3.2. Figure II.3 shows the block diagram of instrumentation for PC based conductivity monitoring instruments.

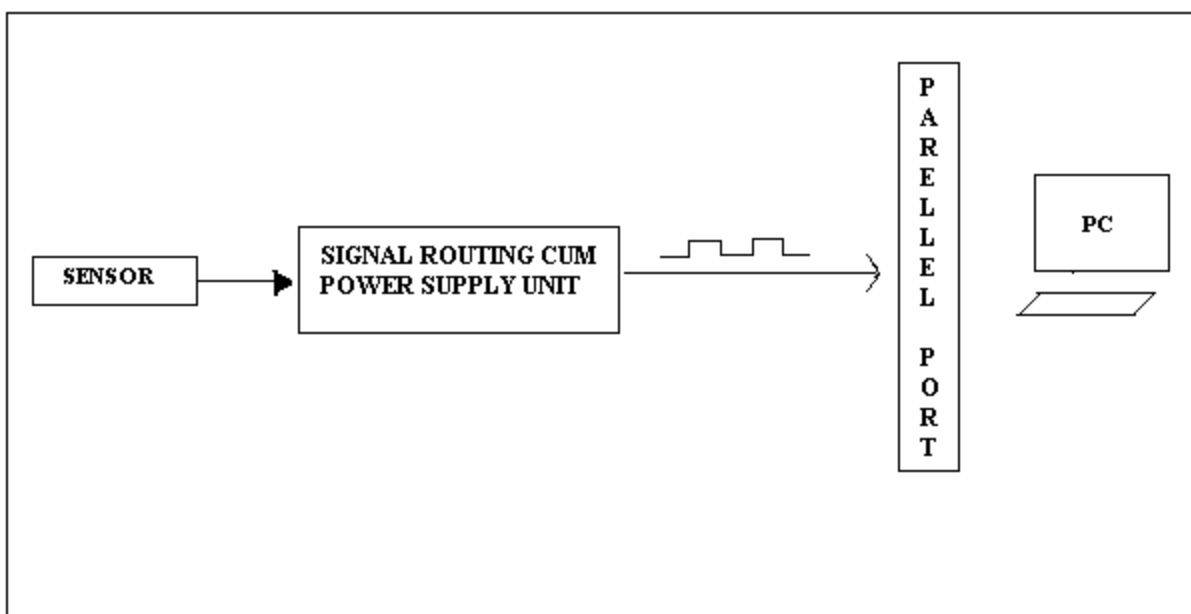


**Fig.II.3.** Block diagram of instrumentation for PC based conductivity monitoring instrument.

### 2.3.4. Salient features

Although there are many commercially available conductivity meters in the market, conductivity based approach in general has not been fully exploited. However pulsating type conductivity

meters have many salient features which allow these sensors to be deployed in diverse applications. Some of the salient features are listed below

- (i) *Simplified instrumentation:* Since the output from the probe is transistor-transistor logic pulses no other pulse conditioning circuits are required. This greatly simplifies the instrumentation. In comparison the conventional instruments require pre-amplification, signal conditioning, post amplification and analog to digital converters.
- (ii) *High resolution and sensitivity:* The conductivity probes offer high precision, high resolution and high sensitivity in measurement.
- (iii) *Response time:* Response time is defined as the time taken by a probe to reach 63% of the final stable value. The response time of pulsating type conductivity probes are less than 100 milli seconds and hence they are suitable for carrying out rapid conductometric titrations.
- (iv) *Communication to long distances:* The instrumentation is capable of transmitting noise free signal from LGO to long distances (up to 100 meters) without distortion or loss in the signal quality.
- (v) *Flexibility in probe design:* There is a lot of flexibility in probe design depending upon the specific application. The oscillator circuit can be either fixed into the probe head using epoxy resin or it can be placed near the probe.
- (vi) *PC based titrations:* Pulsating conductivity probes are readily compatible with PC as the signal produced from the probe is directly in the digital domain. Hence they are highly suitable for carrying out PC based titrations with reduced instrumentation.
- (vii) *Compatible for field use:* Since pulsating conductivity probes work on 5V DC they are portable and therefore compatible for field use.

## **2.4. EMF based measurements**

In the course of this work (refer chapter 3) all EMF measurements were carried out through a PC although the measurements can also be carried out using a standalone embedded unit. For carrying out PC based EMF measurements an appropriate probe (combination type pH electrode, platinum calomel electrodes etc) is connected to a V to f converter which in turn is connected to the signal routing unit. The V to f device converts the potential of the electrochemical system under investigation to digital pulses of 5V magnitude. The pulses are communicated to the PC using an interfacing cable. The GUI described in section 2.5 determines the frequency and converts it to EMF by applying a conversion factor.

## **2.5. Graphical user interface for recording titrations**

In order to carryout conductometric and potentiometric titrations using pulsating sensors a GUI was developed in C language [55]. Apart from carrying out titrations the GUI can also be used to measure conductivity and EMF. The flowchart of the GUI is shown in Figure II.4. The GUI is designed to handle three pulsating type sensors as the signal routing unit can support a maximum of three sensors only. The signal routing unit communicates the pulses generated from all the three sensor heads along with a reference frequency to the PC through an interfacing cable. The GUI simultaneously counts the pulses received from all the probes for a fixed duration to determine the frequencies. The frequency values are then plotted in three different channels as a function of real time. Scaling of axis, choosing appropriate sampling time, conversion of frequency to the parameter of interest, recording titration plots and other host of features are further accessed using the online menu keys.

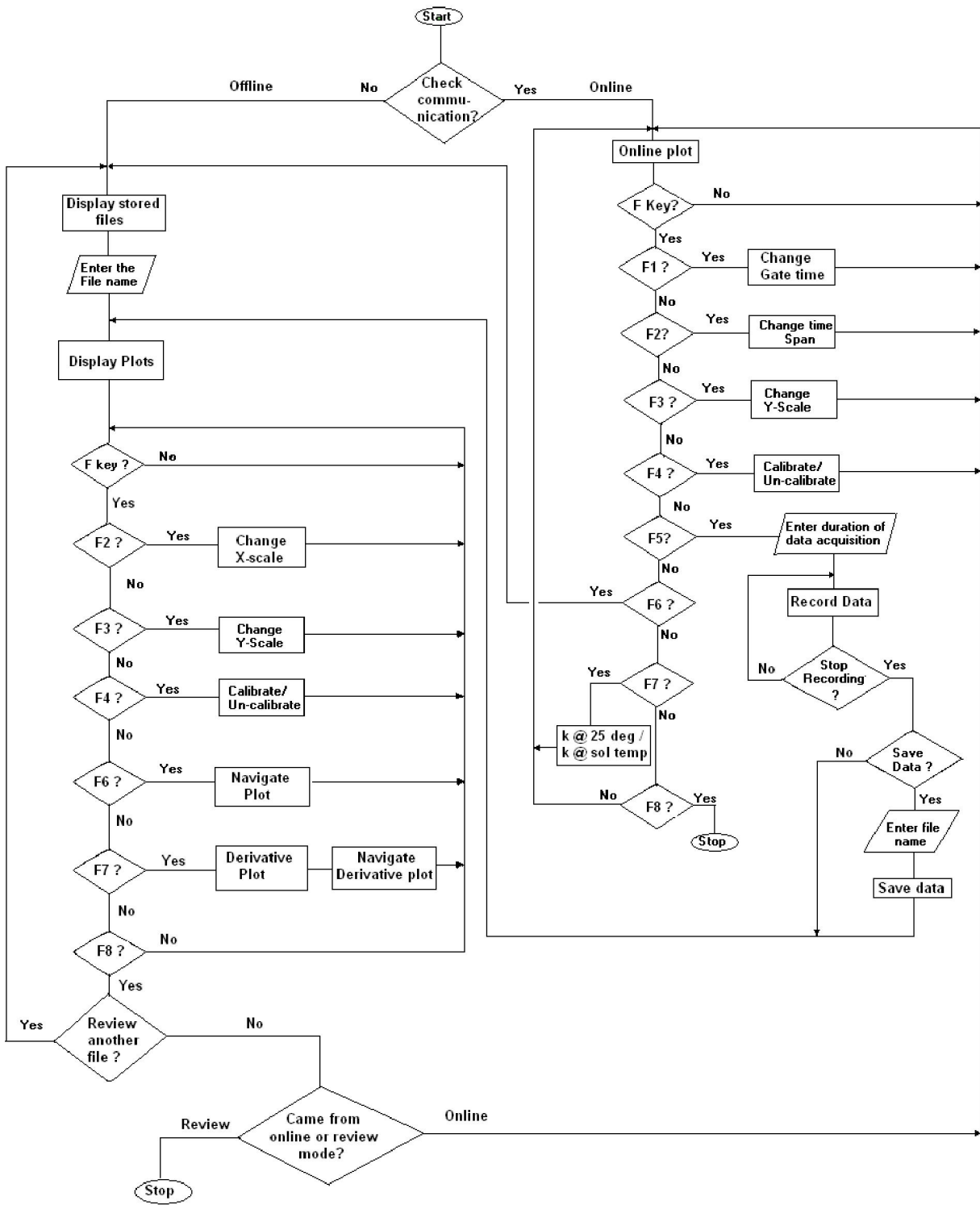
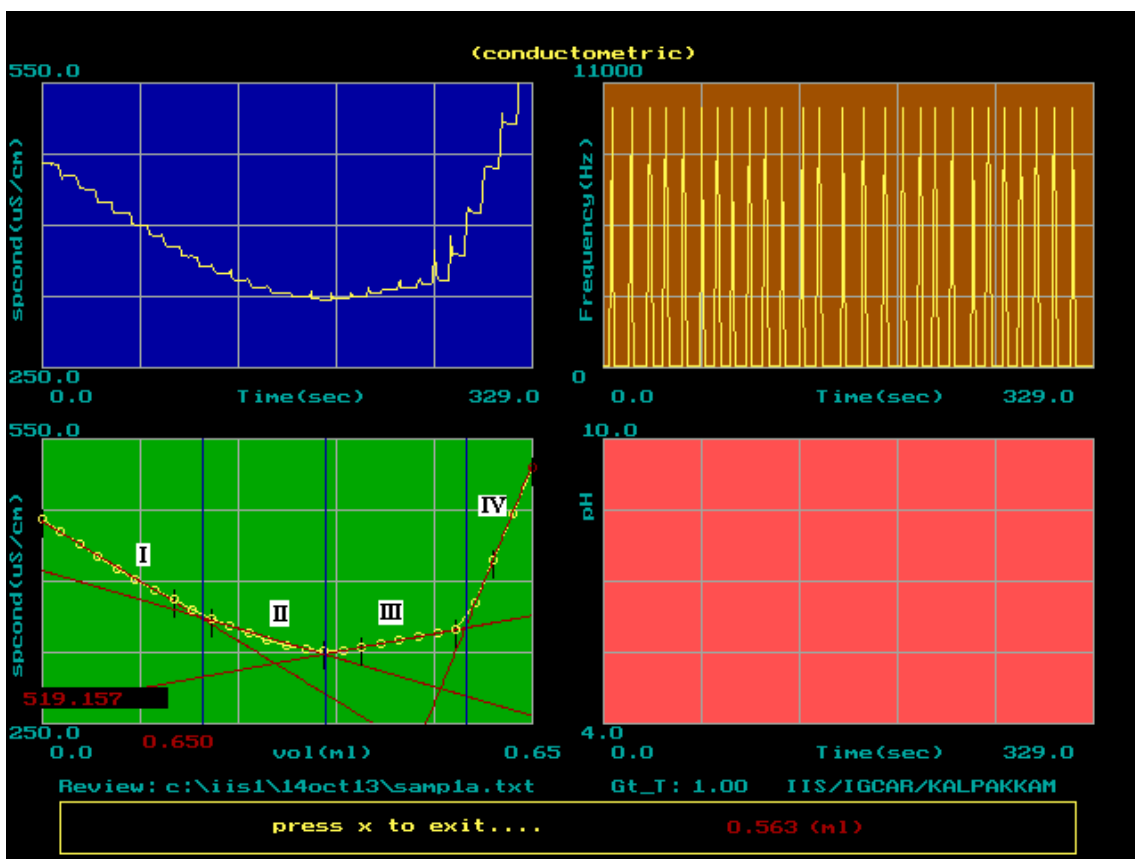


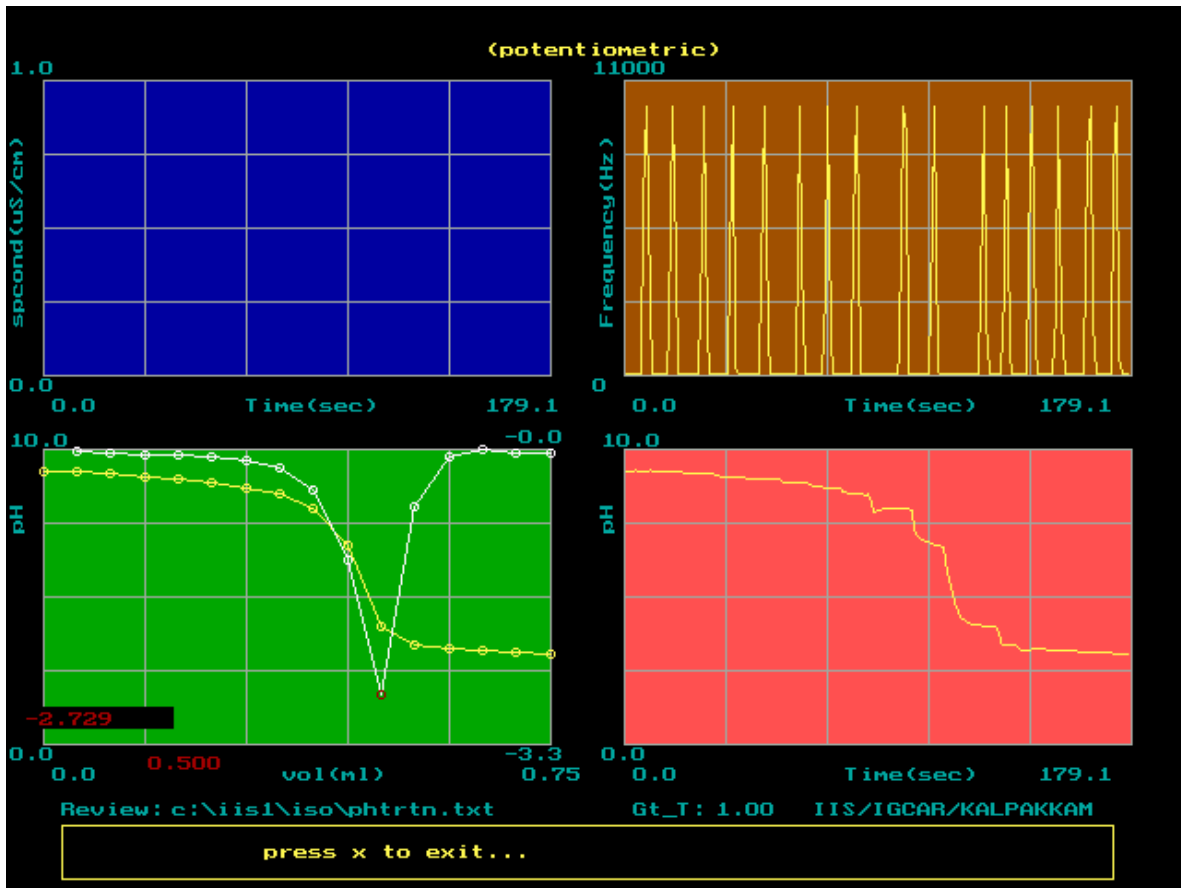
Fig.II.4. Flowchart of the graphical user interface.

Figure II.5 shows a typical screen capture view of a conductometric titration plot obtained using the GUI. The first channel shows the real time shift in conductivity while the second channel shows the number of peaks registered during the course of titration with each peak representing a fixed aliquot of titrant. The third channel which is earmarked for potentiometric titrations is left unused. A fourth channel that gets automatically generated after the completion of titration represents the shift in conductivity in the volume domain. The volume domain plot is generated using the data registered in the first and second channels. The plot shows four distinct regions with three endpoints. The end points are obtained by the intersection of least square fitted lines of adjacent regions while the fitted lines are generated by selecting a pair of points in each region.



**Fig. II.5.** Screen capture view of a PC based conductometric titration plot.

In the case of potentiometric titrations the first channel is left unused where as channels 2 and 3 are engaged. Channel-3 records the real time shift in EMF while channel-2 records the number of peaks registered during the course of titration. A fourth channel in volume domain unfolds immediately after the completion of titration. Figure II.6 shows the screen capture view of a typical potentiometric titration plot along with the derivative plot. In this particular case the shift in pH during an acid base titration was monitored using a combination type pH electrode.



**Fig.II.6.** Screen capture view of a PC based potentiometric titration plot.

### **2.5.1. Salient features of GUI**

The GUI was developed to carryout high resolution conductometric and potentiometric titrations in much simpler way. In order to achieve this the GUI was packed with many user friendly features and some of the main features are listed below

- (i) Simultaneous counting of pulses from all three channels for the determination of frequencies.
- (ii) Real time display of either frequency or parameter of interest in all three channels. The GUI converts the frequency value of a particular channel to the required parameter using the preloaded polynomial coefficients.
- (iii) Recording of conductometric and potentiometric titration plots.
- (iv) Multiple end point detections in both conductometric as well as in potentiometric titrations. In the case of conductometric titrations the end points are obtained by the intersection of least square fitted lines of adjacent regions. In the case of potentiometric titrations the end points are obtained by taking the first derivative of the titration plot.
- (v) Scaling of X and Y axis.
- (vi) Data navigation.
- (vii) Review of stored titration plots.

### **2.6. Reagent volume dispenser**

Conductometric and potentiometric titrations can be carried out either adding the reagent manually using a gas tight Hamilton syringe or using a reagent volume dispenser developed in the laboratory. The latter is used for carrying out rapid titrations. Figure II.7a shows the schematic representation of the entire titration setup used in a conductometric titration while

Figure II.7b shows the zoomed in schematic of the volume dispenser. The dispenser is connected to the second channel of the signal routing unit for carrying out an automated titration. The dispenser consists of an ordinary medical syringe that is locally available in the market. The piston that comes along with the syringe is not used in the set up as the reagent is made to fall under the influence of gravity as distinct drops through the syringe needle. In order to detect the number of drops falling inside the titration vessel a SS wire is placed adjacent to the needle with the wire and the needle forming an electrode pair. The wire is placed such that each drop resides momentarily between the electrodes before getting dislodged. Shorting occurs every time the drop touches the electrodes and this in turn gives rise to a maximum frequency. The frequency drops back to a minimum value once the shorting gets discontinued due to the displacement of the drop from the electrodes. Thus during the course of titration a train of peaks gets registered in the second channel of the PC screen as drops get formed and dislodged from the electrodes. Figure II.8 shows a typical titration plot obtained using the automated dispenser with the second channel showing the distinct peaks. From the figure it is seen that it takes less than a minute to complete the titration. Unlike in the case of manual addition of reagent, where there is no constraint in choosing the sampling time, in titrations involving the volume dispenser the data is sampled for either 0.25 seconds or 0.3 seconds only. This is because the sampling time in an automated titration is limited by the time taken for a drop to form and arrive inside the titration vessel and therefore the data has to be sampled before the arrival of the next drop inside the titration vessel.

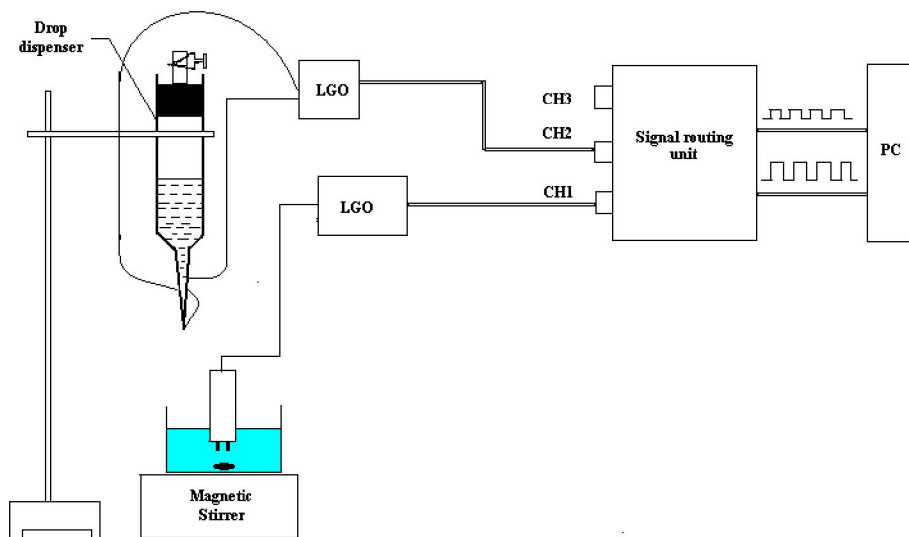


**Fig.II.7a.** Schematic representation of a complete conductometric titration facility using the reagent volume dispenser.

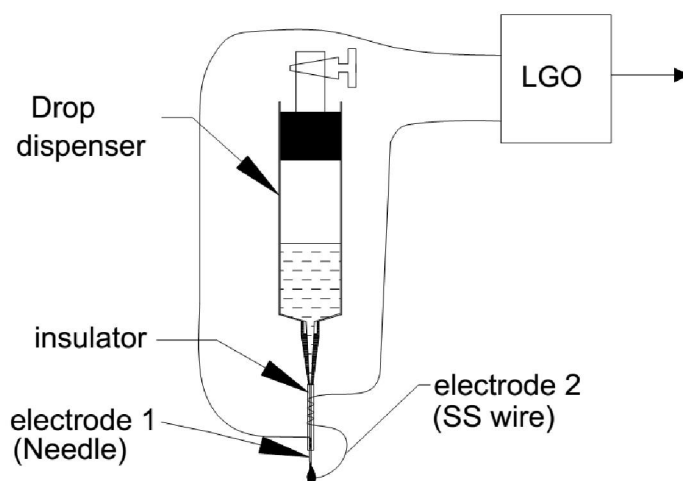


**Fig.II.7b.** Schematic representation of the reagent volume dispenser.

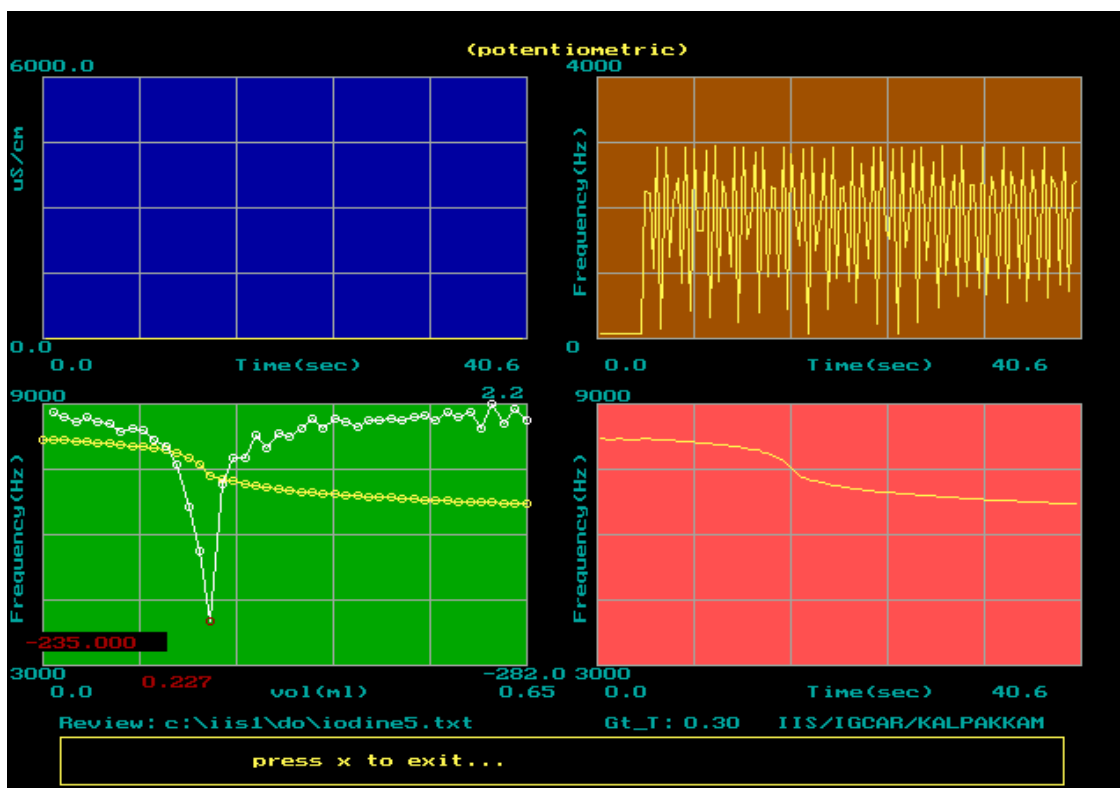


**Fig. II.8.** A typical potentiometric titration plot obtained using the reagent volume dispenser.

## 2.7. Conductometric titration facility

The PC based rapid conductometric titration facility consists of a pulsating type conductivity probe, a signal routing cum power supply unit, a PC loaded with GUI described in section 2.5 and an reagent volume dispenser described in section 2.6. For carrying out a conductometric titration the conductivity probe is connected to the first channel while the volume dispenser is connected to the second channel of the signal routing unit. The photograph of the entire rapid titration facility is shown in Figure II.9. There is also a provision to carryout titrations manually using a gas tight Hamilton syringe. Manual addition of reagent is followed when high resolution titration plots are required even in dilute solutions. In such cases the volume dispenser is disconnected and instead a marker available on the signal routing unit is engaged. In a manual titration the marker is pressed momentarily just before the addition of each aliquot of reagent of

fixed volume. Engaging the marker produces a shorting frequency that gets registered as a peak in the second channel of the PC screen. Figure II.5 shows a typical titration plot obtained by adding the reagent manually using a gas tight Hamilton syringe with the second channel showing the train of registered peaks. In the case of titrations involving the volume dispenser the peaks get automatically registered in the second channel as drops fall into the titration vessel. The end points are obtained once the titration gets over and from the resulting end points the various species present in the sample are quantified and reported. Generally it takes a couple of minutes to complete a titration by using the volume dispenser whereas it takes about ten minutes to complete a titration by adding the reagent manually using a Hamilton syringe.

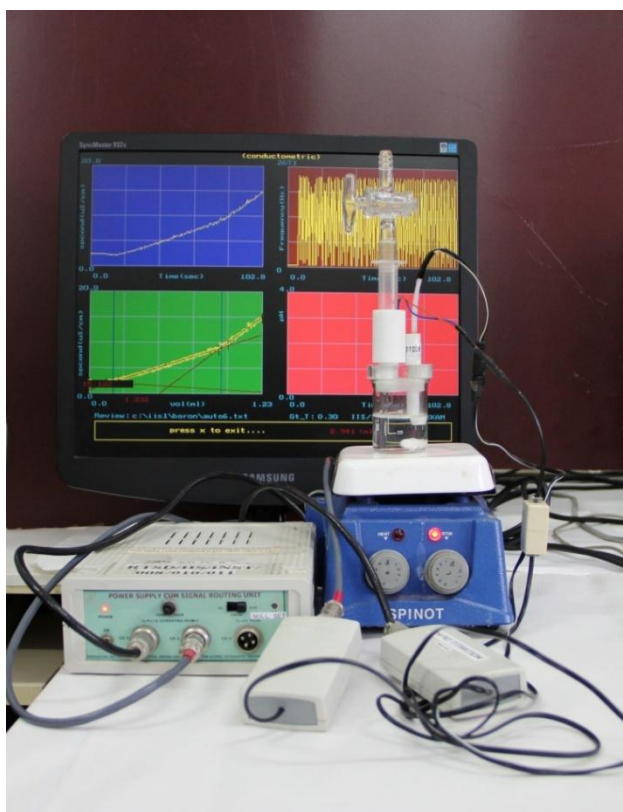


**Fig.II.9.** Photograph of the rapid conductometric titration facility.

## 2.8. Potentiometric titration facility

The PC based rapid potentiometric titration facility consists of a suitable reference-indicator electrode pair, a V to f converter, a power supply cum signal routing unit, a reagent volume dispenser and a PC loaded with the GUI. Figure II.10a shows the block diagram of the entire titration setup while Figure II.10b shows its actual photograph. The V to f device converts the potential of the electrochemical system to digital pulses of 5V magnitude. This approach of converting the analog output to digital domain simplifies the instrumentation and also makes the signal compatible to PC. Further there is a provision for EMF measurements at three different sensitivity ranges namely; X (gain 1), 10X (gain 10) and 100 X (gain 100). The required sensitivity can be selected through the knob on the signal routing unit.

As in the case of conductometric titrations potentiometric titrations too can be carried out either manually or using the volume dispenser. Automated titrations are carried out by connecting the volume dispenser to the second channel of the signal routing unit whereas the marker is engaged for carrying out manual titrations. Figure II.8 shows a typical potentiometric titration plot obtained by using the automated dispenser where the end point is obtained by taking the first derivative of the plot.

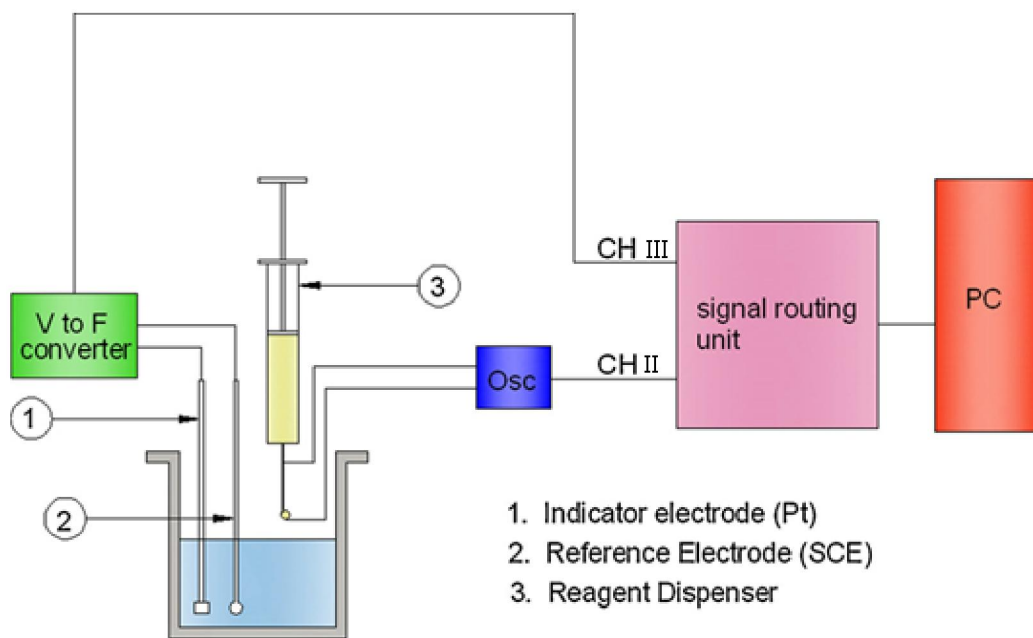


**Fig.II.10a.** Block diagram of the potentiometric titration facility.

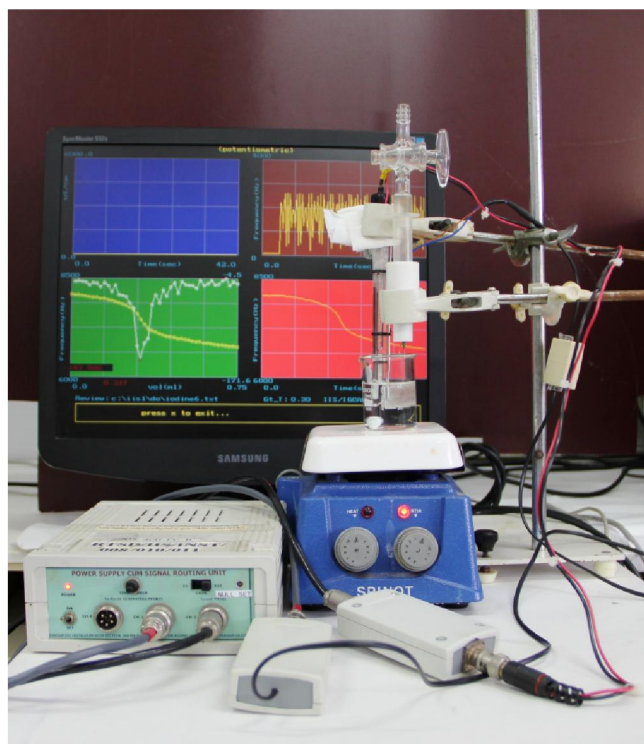


**Fig.II.10b.** Photograph of the rapid potentiometric titration facility.

## **2.9. Commercial instruments used in the thesis**

During the course of this work many commercial instruments were used in order to validate the analytical techniques developed using pulsating sensors. The following commercial instruments were used in this work and a brief description of each device along with its working principle is presented below.

### **2.9.1. UV-Visible spectrophotometer**

A UV-visible spectrophotometer is used to study the interaction of UV- visible light on the compound under investigation. The main components of a UV-visible spectrophotometer are a spectroscopic source (H<sub>2</sub>, D<sub>2</sub>, W lamp), a monochromator, a sample cell, a detector and a signal processor and read out unit [56]. Tungsten filament is used as a source to cover the visible region whereas a deuterium lamp or hydrogen lamp is used to cover the UV region. UV-Visible spectrophotometers are of two types, single beam spectrophotometers and double beam spectrophotometers. Single beam instruments have single light path whereas double beam instruments have two separate light paths, one for the test solution and another for the blank. Thus single beam instruments require the interchange of sample and blank solutions for each wavelength and therefore are better suited to manual than automatic operation [57]. In contrast, double beam instruments automatically vary the wavelength and record the absorbance as a function of wavelength and therefore offer more convenience in recording a spectrum. A UV-Visible instrument can be used for both quantitative as well as qualitative analysis. Quantitative analyses are performed based on the well known Beer Lambert's law [58]. The law states that the absorbance of a solution is linearly related to the concentration (c) of the absorbing species and the path length (b) of the radiation in the absorbing medium. The relationship is shown below

$$\log (I_0 / I) = A = \epsilon b c \quad (6)$$

Where A is the absorbance of the solution,  $I_0$  is the intensity of radiation before entering the solution, I is the intensity of radiation emerging from the solution,  $\epsilon$  is the molar absorptivity in  $\text{mol}^{-1} \text{L cm}^{-1}$ , b is the path length in cm and c is the concentration of solution in  $\text{mol L}^{-1}$ .

The instrument measures the ratio of intensity of light emerging from the sample (I) to the intensity of light entering the sample ( $I_0$ ). The ratio is called transmittance and is related to absorbance by the following formula

$$A = -\log (I / I_0) \quad (7)$$

In the work involving analysis of boron in light water and heavy water by conductometric titration approach (refer chapter 4), a Thermo make double beam spectrophotometer model number UV 2600 was used for validation. Standard curcumin spectrophotometric method was followed to analyze boron [39]. The method involves acidification of sample with hydrochloric acid and evaporating it to dryness in the presence of curcumin reagent. Heating is carried out at  $55^\circ\text{C}$  in a constant temperature bath. This results in the formation of a red rosocyanin complex which is taken up in iso-propyl alcohol and read spectrophotometrically at 540 nm. In the current spectrophotometric work all the analysis were carried out in a 10mm path length cell.

### **2.9.2. Infrared spectrophotometer**

An infrared (IR) spectrophotometer Wilks Miran 1A was used to measure the isotopic purity of heavy water when the concentration of heavy water in the samples exceeded 98% (ref Chapter 5). Mixed rare earth oxide was used as IR source whereas a thermocouple was used as detector. Generally IR spectroscopy is used when the sample is highly enriched in heavy water ( $> 88\%$ ) or when the concentration of heavy water in the sample is very low ( $<9\%$ ). In the intermediate

ranges (between 9% to 88%) a refractometer is used. An IR spectrophotometer is used to study the vibrational excitation of bonds by the absorption of infra red radiation. In modern laboratories three types of spectrophotometers are used, (i) dispersive spectrophotometers, (ii) Fourier transform spectrophotometers and (iii) filter photometers. The first two are used for obtaining complete spectra for qualitative identification whereas filter photometers are designed for quantitative work [59]. Like UV-visible spectrophotometer most of the IR spectrophotometers have the following components, (i) a source, (ii) a wavelength selector, (iii) a sample cell, (iv) a detector and (v) a signal processing and read out unit. However the components of an IR spectrophotometer deviate in many aspects as compared to a UV-Visible spectrophotometer. Infrared sources are heated solids in place of tungsten or deuterium lamps, infrared gratings are much coarser, the IR detector responds to heat rather than photons and the optical components in an IR instrument are constructed out of sodium chloride or potassium bromide [59]. None the less as in the case of quantitative measurements involving UV-visible spectroscopy, here too Beer Lambert's law is used for quantification.

Vibrational absorption occurs in the infrared region where the energy of radiation is insufficient to excite electronic transitions. Vibrational frequency ( $\nu$ ) of a bond is inversely proportional to the reduced mass ( $\mu$ ) of the atoms constituting the bond [60]

$$\nu = (1/2\pi)(k/\mu)^{1/2} \quad (8)$$

where k is the force constant.

Since O-H and O-D have different reduced masses their vibrational frequencies differ which in turn causes their characteristic excitation frequencies to be different. O-H shows a characteristic absorption at  $3400 \text{ cm}^{-1}$  while O-D shows a characteristic absorption at  $2500 \text{ cm}^{-1}$ . In the case of

quantitative measurements involving enriched heavy water (>88%) the absorption is measured at  $3400\text{ cm}^{-1}$  whereas in the case of low grade heavy water (<9%) the absorption is measured at  $2500\text{ cm}^{-1}$ .

### **2.9.3. Ion chromatograph**

Ion chromatography (IC) is an analytical technique in which anions and cations are separated by the difference in the rate of migration through a column containing either anion or cation exchange particles [61]. The ion having the greatest affinity for the column is eluted last while the ion having the least affinity is eluted first. The instrument is highly useful as a number of cations or anions can be analyzed simultaneously in a single run within a very short period (usually less than 30 minutes). IC has been successfully applied to the analysis of ions in many extremely diverse types of samples. Ions have been determined in difficult matrices such as toothpaste, brines and caustics apart from much simpler matrices such as potable water and rain water. The instrument is capable of detecting ions down to a few  $\mu\text{gL}^{-1}$  levels using minimum sample volume. An IC can be used in a variety of instrument configurations with different column sets and eluent. Typically an IC consists of an eluent pump, sample injection valve, separation column, a suppressor coupled to a conductivity detector and, a regenerating pump with electronic timer and control [62]. In this technique a known volume of sample is introduced into a mobile eluent stream which carries the sample to the separator column. The analytes get separated on the column based on their affinity towards the ion exchange particle loaded inside the column. The affinity is defined in terms of distribution coefficient  $K$ , which is simply the ratio of concentrations of a given component in the stationary phase to that in the mobile phase [63]. The eluent containing the separated ions pass through a suppressor column before entering the conductivity detector. The purpose of suppressor column is twofold, (i) it suppresses the

background conductivity of the eluent and (ii) it enhances the analyte conductivity. The resulting chromatogram as recorded by a PC consists of a train of conductivity peaks due to the various analytes as a function of time. In this technique there are number of parameters which can be altered to increase the efficiency of separation and to decrease the analysis time, they are (i) separator column length, (ii) separator column capacity, (iii) eluent strength, (iv) use of organic modifiers in the eluent, (v) flow rate of eluent and (vi) gradient elution [62].

In the work involving analysis of boron in light water and heavy water by direct conductivity approach (refer chapter 4), a Dionex make IC model number ICS-1100 was used for validation. An ion pac IC borate column (9 x 250 mm) was used as the separator column, 2.5 mM methan sulphonic acid + 60 mM mannitol acted as eluent, loop volume was 100 micro liters, flow rate was  $1 \text{ ml min}^{-1}$ , while no concentrator or suppressor was used [64].

#### **2.9.4. Refractometer**

Refraction is a phenomenon in which the direction of light changes as it passes from one medium to the other. Refraction occurs due to the difference in velocity of light in the two mediums. The extent of bending of light is determined by the refractive index of the medium and refractive index in turn is determined using a refractometer. A Karl Zeiss make Abbe refractometer was used to validate the work involving the isotopic determination of heavy water by conductivity approach (refer chapter 5). The instrument was used when samples contained heavy water in the range of 9% to 88%. The instrument consists of a source of monochromatic light, an assembly of two prisms, and a telescope [65]. A drop of sample is placed between the two prisms forming a thin film. One prism acts as an illuminating prism while the other acts as a refracting prism. A light source is projected through the illuminating prism whose bottom surface is roughened in order to generate light rays travelling in all directions from each point on the surface.

Consequently light enters the refracting prism in a variety of angles which is sharply limited by the critical angle [66].The critical ray forms the boundary between the bright light and dark portions of the field when viewed through the telescope. This demarking boundary is adjusted to the cross hairs to read the scale. In order to get quantitative information on the isotopic purity of heavy water by this technique a calibration plot is generated using known standards of heavy water and measuring the signal output of each standard. Heavy water concentration and the signal output obey a linear relationship and this relationship is used to determine the unknown concentration of heavy water in a sample.

---

### 3. DEVELOPMENT OF ANALYTICAL TECHNIQUE FOR TRACE ASSAY OF DISSOLVED OXYGEN BY REDOX TITRATION

---

#### 3.1. Introduction

The chapter deals with the application of an in-house built pulsating sensor based EMF monitoring system towards the development of a simple and high precision analytical technique for the assay of dissolved oxygen (DO) in water at  $\text{mgL}^{-1}$  (ppm) and  $\mu\text{gL}^{-1}$  (ppb) levels. DO measurement is of considerable importance in various fields such as environmental [67, 68, 69], biological [70] and industrial power plants [71, 72]. DO is required for the survival of many aquatic organisms and its measure is an important parameter to ascertain the quality of water. In nuclear industry DO is constantly monitored in the feed waters of steam generator unit. The level of DO in such water is kept below 10 ppb in order to avoid corrosion. The removal of DO from the initial deionized water is achieved using a combination of mechanical and chemical methods. In the first stage DO in the water is lowered from around 8.0 ppm to 50 ppb using mechanical deaeration technique. This is followed by chemical dosing which brings down the DO from 50 ppb to less than 8ppb. Chemical dosing is done using volatile chemicals such as hydrazine [73] which do not add to the total ionic content of the steam generator feed water. An increase in the total ionic content beyond certain allowed level accelerates corrosion and deposition of the ionic species on the turbine blades and other components of the steam generator unit. Similarly the presence of DO above 10 ppb promotes stress cracking corrosion in stainless steel. In view of the above problems it becomes crucial to continuously monitor the DO content along with other ionic impurities present in the steam generator feed water.

There are many techniques available for the measurement of DO. Amperometric [74] and galvanic type [75, 76] meters are the most convenient and extensively used methods for online

measurement. For rapid screening colorimetric methods based on Indigo carmine [77] and Rhodazine-D [78] are being used. Depending on the DO content in the sample the colorimetric reagent produces different colors. From the nature of color shade the concentration of DO in water is predicted. The limitation of this technique is that it gives a narrow range in which DO is present and not its absolute value. In environmental monitoring classical Winkler's titration [79, 80] using starch as indicator is still being followed for the routine determination of biological oxygen demand. The method gives excellent accuracy and precision when DO is present at few ppm levels but it is not recommended when DO is present at sub ppm levels. Flow injection analysis (FIA) [81, 82] is an attractive technique when large number of samples has to be analyzed. Apart from high sample throughput FIA offers reduced reagent consumption, high reproducibility and high degree of flexibility. Luminescence measurement technique using Hach Method [83] 10360 has been adopted as a standard technique by the USEP (United States Environmental Protection Agency) for DO assay in surface, ground, municipal and industrial waste waters. Apart from being rapid and convenient this technique is non destructive unlike the other techniques discussed above. Therefore this technique has gained much acceptance in environmental monitoring analysis.

In the present work a modified PC based Winkler's titration technique has been studied in detail. In the classical Winkler's titration starch is used as indicator to detect the end point whereas the present technique follows the same titration potentiometrically through a PC using a high resolution potentiometric titration device with pulsating sensor based instrumentation. The end point of the titration is obtained by taking the first derivative of the potentiometric titration plot. Using this technique low detection levels are achieved which is otherwise not possible using the traditional Winkler's technique. Such advancement in measuring low levels of DO (at a few ppb)

was made possible due to the use of in-house built high resolution titration facility. In this chapter the basic principle of Winkler's chemistry, the advantages of the current technique over the indicator method, construction of an in-house built DO sampler have been discussed in detail. After successfully standardizing the technique at trace levels the technique was applied for the assay of DO in the steam generator feed waters of Fast Breeder Test Reactor (FBTR) and Madras Atomic Power Station (MAPS), Kalpakkam. Probably for the first time a titration technique is applied to determine DO at few ppb levels in such crucial applications.

## **3.2. Experimental**

### **3.2.1. Materials and reagents**

#### **3.2.1.1. Alkaline potassium iodide (~8M sodium hydroxide/~ 4M potassium iodide)**

About 16g of NaOH was dissolved in 25mL of deionized water and the solution was allowed to cool. To this solution about 33g of KI was added and the solution was shaken vigorously. Water was added in small quantities while shaking and the solution was finally made to 50 mL. After further shaking the solution was filtered and the filtrate was made up to 50 mL. It is observed that at such high concentration levels the chemicals tend to dissolve slowly and therefore filtration of solution is highly recommended.

#### **3.2.1.2. Manganese sulphate solution (~3M $\text{MnSO}_4 \cdot \text{H}_2\text{O}$ )**

To 40 mL deionized water about 25g of manganese sulphate was added. The solution was shaken well to dissolve as much salt as possible. Shaking was continued by adding small quantities of water and the solution was made up to 50mL. After further shaking the solution was filtered and the filtrate was finally made up to 50 mL.

### **3.2.1.3. 5M Sulphuric acid**

5M sulphuric acid was prepared by diluting concentrated sulphuric acid (AR grade).

### **3.2.1.4. Standard sodium thiosulphate solution**

A 0.1 M sodium thiosulphate solution was prepared by dissolving around 0.64g of sodium thiosulphate in 25 ml of deionized water. The solution was standardized against potassium iodate. All subsequent working standards were prepared from this stock solution through appropriate dilution.

### **3.2.1.5. 0.05M Iodine solution prepared in 2% (w/v) KI solution**

0.05M iodine in 2% (w/v) KI solution was prepared by dissolving 0.64g of iodine in a 40 mL solution containing 1g of KI. After dissolving the iodine the solution was made up to 50 mL. The resulting solution was standardized against standard arsenious oxide solution.

### **3.2.1.6. Potentiometric titration facility**

The potentiometric titration facility along with the GUI described in sections 2.8 and 2.5 respectively of chapter 2 was used in this current work. Further all the titrations were carried out in gain 10, ie. 10X sensitivity mode.

### **3.2.1.7. DO sampler**

A DO sampler of 100 mL capacity was made in the laboratory for collecting the water samples. The sampler was made out of Perspex and was designed in such a way that it eliminates the ingress of any air bubble during sampling. The schematic of the sampler is shown in Figure III.1. The sampler is divided into two parts- a conical upper part and a cylindrical bottom part. The two parts are joined by means of a thread provided externally on the bottom part. It was observed that providing the thread internally resulted in the occasional entrapment of air bubbles between the

threads during sampling. The bottom part contains both the inlet and the outlet that are controlled by Tarson valves. During sampling water enters through the valve at the bottom and exits via the valve at the top. The upper part houses a replaceable septum through which the Winkler's reagents are administered into the vessel using Hamilton syringe. The upper part is deliberately made conical in order to facilitate the easy and smooth flow of water during sampling.

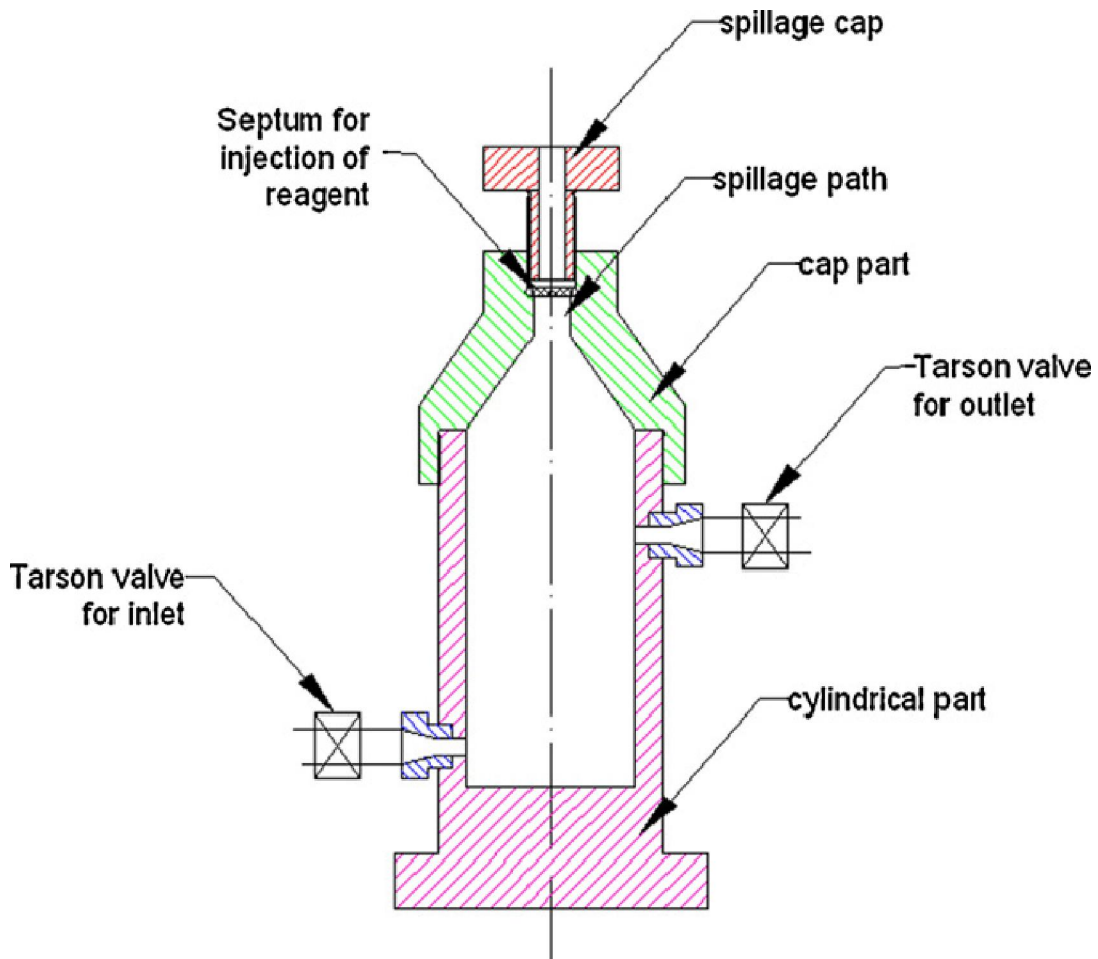


**Fig.III.1.** The schematic of the DO sampler used in collecting water samples.

### 3.3. Methodology

The first step involves the collection of water sample using the DO sampler described in section 3.2.1.7. The source outlet is connected to the DO sampler's inlet and representative sample is

collected after flushing the container for about 6-7 minutes. Immediately after sampling the inlet valve is closed and the following reagents are added in quick succession, (i) 0.5mL of  $\text{MnSO}_4$  and (ii) 0.5 mL of alkaline KI. The outlet valve is closed and the sampler is inverted for about 10-12 times when a brown  $\text{MnO}(\text{OH})_2$  precipitate appears. Under this condition the sample can be preserved up to 10 hours and within this timeframe the sampler is brought back to laboratory from the sampling point for carrying out the titration. Before starting the titration 1.0 mL of  $\text{H}_2\text{SO}_4$  is added to the sampler and the sampler is inverted for about 10-12 times. The addition of sulphuric acid dissolves the brown precipitate and makes the sample acidic. In order to carry out the titration a suitable volume of the sample (25 or 50 mL) is taken in a titration vessel. A pair of Pt-SCE electrode is mounted over the vessel and the sample is titrated against freshly standardized sodium thiosulphate solution. The titration endpoint is obtained by taking the first derivative of the plot and from the resulting end point the DO present in the sample is calculated.

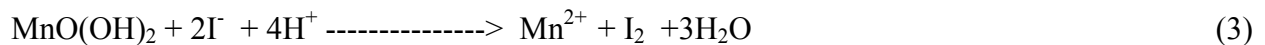
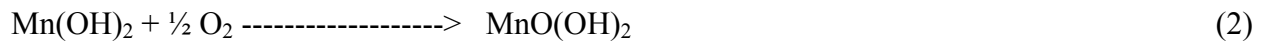
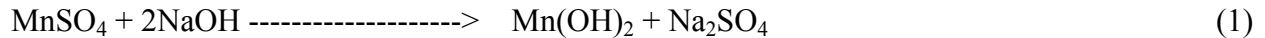
### **3.4. Results and discussion**

#### **3.4.1. Principle**

Winkler's titration is basically an iodometric titration. As DO does not directly oxidize iodide to iodine a multistep oxidation involving manganese hydroxide is performed. The successive addition of manganese sulphate and alkaline KI into the sample results in the in-situ generation of manganese hydroxide ( $\text{Mn}(\text{OH})_2$ ).  $\text{Mn}(\text{OH})_2$  reacts with the DO present in the sample and gets transformed to a hydrated tetravalent oxide of manganese [ $\text{MnO}(\text{OH})_2$ ].  $\text{MnO}(\text{OH})_2$  is a brown precipitate that can be dissolved by acidifying the sample. Under acidic condition iodide reduces the tetravalent manganese to  $\text{Mn}^{2+}$  while itself getting oxidized to iodine. Acidification is done prior to the start of titration in order to avoid the loss of iodine. The liberated iodine which is

representative of DO present in the sample is determined by titrating it against a freshly standardized sodium thiosulphate solution.

The list of reactions involved in the above process is given below



### 3.4.2. Advantages of the current technique over classical Winkler's titration

In classical Winkler's titration starch is used as indicator and the end point is detected by the disappearance of blue color. This method of end point detection is subjected to personal errors and the errors become significant when analyzing samples at sub ppm levels. At low levels of DO concentration the visual detection of end point becomes difficult and as a consequence the precision and accuracy of the final result gets affected. However personal errors associated with the visual detection of end point is avoided in the modified Winkler's technique as the end point is detected by taking the first derivative of the plot. Moreover the use of high resolution titration facility ensures a sharp jump in potential near the end point even when working with dilute solutions (DO to a few ppb levels). This in turn helps in unambiguous detection of end point while taking the first derivative plot.

### **3.4.3. Initial studies on potentiometric based Winkler's titration technique**

It was observed that there are many recipes available in the literature to prepare the various reagents required for Winkler's titration. In the present work the current recipe described in section 3.2 was standardized and evaluated in order to avoid confusion. Further the quantity of various reagents required for the treatment of sample was also optimized. It was found that the addition of 0.5 mL of manganese sulphate, 0.5 mL of alkaline potassium iodide and 1mL of 5M sulphuric acid to 100 mL sample would suffice.

Before applying this new technique at trace levels the method was used for determining DO in tap water samples. Two batches of tap water were collected in a time interval of two hours from the same sampling point from our laboratory using the DO sampler. Three samples from each batch were analyzed in accordance with the methodology described in section 3.3. The precision in measurement of the first batch of sample (designated as S1) was found to be 1.3 % RSD ( $5.83 \pm 0.075$ ,  $n=3$ ) while the precision in measurement of the second batch of sample (designated as S2) was also found to be 1.3% RSD ( $5.78 \pm 0.075$ ,  $n=3$ ). Table III.1 shows the titration end points along with the corresponding DO concentrations obtained by using this potentiometric titration approach. The results were compared with an independent parallel set of experiments carried out by following the conventional Winkler's titration and the results from both the techniques agreed well (refer Table III.2).

**Table III.1.** Assay of dissolved oxygen in tap water samples by potentiometric titration technique.

S. no.	Description of sample	End point (mL)	Dissolved oxygen (ppm)
1.	25 mL of tap water sample (S1). Designated as (S1A1).	0.720	5.87
2.	25 mL of tap water sample (S1). Designated as (S1A2).	0.720	5.87
3.	25 mL of tap water sample (S1). Designated as (S1A3).	0.704	5.74
4.	25 mL of tap water sample (S2). Designated as (S2A1).	0.704	5.74
5.	25 mL of tap water sample (S2). Designated as (S2A2).	0.704	5.74
6.	25 mL of tap water sample (S2). Designated as (S2A3).	0.720	5.87

**Table III.2.** Comparison of pulsating potentiometric titration technique with classical Winkler's titration method.

Sample Designation	DO obtained by pulsating potentiometric titration approach (ppm)	DO obtained by Winkler's titration approach (ppm)
S1A1	5.87	5.95
S1A2	5.87	5.99
S1A3	5.74	5.87
S2A1	5.74	5.83
S2A2	5.74	5.83
S2A3	5.87	5.79

### 3.4.4. Potentiometric titrations at trace levels

The main purpose of this work was to bring out a suitable titrimetric technique which can be used reliably at ppb levels. With the encouraging results obtained from the initial study analysis of DO was carried out at sub ppm and ppb levels. As DO standards are not readily available standard iodine solution equivalent to DO was selected. This approach was followed because after adding all the reagents involved in Winkler's chemistry the iodine representative of DO in the sample is liberated. Titrations were carried out by two different methods of reagent addition. In one method the reagent was added from a semi automated volume dispenser (refer 2.6.) while in the other method the reagent was added manually using a Hamilton syringe. The titration plots obtained by the two different modes of reagent addition are reproduced in Figures III.2 and III.3.

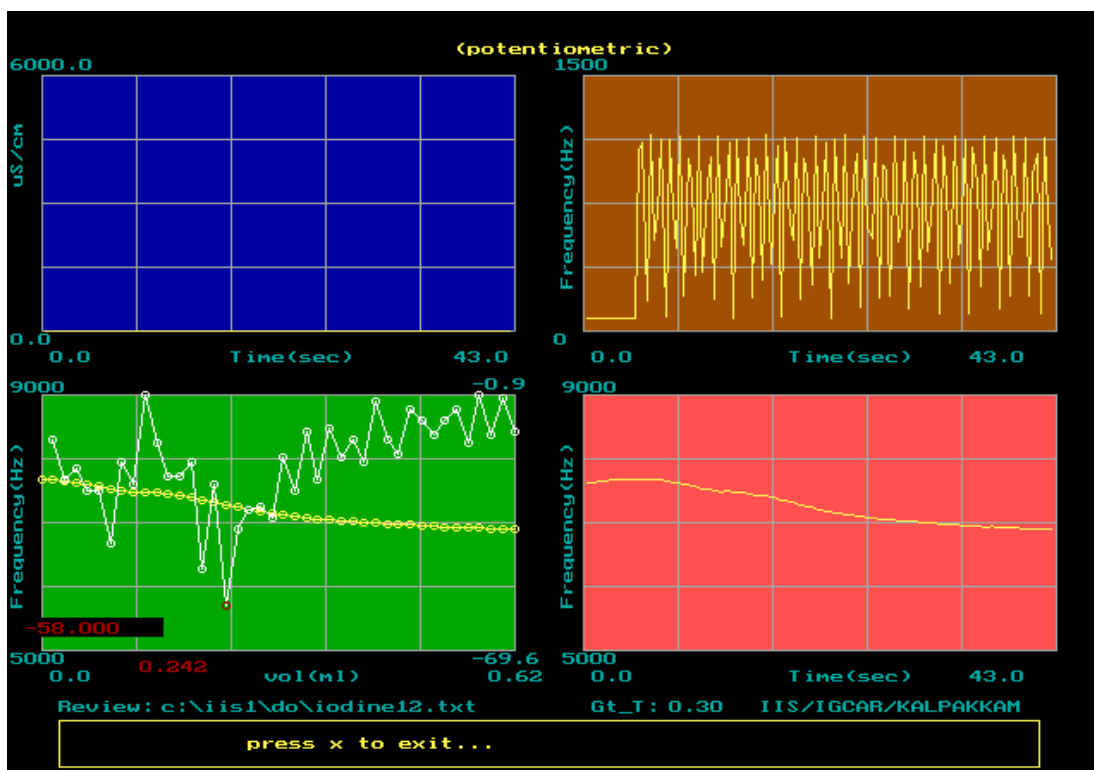


**Fig.III.2.** Titration of 50 mL of  $2.47 \times 10^{-3}$  mM iodine in 0.5%(w/v) KI (equivalent to 39.5 ppb DO) against 0.00103M sodium thiosulphate using the automated dispenser. The DO corresponding to end point (0.242 mL) is 39.8 ppb as against 39.5 ppb. The sampling time is 0.3 seconds while each peak in the second channel represents  $15 \mu\text{L}$ .

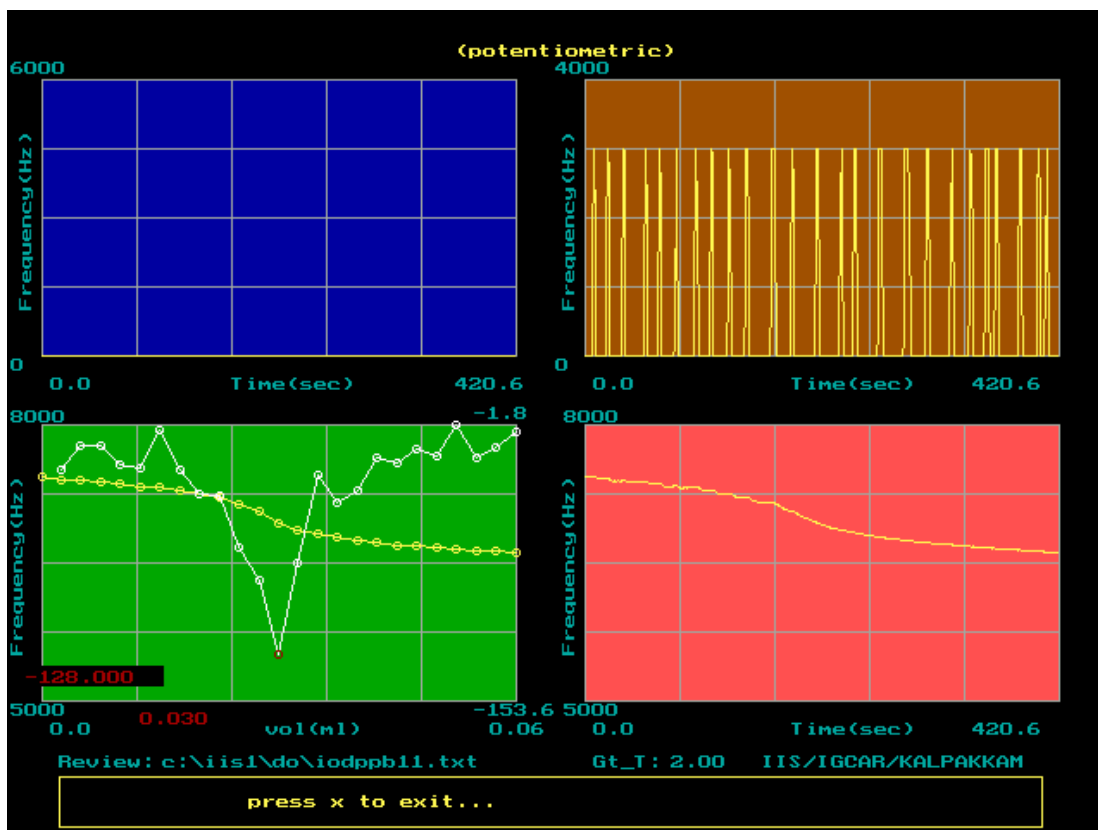


**Fig.III.3.** Titration of 25 mL of  $6 \times 10^{-4}$  mM iodine in 0.5% (w/v) KI (equivalent to 9.6 ppb DO) against 0.001M sodium thiosulphate using manual addition of reagent. (Sampling time = 2 seconds, steps of titrant addition =  $2.5 \mu\text{L}$ ). The sample contains 9.6 ppb DO (end point: 0.03mL).

From Figure III.2 it is seen that the derivative plot is not smooth although the plot gives a distinct end point. The plot was obtained by using the automated volume dispenser with a data sampling time of 0.3 seconds (refer section 2.6 for working of the dispenser and the choice of sampling time). In dilute solutions such small sampling times are insufficient to obtain stable potential values as the reaction becomes kinetically slow. As a consequence the precision in measurement deteriorates which in turn affects the smoothness of the derivative plot.

However smooth derivative plots were obtained using the volume dispenser for samples containing DO above 1ppm. At higher DO concentrations the reaction becomes kinetically favorable and therefore small sampling times do not affect the measurement precision. Figure

III.4 illustrates this argument where a smooth derivative plot was obtained for a sample containing 1.86 ppm of DO. In contrast to Figure III.2 Figure III.3 shows a smooth derivative plot with a distinct end point at a much lower DO concentration of 9.6 ppb. The plot was obtained by adding the titrant manually using a Hamilton syringe with a data sampling time of 2 seconds. Such higher sampling times are required in order to give allowance for the delayed kinetics in dilute solutions. This leads to better precision in measurement and also gives smoother derivative plots as reflected in Figure III.3.

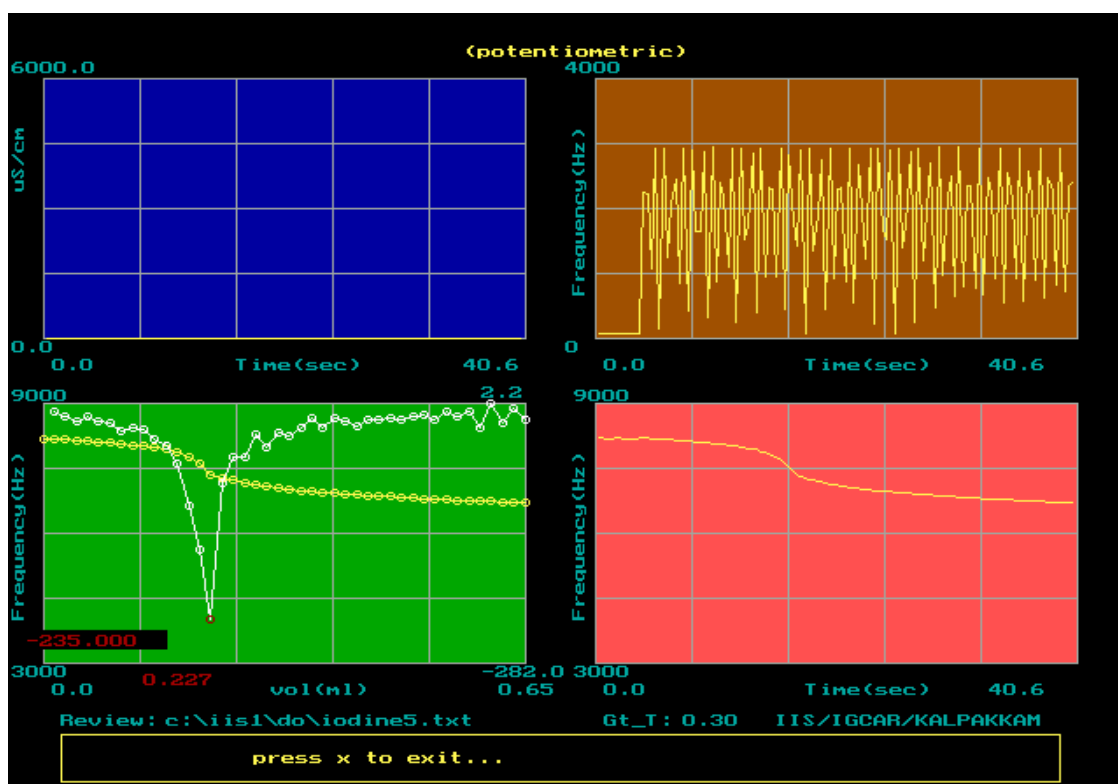


**Fig.III.4.** Titration of 25mL of 0.116 mM iodine in 0.5% (w/v) KI (equivalent to 1.86 ppm DO) against 0.0257M sodium thiosulphate using the automated volume dispenser. Sampling time is 0.3 seconds while each peak in the second channel represents 15  $\mu$ L of titrant. DO corresponding to the end point (0.227 mL) is 1.87ppm.

During the course of this work a novel method for unambiguous detection of end point was developed while working with dilute solutions. In this method the electrodes are short just before the addition of each aliquot of reagent and the shorting is discontinued once the aliquot is added. The provision of shorting the electrodes has been provided in our titration setup. By shorting the electrodes the potential becomes zero and regains a value corresponding to solution potential once the shorting is discontinued. At equivalence point a sharp change in potential is observed from which the end point is easily judged without any ambiguity. The method therefore gives the reaction end point without taking the first derivative of the plot. A typical titration plot obtained using the above technique is shown in Figure III.5.

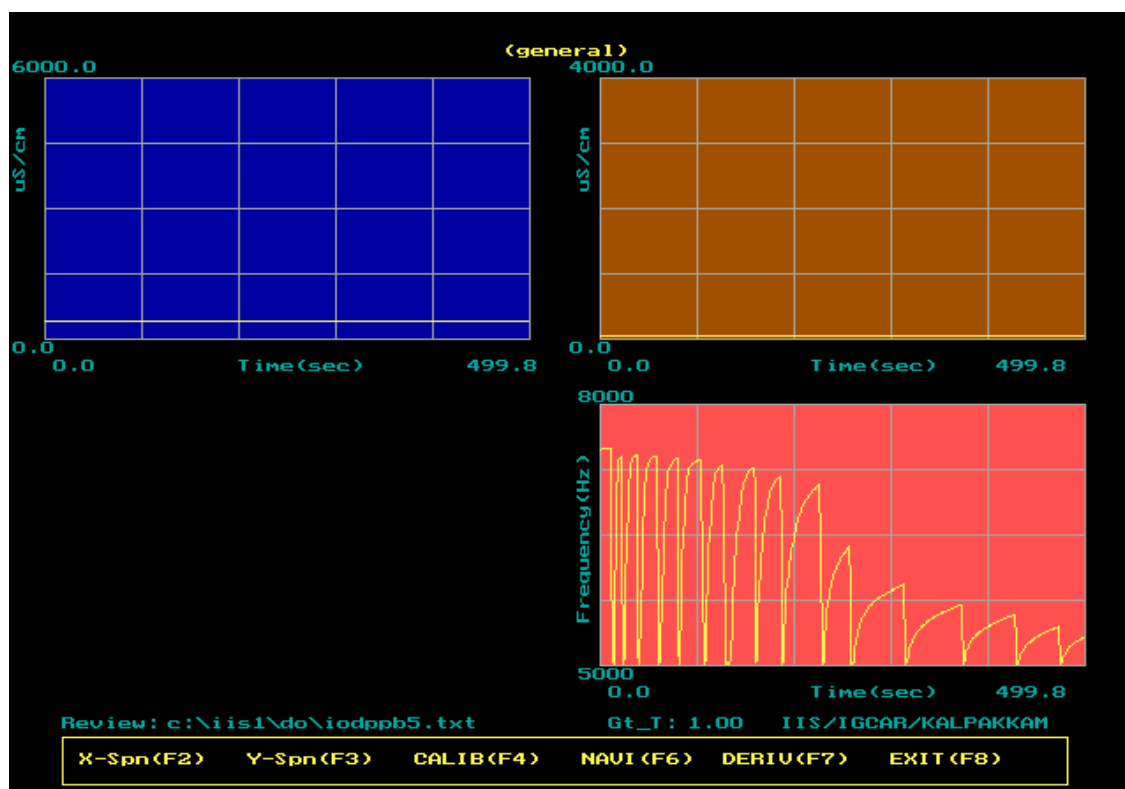


**Fig.III.5.** Online titration plot of standard iodine solution (equivalent to 16 ppb DO) against 0.001M sodium thiosulphate using ‘shorting electrodes approach’, 10th step of addition (corresponding to 50  $\mu$ L volume) is the end point.

After successfully analyzing samples at trace level using iodine equivalent of DO the method was applied to actual samples. Water containing trace DO was produced by adding controlled quantity of sodium sulphite solution to the collected water sample prior to the addition of Winkler's reagents. Sodium sulphite acts as a scavenger of DO and removes it according to the following equation



Figure III.6 shows a typical high resolution plot obtained by titrating a tap water sample pre treated with sodium sulphite solution.

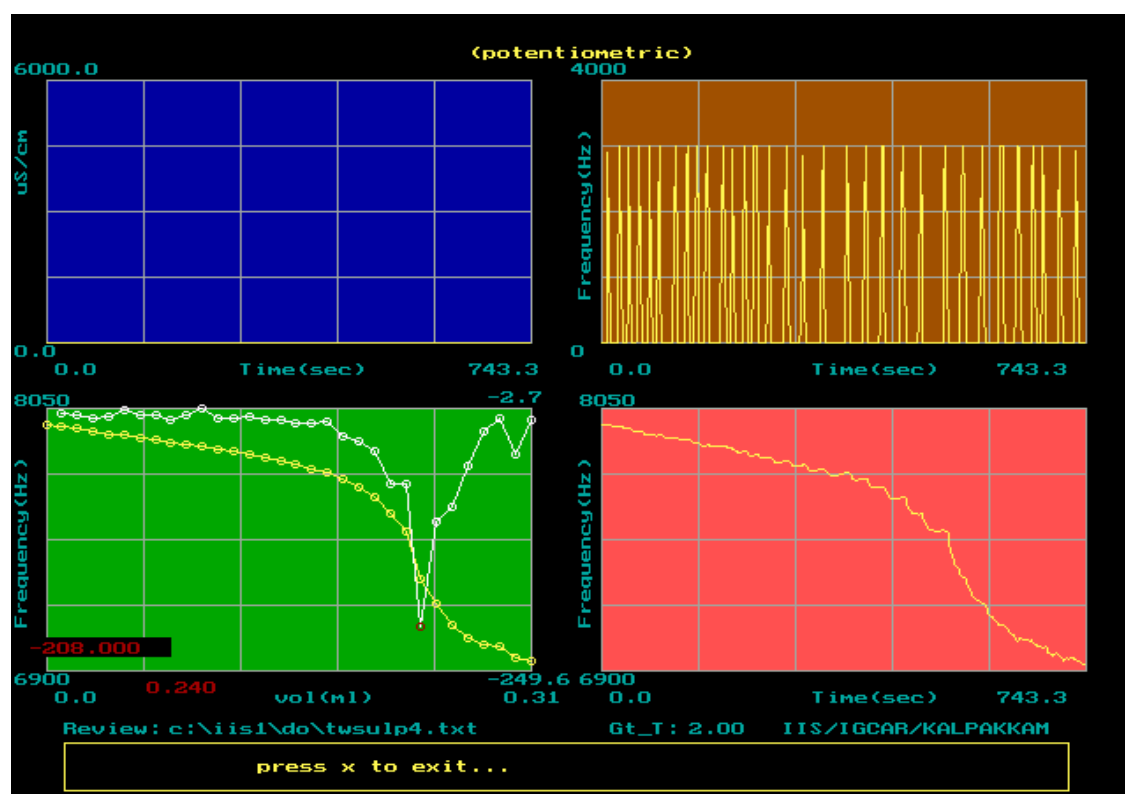


**Fig.III.6.** 100mL tap water sample collected in DO sampler, added small aliquot of 1% (w/v)  $\text{Na}_2\text{SO}_3$  to bring down DO to ppb level. Added  $\text{MnSO}_4$ ,  $\text{NaOH/KI}$  and 5M sulphuric acid as recommended in Winkler technique. 25mL of sample titrated against 0.001M sodium thiosulphate in 10  $\mu\text{L}$  steps by manual addition. The sample contains 77 ppb of DO (end point: 0.24 mL).

The sample was found to contain 77 ppb of DO as against 79 ppb obtained by an electrochemical DO meter. Table III.3 summarizes the results obtained by analyzing water samples pre treated with sodium sulphite solution by the current technique and also by using an electrochemical DO meter.

**Table III.3.** Comparison of pulsating potentiometric titration technique with electrochemical DO meter for assay of dissolved oxygen.

Nature of sample	By pulsating-potentiometric titration (ppm DO)	By electrochemical DO meter (ppm DO)
Sulphite treated tap water-I	0.077	0.079
Sulphite treated tap water-II	0.012	0.010
Sulphite treated tap water-III	0.054	0.054
Sulphite treated tap water-IV	0.074	0.070
Sulphite treated tap water-V	0.032	0.029
Sulphite treated tap water-VI	0.067	0.065
Sulphite treated tap water-VII	0.025	0.022
Sulphite treated tap water-VIII	0.044	0.041
Sulphite treated tap water-IX	0.023	0.026
Sulphite treated tap water-X	0.047	0.045
Sulphite treated tap water-XI	0.035	0.039
Sulphite treated tap water-XII	0.049	0.051
Sulphite treated tap water-XIII	0.054	0.049
Sulphite treated tap water-XIV	0.015	0.017

*\*Samples were prepared by adding sodium sulphite to tap water.*

To test this technique further DO was analyzed in the steam generator feed waters of FBTR and MAPS. Samples were collected from the reactor site in the DO sampler. Immediately after sample collection the DO was fixed by adding  $MnSO_4$  followed by alkaline KI. Under this condition the samples were brought back to the laboratory, treated with sulphuric acid and titrated against thiosulphate solution. In all cases the time elapsed from fixing the DO at the sampling site to the completion of titration was less than 2 hours. Figure III.7 shows a typical high resolution titration plot of a sample containing 8.64 ppb of DO obtained from steam generator feed water of MAPS while Table III.4 shows the results obtained by this technique and by using standard electrochemical DO sensor.

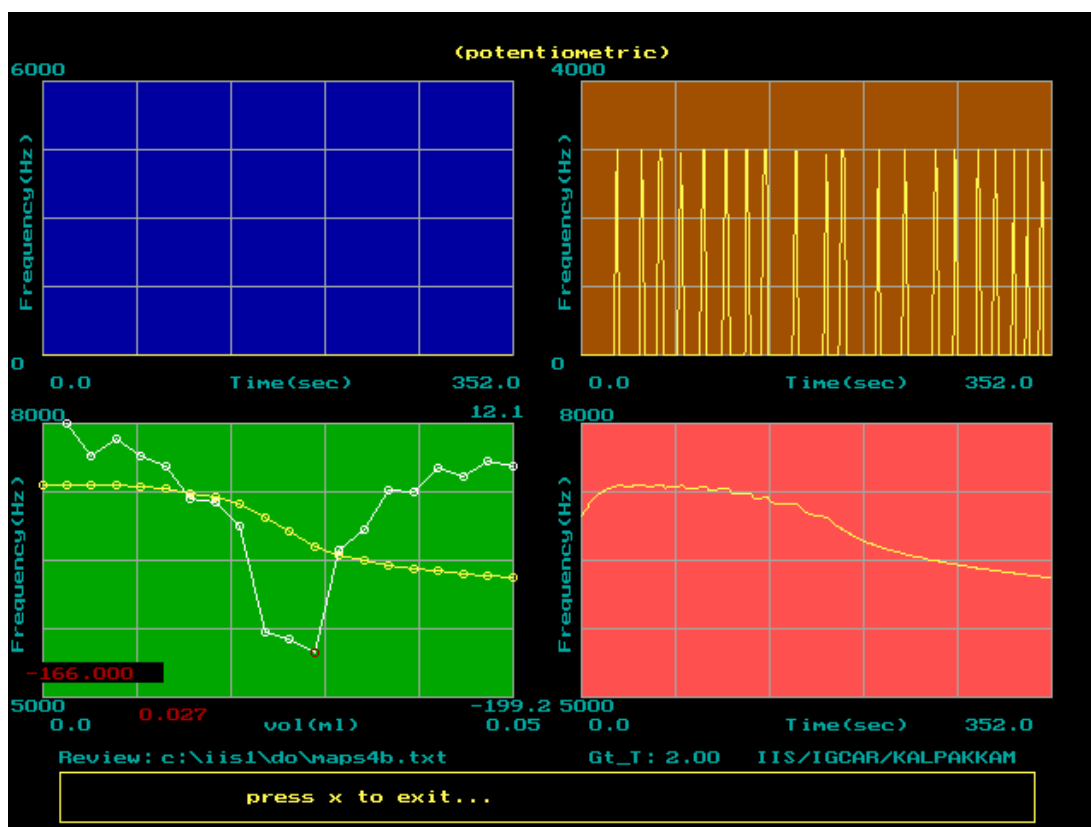


**Fig.III.7.** Titration of 25 mL of sample collected from steam generator feed water of MAPS against 0.001M sodium thiosulphate by manual addition of reagent. Sampling time is 2 seconds, end point is 0.027 mL and the volume corresponding to each aliquot of reagent addition is  $2.5\mu L$ . The DO present in the sample is 8.64 ppb.

**Table III.4.** Comparison of analytical results obtained using potentiometric titration technique with electrochemical DO meter.

Nature of sample	Using present technique (ppb DO)	By electrochemical meter (ppb DO)
FBTR sample-2	6	6
FBTR sample-3	9	9
FBTR sample-4	10	10
FBTR sample-5	13	12
FBTR sample-6	11	10
FBTR sample-7	9.5	8
MAPS sample-a	7	6.5
MAPS sample-b	10	11
MAPS sample-c	9	10
MAPS sample-d	11	11
MAPS sample-e	8	8
MAPS sample-f	9.5	8.5
FBTR sample (January 10)-c	11	12
FBTR sample (January 10)-d	12	10
FBTR sample (January 10)-e	9	7
FBTR sample (January 18)-a	9	8
FBTR sample (January 18)-b	8	7
FBTR sample (January 18)-c	9	7
FBTR sample (January 18)-d	8	9

*\*The samples were collected from the steam generator feed waters of FBTR and MAPS.*

Finally in order to examine the precision of measurements down to 10 ppb level a series of water samples collected from steam generator unit of FBTR were analyzed using the present technique. The results with respective precision in measurement of each sample are tabulated in Table III.5.

**Table III.5.** Precision in measurement of DO down to 10 ppb levels by potentiometric titration technique.

Description of sample	Concentration ppb(DO)
STGDO-1	9.7 ± 0.14 (n=5)
STGDO-2	9.7 ± 0.14 (n=5)
STGDO-3	9.0 ± 0.13 (n=5)
STGDO-4	10.1 ± 0.13 (n=5)
STGDO-5	10.1 ± 0.13 (n=4)
STGDO-6	9.7 ± 0.14 (n=5)
STGDO-7	10.0 ± 0.14 (n=4)
STGDO-8	9.0 ± 0.14 (n=5)
STGDO-9	9.6 ± 0.14 (n=5)
STGDO-10	9.0 ± 0.14 (n=4)
STGDO-11	10.0 ± 0.14 (n=4)
STGDO-12	8.0 ± 0.13 (n=5)
STGDO-13	8.0 ± 0.13 (n=5)
STGDO-14	8.2 ± 0.13 (n=4)
STGDO-15	8.0 ± 0.14 (n=5)
STGDO-16	8.2 ± 0.13 (n=5)

\* 25 mL aliquot of sample was taken for titration. 'n' refers to number of titrations for each sample.

### **3.4.5. Kinetic investigations**

Kinetic investigations were carried out to find out the acceptable time intervals between (i) fixing of DO in the sample and titration and (ii) between acidification and titration. Samples were acidified and titrated at the following time intervals after the formation of  $\text{MnO}(\text{OH})_2$  precipitate (after fixing DO): 5 minutes, 1 hour, 2 hours, 4 hours and overnight. It was observed that even if the sample was preserved overnight after addition of manganese sulphate and alkaline potassium iodide there was no change in DO content from the fresh sample. In order to evaluate the loss of iodine after acidification with sulphuric acid the acidified samples were titrated at various time intervals. It was found that there is a considerable loss of iodine (20%) if titrations were performed after 3 hours from acidification while there is no loss of iodine if titrations were performed within 2 hours from acidification. Hence from the study it is recommended not to preserve the sample beyond 8 hours after the addition of manganese sulphate and alkaline potassium iodide while it is preferable to titrate the sample soon after acidification.

### **3.5. Conclusion**

In this chapter a simple yet powerful titration technique has been described using which DO in water samples down to a few ppb levels could be measured. Perhaps for the first time such a simple technique has been used to determine DO at trace level. In the present work an in house developed DO sampler was used to collect samples directly from the source without the ingress of any air bubble. Use of such sampler gave representative samples for the offline analysis of DO at trace level. After chemical treatment the titration with display of online titration plot and quick processing of data to get information about the end point can be completed within a couple of minutes. The precision in measurement of DO in water at 10 ppb level is 0.14 (n=4), Relative Standard Deviation: 1.4%.

---

## 4. DETERMINATION OF TRACE BORON IN LIGHT WATER AND HEAVY WATER

---

### 4.1. Introduction

Boron is a metalloid and it is found only in low abundance in the earth's crust. It finds widespread use in different industries such as glass making [84], pharmaceutical [85], nuclear [86], fertilizer [87], and cosmetics [88]. In nuclear industry boron is used as neutron poison because of its high neutron absorption cross section. It is added to the moderators of Pressurized Heavy Water Reactor (PHWR) in the form of  $B_2O_3$ . Naturally occurring boron is made up of two stable isotopes namely  $B^{11}$  (80.1%) and  $B^{10}$  (19.9%). While  $B^{11}$  has a neutron absorption cross section of only 5 mbarns,  $B^{10}$  has a neutron absorption cross section of 3840 barns [89]. The high neutron absorption cross section of  $B^{10}$  makes  $B_2O_3$  as an excellent candidate for neutron poison. Apart from its use in the moderator it is also used in making reactor control rods which again acts as neutron poison. Such wide applications of boron compounds in the various fields mentioned above causes the surrounding water bodies to be contaminated with boron. Boron in water is mainly present as boric acid [90] and its concentration can go up to a few  $mgL^{-1}$  (ppm) levels in certain drinking water bodies. However the recommended concentration of boron in drinking water is below 0.5 ppm according to World Health Organization [91]. Therefore from safety point of view it becomes essential to monitor the concentration of boron in drinking water. Moreover in nuclear industry the concentration of boron in the moderator is monitored periodically for the smooth operation of PHWR.

There are various techniques available for the assay of boron at trace levels such as atomic absorption spectroscopy (AAS) [92], inductively coupled plasma atomic emission spectroscopy

(ICPAES) [93], isotope dilution-thermal ionization mass spectrometry (ID-TIMS) [94], inductively coupled plasma mass spectrometry (ICPMS) [95] ion chromatography [96], spectrophotometry [40,97], neutron activation analysis (NAA) [98,99], and flow injection analysis (FIA) [100,101]. Each of these techniques has its own limitations. AAS is a less sensitive and precise technique besides being susceptible to severe matrix interference. ID-TIMS, ICPEAS and ICPMS are extremely sensitive and precise techniques which are used for the trace determination of boron in a variety of matrices. None the less these instruments are extremely costly and therefore limited laboratories such as labs in nuclear facilities have access to them. Ion chromatography is yet another technique that finds routine application in nuclear facilities such as PHWR where determination of boron in the moderators is essential. During reactor operation boron in the moderator is maintained below  $30 \mu\text{gL}^{-1}$  (ppb) and ion chromatography is the technique of choice for such trace analysis. Apart from having low detection limit the technique is rapid and requires only a few micro liter of sample solution. Spectrophotometric techniques involving carminic acid and curcumin are very popular for the determination of boron. While carminic acid method is used when samples contain boron above 2ppm, curcumin method is used even if samples contain boron at ppb levels. Although carminic acid method is less sensitive as compared to curcumin method, it is much less laborious. Hence this technique is generally used for routine analysis of boron in quality control laboratories of PHWRs. However both the methods are time consuming as they require about 30 to 45 minutes for the color to develop. NAA is a nuclear analytical based technique that provides excellent sensitivity and precision. However the technique is accessible to very few laboratories where neutron irradiation source is available. Moreover the method is quite time consuming to be used for routine analysis in a plant. FIA using conductivity detector was reported by Kumar [100] for

the determination of boric acid in heavy water moderator samples. Though the authors have specified the range of analysis as 0 – 20 ppb, they have not worked out with light water or heavy water samples containing boron at ppb level which is required in PHWRs.

From the literature survey it is found that either the methods are sensitive but highly expensive or cost effective but time consuming and laborious. In this chapter a conductivity based approach which is cost effective, rapid and sensitive has been investigated. The chapter describes in detail the two different approaches that are followed for the determination of boron depending on the boron content in the sample. A conductometric titration approach is followed when the samples contain boron above 0.2 ppm and a direct conductivity approach is followed when samples contain boron less than 0.2 ppm and is relatively free from other impurities. The conductometric titration approach can be adopted for relatively pure samples as well as to samples containing specific impurities such as trace acid or alkali. This chapter describes the basic principle behind both the techniques, the nature of conductometric titration plots obtained in light water as well as in heavy water matrices and the impact of both interfering and non interfering impurities on the titration plot. Interfering impurities include trace quantities of acids and bases while non interfering impurities include common ionic salts like KCl. Further the influence of isotopic effect on the slope of calibration curves obtained in light water and heavy water matrices by the direct conductivity approach is also discussed. Probably for the first time a conductivity based approach for the assay of boron at trace level has been studied in depth in both light water and heavy water matrices.

## 4.2. Experimental

### 4.2.1. Materials and reagents

All the chemical reagents used in this work were of AR grade. Millipore water having conductivity  $< 1.0 \mu\text{S cm}^{-1}$  was used for preparing all the reagents and standard solutions.

#### 4.2.1.1. Preparation of boric acid solution

About 1.61g of boron trioxide ( $\text{B}_2\text{O}_3$ ) was dissolved in 500 mL of deionized water to give a 1000 ppm of boron stock solution. Boron trioxide when dissolved in water produces boric acid according to the following reaction



The resulting stock solution was standardized against sodium hydroxide. To 25 mL stock solution 2g of mannitol was added and titrated against 1.0M NaOH using phenolphthalein indicator. This standardized stock solution was used to prepare dilute working standards both at ppm and ppb levels through appropriate dilutions.

Similarly a boron stock solution was prepared in heavy water by dissolving 0.16g of  $\text{B}_2\text{O}_3$  in 50 mL  $\text{D}_2\text{O}$  to give  $\text{D}_3\text{BO}_3$ .



The resulting solution was standardized against NaOH and was used to prepare synthetic samples of boron in heavy water.

#### 4.2.1.2. Preparation of mannitol solution

A 20% (w/v) mannitol solution was prepared by dissolving 20g of mannitol in 100 mL of deionized water. The solution was used in direct conductivity measurement approach which is

recommended when samples contain boron less than 0.2ppm. For conductometric titrations a fixed quantity of solid mannitol was added to the sample before the start of titration.

#### **4.2.1.3. Preparation of standard NaOH solution**

A 1M sodium hydroxide solution was prepared and standardized against oxalic acid. Further dilute solutions were freshly prepared directly from this working standard using appropriate dilution.

#### **4.2.1.4. Reagents for interference study**

The following salt solutions from the respective salts were prepared for interference study: NaCl, KCl, LiCl, NaNO<sub>3</sub> and Na<sub>2</sub>SO<sub>4</sub>. Also appropriate concentrations of HCl and NH<sub>4</sub>OH were prepared from respective analytical reagent grade chemicals.

#### **4.2.1.5. Heavy water**

Heavy water used in this work was provided by Madras Atomic Power Station (MAPS) Kalpakkam, India. The heavy water had an isotopic purity above 99.5%.

#### **4.2.1.6. Conductometric titration facility**

The conductometric titration facility along with the graphical user interface described in sections 2.7 and 2.5 respectively were used to carry out the PC based titrations.

### **4.3. Methodology**

The PC based Conductometric titrations were carried out in Teflon cells containing a pair of stainless steel sensing electrodes embedded across the cell. In some cases titrations were carried out using Teflon beakers and a vertical type conductivity probe. The vertical probe has a pair of platinum electrodes fixed at the bottom which senses the solution conductivity. For carrying out a titration the sample was taken in the titration vessel and kept under mild stirring to bring the

solution to a homogeneous mixture. Before starting the titration the sample was flushed with argon for about 5 minutes. Flushing of argon before the start of titration and also during the titration is necessary to remove the dissolved carbon dioxide ( $\text{CO}_2$ ) from the sample. The presence of dissolved  $\text{CO}_2$  in the form of carbonic acid results in the excess consumption of sodium hydroxide during titration. Although the slope due to the reaction between carbonic acid and sodium hydroxide can be easily identified and accounted from the high resolution titration plot, it is still advisable to eliminate dissolved  $\text{CO}_2$  when analyzing boron at trace levels. After flushing the sample with argon for about 5 minutes solid mannitol was added to the sample in order to bring the mannitol concentration to 2% (w/v). The resulting solution was titrated against standardized sodium hydroxide solution in small aliquots. From the resulting end point the amount of boron in the sample was calculated.

In the direct conductivity approach 45 mL of sample was taken inside the Teflon conductivity probe. The sample was kept under mild stirring and was flushed with argon for about 5 minutes. Under this condition the sample conductivity was recorded continuously through the PC. Typically the average of 15 stable values was taken in order to obtain the background conductivity of the sample ( $k_1$ ). 5mL of 20% (w/v) mannitol was introduced to the conductivity cell which caused the solution conductivity to increase as a result of the reaction between boron and mannitol. The resulting average conductivity ( $k_2$ ) was noted and the flow of argon inside the sample was discontinued. From the shift in conductivity ( $k_2-k_1$ ) the amount of boron in the sample was obtained using the pre-established polynomial relationship between shift in conductivity and boron concentration.

## 4.4. Results and discussion

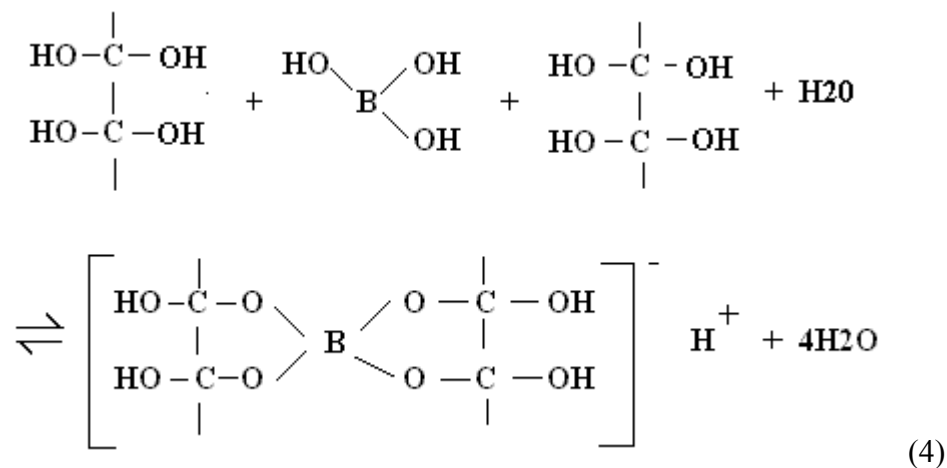
### 4.4.1. Principle

#### 4.4.1.1. Conductometric titration technique

This technique is adopted when samples contain boron above 0.2 ppm. Boron in aqueous solution mainly exists as boric acid due to its large  $pK_a$  value (8.98) [102].



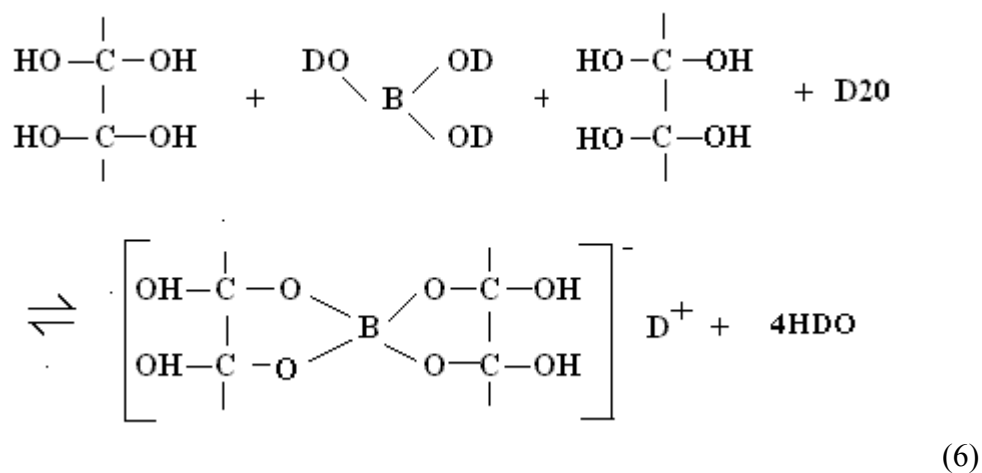
As a result it has insignificant conductivity in aqueous solution. However, the problem can be circumvented by adding mannitol to the sample prior to titration. Mannitol is a polyhydroxy alcohol which combines with boric acid to form an ester. The resulting boron mannitol compound has a  $pK_a$  value lower than boric acid [102,103] and its conducting power increases to some extent as compared to boric acid. The reaction between mannitol and boric acid is shown below



In the above reaction two molecules of mannitol react with one molecule of boric acid to give a boron mannitol complex. For the sake of brevity the boron mannitol complex is represented as HX and the corresponding equilibrium is shown below



A similar set of equations can be readily derived in heavy water matrix



#### 4.4.1.2. Direct Conductivity approach

This technique is adopted when samples contain boron at trace levels (< 200 ppb). A fixed concentration of mannitol is added to the sample and the resulting shift in conductivity before and after the addition of mannitol is monitored. The increase in conductivity is due to the generation of either  $\text{H}^+$  or  $\text{D}^+$  ions depending on the sample matrix (refer equation 5 and 7). From the resulting shift in conductivity the concentration of boron is calculated using the pre-established polynomial relationship between the two variables in the particular matrix (either  $\text{H}_2\text{O}$  or  $\text{D}_2\text{O}$ ) under consideration.

## 4.4.2. Conductometric titration approach for the assay of boron

### 4.4.2.1. Titration plots in light water matrix

Figure IV.1 shows a typical titration plot obtained by titrating 0.1 ppm of boron in light water against sodium hydroxide using the methodology described in section 4.3. The plot shows three distinct regions which can be accounted by considering the equilibrium represented in equation 5.

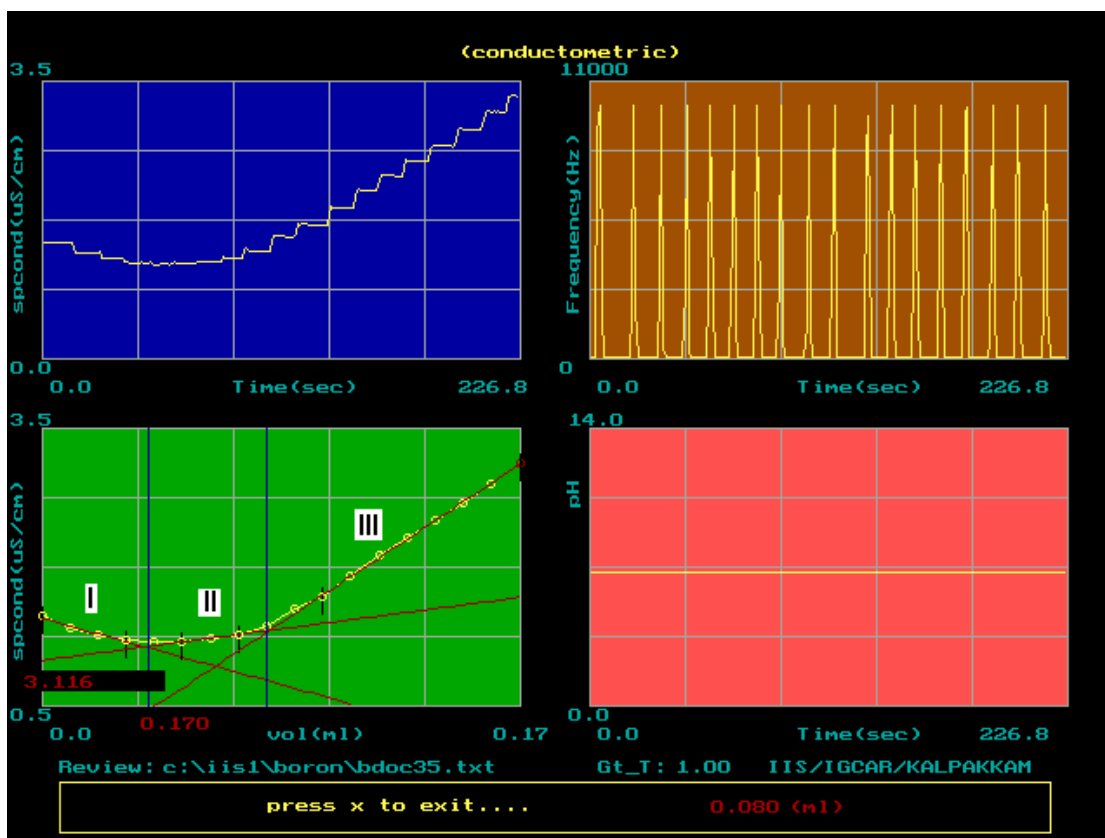


**Fig.IV.1.** Titration plot of 50mL of 0.1 ppm boron in light water against sodium hydroxide. To 50mL sample 1g of mannitol was added and titrated against 0.005N NaOH in 10 micro liter steps. Argon was flushed to avoid interference from dissolved carbon dioxide. The end point occurs at 0.08 mL which corresponds to a boron concentration of 0.086 ppm.

The first region, showing a negative slope, is obtained due to the replacement of highly conducting  $H^+$  ions in the dissociated form by the less conducting  $Na^+$  ions



The second region is obtained due to the replacement of HX molecule with  $\text{Na}^+$  and  $\text{X}^-$  ions



HX molecule being un-dissociated does not contribute to the solution conductivity whereas the replaced ions ( $\text{Na}^+$  and  $\text{X}^-$ ) make a small positive contribution. This results in a positive slope as reflected in region II. Region II continues till all the HX gets exhausted after which there is a steep rise in conductivity due to the accumulation of excess titrant ( $\text{Na}^+$  and  $\text{OH}^-$ ) in the reaction vessel. This is reflected in region III.

#### 4.4.2.2. Titration plots in heavy water matrix

Figure IV.2. shows a typical titration plot obtained in heavy water by following the methodology described in section 4.3. Compared to the titration plot obtained in light water matrix the plot shows only two regions. The region showing the initial decrease in conductivity (refer region I of Figure IV.1) is missing in the present case. This is due to the fact that the equilibrium involved in heavy water matrix (refer equation 7) lies predominantly to the left hand side of the equation. This causes DX as the majority species available for reaction as shown below



In the above reaction a non-conducting DX molecule is replaced by two conducting ions namely  $\text{Na}^+$  and  $\text{X}^-$ . This results in a positive shift in conductivity and the same is reflected in region I of the titration plot. After crossing the end point the conductivity increases sharply as excess titrant ( $\text{Na}^+$  and  $\text{OH}^-$ ) starts accumulating in the titration vessel. This is reflected in region II.

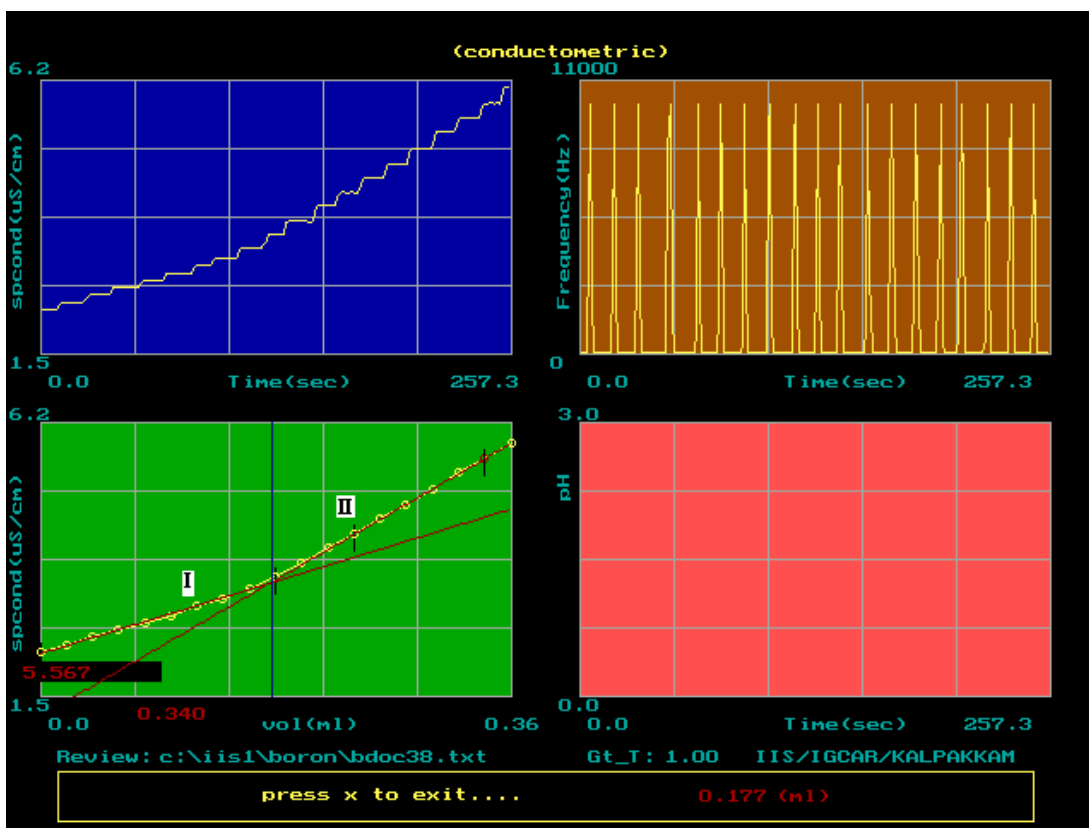


**Fig.IV.2.** Titration plot of 50mL of 0.2 ppm boron in heavy water against NaOH. To 50mL sample 1g of mannitol was added and titrated against 0.005N NaOH in 20 micro liter steps. Argon was flushed to avoid interference from dissolved carbon dioxide. The end point (0.177 mL) corresponds to a boron concentration of 0.19 ppm.

#### 4.4.2.3. Performance evaluation of titration approach

In order to access the performance of conductometric titration approach a large number of titrations were carried out in both light water as well as in heavy water matrices. Synthetic samples spiked with boron in the range of 0.2 ppm to a few ppm were analyzed using this technique. Parallely the samples were also analyzed by standard curcumin method [39]. The results of the study are shown in Table IV.1. From the table it seen that the method provides excellent accuracy and reproducibility not only at ppm levels but also at sub ppm levels. Further

the titration approach is much less laborious and rapid as compared to standard curcumin or carminic acid spectrophotometric methods.

**Table IV.1.** Recovery of boron by conductometric titration approach and by spectrophotometric approach.

Sample	Boron sought (ppm)	Matrix used	Boron recovered by titration approach (ppm)	Boron recovered by spectrophotometric approach (ppm)
S-1	0.75	Light water	$0.75 \pm 0.02$	$0.74 \pm 0.03$
		Heavy water	$0.74 \pm 0.02$	$0.76 \pm 0.02$
S-2	1.5	Light water	$1.52 \pm 0.03$	$1.49 \pm 0.03$
		Heavy water	$1.51 \pm 0.03$	$1.48 \pm 0.05$
S-3	0.25	Light water	$0.25 \pm 0.01$	$0.26 \pm 0.02$
		Heavy water	$0.27 \pm 0.01$	$0.26 \pm 0.02$
S-4	2.5	Light water	$2.53 \pm 0.04$	$2.51 \pm 0.05$
		Heavy water	$2.45 \pm 0.05$	$2.42 \pm 0.06$
S-5	0.21	Light water	$0.22 \pm 0.01$	$0.24 \pm 0.02$
		Heavy water	$0.20 \pm 0.02$	$0.22 \pm 0.02$
S-6	0.5	Light water	$0.49 \pm 0.01$	$0.50 \pm 0.02$
		Heavy water	$0.48 \pm 0.01$	$0.51 \pm 0.02$
S-7	2.2	Light water	$2.33 \pm 0.03$	$2.25 \pm 0.04$
		Heavy water	$2.30 \pm 0.04$	$2.28 \pm 0.06$
S-8	1.6	Light water	$1.62 \pm 0.02$	$1.57 \pm 0.03$
		Heavy water	$1.57 \pm 0.03$	$1.54 \pm 0.04$
S-9	2.0	Light water	$1.93 \pm 0.04$	$1.95 \pm 0.04$
		Heavy water	$1.85 \pm 0.03$	$1.80 \pm 0.06$
S-10	1.0	Light water	$1.05 \pm 0.02$	$0.97 \pm 0.03$
		Heavy water	$1.0 \pm 0.01$	$0.91 \pm 0.035$
S-11	1.5	Light water	$1.49 \pm 0.03$	$1.50 \pm 0.04$
		Heavy water	$1.47 \pm 0.02$	$1.55 \pm 0.05$

#### 4.4.2.4. Effect of non reacting impurities on titration plots

Although the presence of non-reacting impurities increases the overall conductivity of the solution, they do not take part in the reaction between boron mannitol complex and sodium hydroxide. The following are the list of non reacting salts used in the current work: KCl, NaCl, LiCl, NaNO<sub>3</sub> and Na<sub>2</sub>SO<sub>4</sub>. Each individual salt solution was added to the sample at different concentration levels ranging from 50 ppm to 500 ppm. From the study it was found that the titration plot of a pure boron sample and that of a plot obtained in the presence of a non interfering salt look similar. Moreover it was found that concentration levels up to 500ppm of each individual salt can be tolerated when titrating samples containing 1ppm of boron. It was observed that in some cases there is a difference of 4-5% in the results which can be minimized by reducing the aliquot volume of reagent addition during titration. From the study it was established that boron can be quantified in the presence of elevated background conductivities provided a high resolution conductivity probe is used for carrying out the titrations. Table IV.2 shows the recovery of 1ppm of boron in the presence of 500 ppm of each individual non interfering impurity.

**Table IV.2.** Recovery of boron in the presence of non interfering impurities.

Sl.no	Boron sought (ppm)	Boron found (ppm)	Nature of impurity at a level of 500 ppm
1.	1.0	1.05	KCl
2.	1.0	0.96	LiCl
3.	1.0	1.04	NaNO <sub>3</sub>
4.	1.0	1.0	NaCl
5.	1.0	0.96	Na <sub>2</sub> SO <sub>4</sub>

#### 4.4.2.5. Effect of reacting impurities on titration plots

In nuclear fuel samples boron is present as trace impurity and it is separated from the sample matrix by pyrohydrolytic distillation. During distillation small quantities of F, N and Cl are likely to enter the condensate and make the sample either acidic or basic. However the current technique permits the assay of boron in pyrohydrolytic distillates by slightly modifying the procedure as discussed below.

The end points of a titration plot obtained in the presence of acidic or basic impurities tend to differ from the end points obtained without the presence of these impurities. The presence of an acidic impurity causes the sample to consume more NaOH for neutralization while the presence of a basic impurity causes the sample to consume less NaOH. Therefore acidic impurities give rise to positive errors while basic impurities give rise to negative errors. Figure IV.3. shows a plot obtained by titrating 1ppm of boron in the presence of trace HCl. The titration plot shows three distinct regions which can be explained with the help of equation 5. The presence of HCl causes the equilibrium to shift to the left hand side and thus suppressing the dissociation of HX complex. As a consequence all the boron in the sample remains as un-dissociated boron mannitol complex.

The first region in the titration plot is obtained due to the replacement of highly conducting  $H^+$  ions by less conducting  $Na^+$  ions. The  $H^+$  ions participating in the reaction are derived from the trace HCl which was added as impurity. The second region is obtained due to the replacement of un-dissociated HX complex with  $Na^+$  and  $X^-$  ions. As all the boron in the sample is present as HX this region alone represents the total boron content in the sample and consequently the volume corresponding to this region is taken for quantifying boron. Finally the third region in the titration plot is obtained due to the excess accumulation of titrant after the end point.

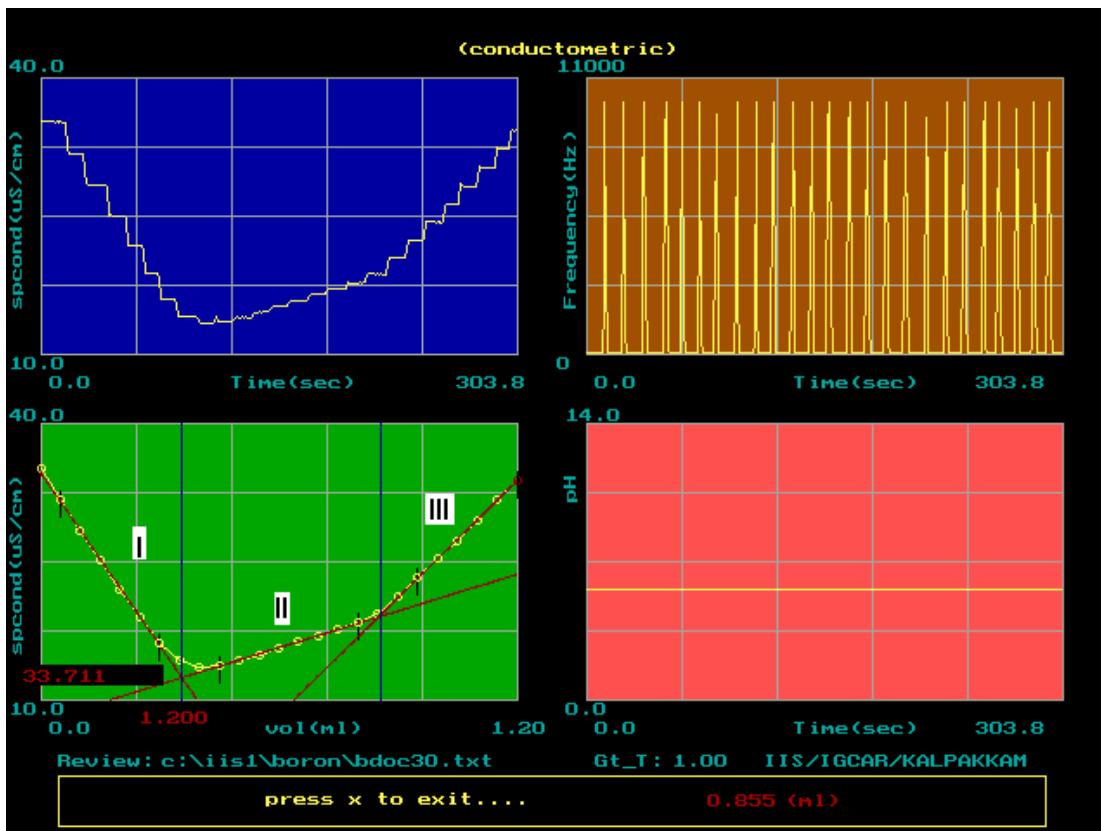


**Fig. IV.3.** Titration plot of 25mL of 1 ppm boron in light water containing trace hydrochloric acid against sodium hydroxide. To 25mL sample 0.5g of mannitol was added and titrated against 0.005N NaOH in 50 micro liter steps. Argon was flushed to avoid interference from dissolved carbon dioxide. The titration end points are 0.36 mL and 0.86 mL. The boron content in the sample is 1.08 ppm as against 1ppm.

Unlike acidic impurities the presence of basic impurities reduces the titrant consumption. In the present study ammonium hydroxide was chosen as the interfering impurity. As ammonium hydroxide is basic it destroys a part of boron mannitol complex according to the following reaction.



However the lost HX can be recovered by adding a small excess of strong acid before carrying out the titration. The introduction of strong acid retrieves the lost HX as shown below



The addition of strong acid not only retrieves the lost HX but also makes the sample acidic due to the accumulation of excess acid. As a consequence the conductometric titration plot of a sample containing basic impurity that has been acidified with a strong acid looks similar to the plot obtained when titrating a sample initially containing trace acidic impurity (refer Figure IV.3).

#### **4.4.3. Direct conductivity approach for the assay of boron**

In direct conductivity approach the shift in conductivity of the sample before and after the addition of mannitol is monitored. Table IV.3 shows the shift in conductivity obtained in light water as well as in heavy water matrices. It is observed that the shift in frequency per unit change in boron concentration is considerably less in heavy water matrix as compared to light water matrix. A change in boron concentration by 20 ppb from the blank level results in a frequency shift of 19 Hz in heavy water matrix as against 109 Hz in light water matrix. Such a difference is attributed to isotopic effect. The ionic mobility of heavier  $\text{D}^+$  isotope is much less as compared to that of the lighter  $\text{H}^+$  isotope and hence there is a considerable difference in frequency shifts in the two matrices. However the use of high resolution conductivity measurement device allowed capturing the small shift in specific conductance due to the presence of trace boric acid mannitol complex in heavy water.

**Table IV.3.** Shift in pulse frequency in heavy water – mannitol and light water – mannitol mixtures with step-wise addition of boric acid at ppb levels.

Sample	Concentration of boron, ppb	Measured frequency, Hz	Frequency shift from blank, Hz
Heavy water + Mannitol (45 mL+5 mL 20% w/v)	0	6158.9 ± 0.6	0
	20	6177.8 ± 0.53	18.9
	40	6201.5 ± 0.51	42.6
	60	6228.9 ± 0.49	70
	79.9	6258.7 ± 0.44	99.8
	99.9	6289.8 ± 0.47	130.9
	119.9	6322.1 ± 0.35	163.2
	139.8	6356.1 ± 0.33	197.2
	159.7	6390.3 ± 0.47	231.4
	179.7	6425.5 ± 0.51	266.6
199.6	6461.3 ± 0.46	302.4	
Light water + Mannitol (45 mL+5 mL 20% w/v)	0	3608.9 ± 0.37	0
	10	3665.2 ± 0.91	56.3
	20.0	3717.7 ± 0.73	108.8
	29.9	3767.3 ± 0.88	158.4
	39.8	3815.7 ± 1.0	206.8
	49.8	3862.7 ± 0.98	253.8
	59.6	3911.4 ± 1.05	302.5
	79.4	4004.3 ± 1.23	395.4
	99.0	4094.1 ± 1.27	485.2

*\*In each case, standard deviation is determined from 15 data points collected at 2sec sampling time during measurement (n = 15).*

From Table IV.3 it is seen that the shift in frequency shows a smooth increasing trend with increasing boron concentration in both the matrices. The calibration plot between shift in pulse frequency from blank sample and concentration of boron in light water is shown in Figure IV.4. This relationship was established using the data presented in Table IV.3. Similarly Figure IV.5 shows the calibration plot between shift in frequency and concentration of boron in heavy water matrix.

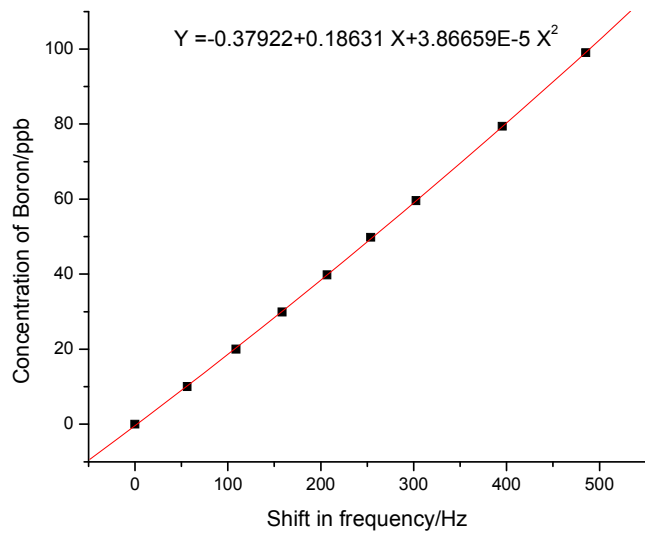


**Fig.IV.4.** Calibration plot between shift in frequency and concentration of boron in light water matrix.

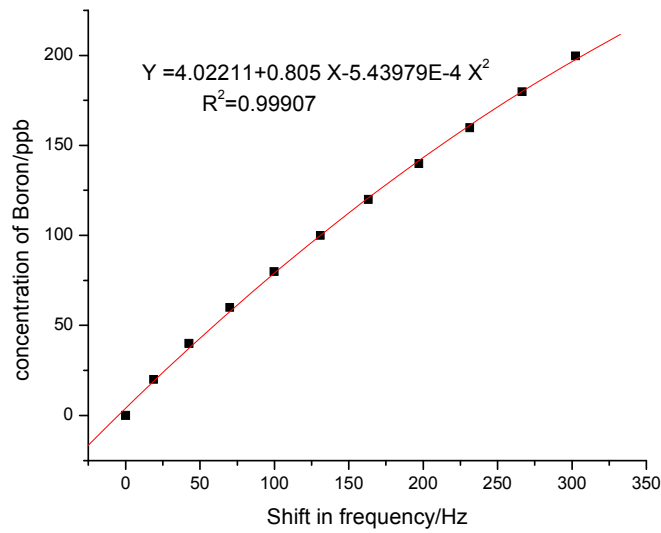


**Fig.IV.5.** Calibration plot between shift in frequency and concentration of boron in heavy water matrix.

#### 4.4.3.1. Performance evaluation of direct conductivity approach

The performance of direct conductivity based approach was evaluated by recovering boron from synthetic light water and heavy water samples. Boron in these samples were spiked in the range of 20- 100 ppb and were analyzed by both direct conductivity approach and by ion chromatography. The results of the study are given in Table IV.4. From the results it is seen that the direct conductivity approach compares well with a well established technique like ion chromatography.

**Table IV.4.** Assay of boron in synthetic samples by direct conductivity approach and by ion chromatography.

Sample	Boron sought (ppb)	Matrix used	Boron recovered by direct conductivity approach (ppb)	Boron recovered by ion chromatography approach (ppb)
S-1	25	Light water	27.2 ± 0.90	26.6 ± 0.62
S-2	90	Light water	88.9 ± 2.28	88.1 ± 1.93
S-3	50	Light water	53.2 ± 1.30	48.7 ± 1.70
S-4	20	Light water	18.6 ± 0.76	18.7 ± 0.63
S-5	30	Heavy water	28.7 ± 0.69	29.1 ± 0.64
S-6	85	Heavy water	83.7 ± 2.42	84.1 ± 1.84

*\*Each experiment was repeated three times (n=3)*

#### 4.5. Analysis of MAPS moderator samples

After obtaining highly satisfactory results on synthetic samples by both titration approach (refer 4.4.2.3) as well as by direct conductivity approach (refer 4.4.3.1), boron was analyzed in the

moderator samples collected from MAPS reactor. Boron is added to the heavy water moderator at ppm levels during the reactor startup in order to suppress the excess reactivity of fresh fuel and also to compensate for the xenon built. It is slowly recovered by passing the moderator through ion exchange beds and its concentration is maintained around 20-30 ppb during the reactor operation. In the present study heavy water samples were collected during reactor startup as well as during reactor operation. Conductometric titration approach was followed to analyze samples collected during reactor startup while the direct conductivity approach was followed to analyze samples collected during reactor operation. Table IV.5 summarizes the results obtained using the proposed techniques as against the standard techniques.

**Table IV.5.** Assay of boron in heavy water samples collected from the moderator system of a PHWR.

Sample identification	Concentration of boron			
	Present technique		Spectrophotometric (in ppm)	Ion chromatography (in ppb)
	App-A (in ppb)	App-B (in ppm)		
MAP-OP-1	20.1 ± 0.6	-	-	18.8 ± 0.7
MAP-OP-1	20.0 ± 0.64	-	-	19.9 ± 0.7
MAP-OP-1	19.8 ± 0.62	-	-	20.3 ± 0.64
MAP-OP-1	21.7 ± 0.58	-	-	20.8 ± 0.7
MAP-OP-1	24.5 ± 0.66	-	-	25.0 ± 0.7
MAP-OP-1	24.3 ± 0.61	-	-	25.1 ± 0.73
MAP-ST-1	-	1.03 ± 0.02	1.06 ± 0.03	-
MAP-ST-1	-	0.78 ± 0.01	0.65 ± 0.015	-
MAP-ST-1	-	1.2 ± 0.025	1.2 ± 0.02	-
MAP-ST-1	-	0.55 ± 0.01	0.51 ± 0.014	-
MAP-ST-1	-	0.55 ± 0.01	0.54 ± 0.015	-

\*MAP-OP-Heavy water samples collected during normal operation period of the reactor.

MAP-ST-Heavy water samples collected during start-up of the reactor.

The uncertainty in measurement is determined in three aliquots of each sample (n=3).

App –A refers to direct conductivity approach.

App-B refers to conductometric titration approach.

#### 4.6. Conclusion

In this chapter two simple and rapid conductivity based approaches have been presented for the assay of boron at trace level. Using the titration approach the final result can be obtained in a

couple of minutes. Moreover this technique can be applied in the presence of trace acidic or basic impurities. Probably this is the only titration technique for the assay of boron in water samples at sub-ppm levels. The present titration technique has been successfully examined for the determination of boron in water and heavy water samples at ppm and sub ppm levels. The precision in measurement was found to be 1.0% relative standard deviation at 1 ppm boron level. In addition to the high resolution titrimetric technique, a direct conductivity monitoring approach with a high resolution conductivity meter has been proposed for rapid assay of boron in heavy water down to a few ppb levels in the context of rapid assay of boron in moderator system of PHWRs. The precision in measurement using this technique was found to be 4.1% relative standard deviation at 20 ppb boron level.

---

## 5. DETERMINATION OF ISOTOPIC PURITY OF HEAVY WATER IN MIXTURES OF LIGHT WATER AND HEAVY WATER BY CONDUCTIVITY APPROACH

---

### 5.1. Introduction

Heavy water is used as a moderator as well as a coolant in Pressurized Heavy Water Reactors (PHWRs) [104]. As a moderator it is used in slowing down fast neutrons whereas as a coolant it is used to carry away the heat generated during fission reaction. In order to use heavy water as a moderator an isotopic purity in excess of 99.75% is required [105]. Similarly an isotopic purity above 98% is required for its use as a coolant. As the source of heavy water is natural water which contains around 150 ppm of heavy water [105], it becomes necessary to enrich natural water before it becomes acceptable for nuclear application. The enrichment is achieved in heavy water production plants which run on chemical exchange processes [106]. In India such plants are located at Manuguru, Kota, Tutucorin, Baroda, Hazira, Thal and Talcher. Prior to the setting up of these plants India used to import heavy water in order to meet its nuclear demand. But now India has become self sufficient in heavy water production and is exporting heavy water to other countries.

In the quality control laboratories attached to these heavy water production plants it becomes mandatory to periodically monitor the percentage enrichment of heavy water at every stage of production. Moreover in PHWRs too there is a necessity to monitor the percentage purity of coolant as there is chance of mixing of the coolant with light water during the steam generation process. Unfortunately there is no single method which can be used to determine the percentage enrichment from few  $\text{mgL}^{-1}$  (ppm) to levels exceeding 99.8%. Infra red (IR) spectroscopy [43,44,45,46] is the method of choice if the heavy water content is either above 88% or less than

9%. The method is less often used in the intermediate ranges as the accuracy and precision deteriorates in comparison to the extreme ranges. Mass spectrometry is routinely used for analysis of heavy water at a few ppm levels [107,108]. Although the technique produces excellent result a skilled person is required to operate the instrument. Also the technique suffers from memory effect which is caused by the contamination of previous sample on to the current sample [109]. The effect becomes especially pronounced if the previous sample happens to be more concentrated than the current sample being analyzed. Density measurement using high sensitive density meter [110] or using techniques such as pykometry, float method, drop method is used for the assay of heavy water in the intermediate ranges. The method is not only labor intensive but also time consuming for routine applications. Compared to density measurement techniques refractive index technique [47,48,49] is much simpler and is widely used in the intermediate ranges. Although the method is capable of covering the entire range from 0-100% the method produces less accurate results at low and high ranges. Gas chromatography using thermal conductivity detector is yet another method whose application is limited to certain range only (upto 15%). Even though the method is suitable in this range the method is not rapid enough for routine analysis.

From the above brief introduction it is clear that conductivity based approach has not yet been attempted previously for the isotopic assay of heavy water and that no single method covers a wide range. In this chapter a novel PC based pulsating type conductivity measurement approach has been investigated in detail for analyzing the percentage composition of heavy water in mixtures of light water and heavy water. In this technique a specific weak acid of fixed concentration is produced in mixtures of light water and heavy water taken in different ratios. The shift in conductivity before and after the generation of the weak acid is monitored accurately

using an in house built pulsating type conductivity meter. The shift in conductivity is then related to the percentage of heavy water in the sample using a suitable polynomial relation. This chapter describes in detail the principle of the method, the choice of weak acid selected for investigation, role of temperature on conductivity measurement, circumventing the effect of temperature and the use of in-house made mini conductivity cells to measure conductivities with low sample volumes. Though the present technique is a destructive, it requires only 1ml of sample for each analysis and covers a wide range of heavy water percentage in the sample mixtures from 1% to 99%.

## **5.2. Experimental**

### **5.2.1. Materials and reagents**

All chemicals used in the work are of AR grade or GR grade. Millipore water with conductivity less than  $1\mu\text{Scm}^{-1}$  was used throughout the work.

#### **5.2.1.1. Boron Stock solution**

A 1000 ppm boron stock solution was prepared by dissolving about 1.65g of boron trioxide in 500mL of distilled water. The resulting solution was standardized against a freshly prepared and standardized sodium hydroxide using phenolphthalein indicator.

#### **5.2.1.2. Heavy water**

Heavy water was obtained from Madras Atomic Power Station (MAPS) Kalpakkam. The heavy water sample was found to have an isotopic purity of 99.68% (w/w) using infrared spectroscopic technique.

### **5.2.1.3. 20% w/v mannitol solution**

25mL of 20% w/v solution of mannitol was prepared by dissolving 5g of mannitol in 25mL deionized water. The solution was always freshly prepared before the start of each campaign.

### **5.2.1.4. Constant temperature bath**

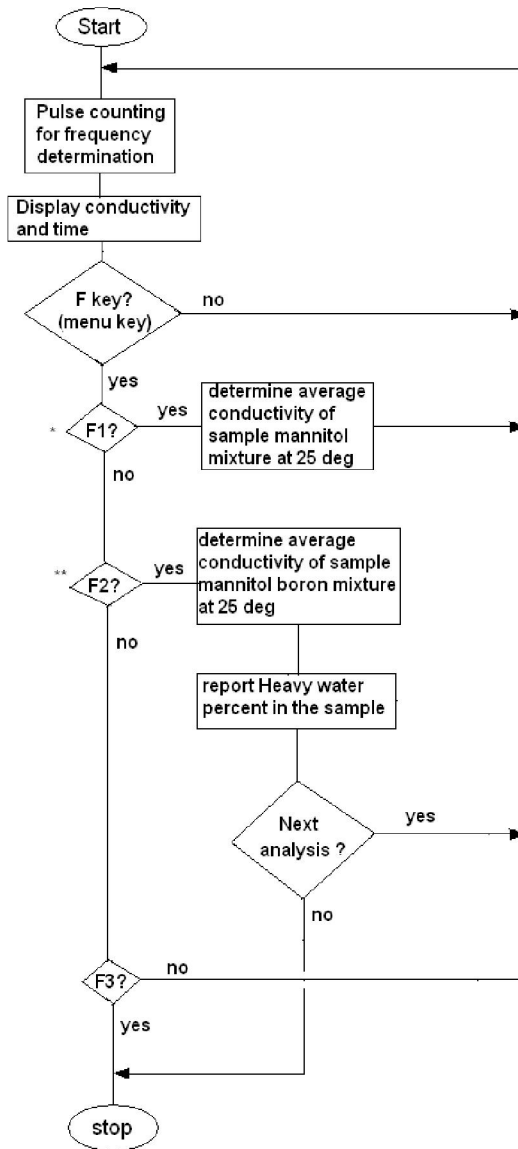
A Thermo make, Hakke DC 10, constant temperature bath was used to take conductivity measurements at a constant temperature of 25 °C. The bath maintains the temperature with an accuracy of  $\pm 0.1$  °C.

### **5.2.1.5. Pulsating conductivity meters**

In the present work three different conductivity probes having different geometries were used. All the probes were made of Teflon and a pair of SS rods acted as sensing electrodes. The probes were calibrated by following the multipoint KCl approach described earlier in section 2.3.2 of chapter 2. In the first phase of work a conductivity probe requiring 50mL of sample volume was used to measure the solution conductivities. The sensing electrodes were 1mm thick, 30 mm in length and were separated by a distance of 4mm. In the next phase of work a conductivity probe requiring 5ml of sample volume was used. The sensing electrodes were 1.6mm thick, 20 mm in length and were separated by a distance of 7mm. In the final stage of work a miniaturized conductivity cell requiring only 1ml of sample volume was used. The electrode geometry of this miniaturized probe is as follows; 2.5mm thick, 14.4 mm in length and having an electrode separation of 1.5mm. In all cases appropriate care was taken to provide good insulation to the electrodes projecting outside the Teflon cells (i.e., not in contact with the test solution) in order to avoid shorting when placed inside a constant temperature bath.

### 5.3. Graphical User Interface

An in-house developed graphical user interface (GUI) in C language was used to carry out the PC based measurements. Figure V.1 shows the flowchart of the interactive GUI.



- \* F1: The key to be operated after mannitol addition to sample and ensuring proper mixing
- \*\* F2: The key to be operated after boric acid addition to sample and ensuring proper mixing

**Fig.V.1.** Flow chart of the graphical user interface developed in C language.

The GUI determines the frequency obtained from the conductivity meter and converts it to the corresponding conductivity value using the pre established and pre loaded polynomial relationship between frequency and conductivity. Typically the GUI takes the average of fifty stable conductivity readings before prompting the user to proceed with the next stage of reagent addition. After the addition of all the reagents the GUI tabulates a list of conductivity values obtained before and after the addition of each reagent. From the tabulated list the shift in conductivity due to the generation of fixed quantity of boron mannitol complex is determined. Using this data and the preloaded polynomial relationship between shift in conductivity and percentage composition of heavy water, the GUI computes and displays the final result.

#### **5.4. Methodology**

Figure V.2 shows the schematic diagram of the entire experimental set up used in the determination of isotopic purity of heavy water. 1mL of sample containing light water and heavy water mixture was taken in a specially designed miniaturized conductivity cell. The cell was placed in a constant temperature bath maintained at 25°C. To the sample appropriate amount of boric acid followed by mannitol was added in order to bring the overall concentration of boron and mannitol to 10 ppm and 2% w/v respectively. After each reagent addition the solution was mixed homogenously and the cell was transferred back to the temperature bath. The stable conductivity values before and after the addition of each reagent was recorded by the GUI. From the resulting shift in conductivity due to the generation of boron mannitol complex the percentage heavy water in the sample was determined by the GUI using the pre established relationship existing between the two variables.

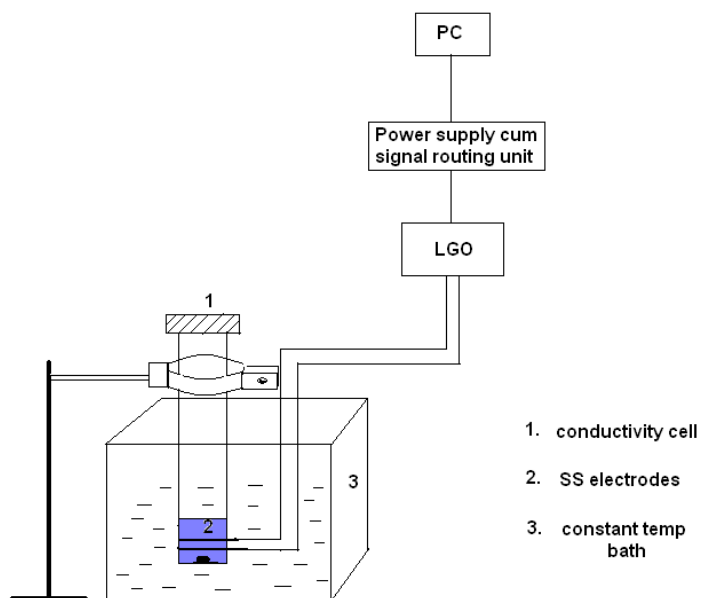


**Fig.V.2.** Schematic diagram of the experimental set up used for the assay of isotopic purity of heavy water.

## 5.5. Results and discussion

### 5.5.1. Principle

In this method a fixed concentration of a weak acid is generated in the sample containing a mixture of light water and heavy water. The resulting change in conductivity of the sample before and after the generation of the weak acid is measured accurately. As light water and heavy water are isotopically different the mobility and also the dissociation of the weak acid in the two media will be different. This leads to a gradual decrease in conductivity of weak acid in light water and heavy water mixtures with a gradual increase in heavy water content in the sample. Thus the conductivity shift in the sample before and after the generation of weak acid is a measure of isotopic purity of heavy water in the sample.

### **5.5.2. Choice of reaction**

The choice of ion pair should be such that it does not appear as a common impurity in the sample. Moreover it should preferably be somewhat weakly dissociating so that the additional effect of isotopic media on the dissociation equilibria adds to the overall isotopic effect. In the present study boron-mannitol complex with hydrogen as counter ion was selected to monitor the shift in conductivities in the sample solution. The ion pair is generated by adding fixed quantities of boric acid followed by mannitol to the sample. Boron mainly exists as boric acid in aqueous medium due to the extremely large pKa value of boric acid (8.98) [102]. As a consequence the presence of boric acid in a sample shows negligible effect on the sample conductivity. However the addition of mannitol to the sample transforms the weakly conducting acid to a relatively stronger acid by the formation of boron mannitol complex and thereby increasing the solution conductivity.

### **5.5.3. Scoping study on the feasibility of conductivity approach**

In order to realize the concept initial experiments were conducted by taking 50mL of sample volume for each analysis. Accordingly a suitable Teflon cell described in section 5.2.1.5 was used. Synthetic samples of D<sub>2</sub>O-H<sub>2</sub>O mixture containing D<sub>2</sub>O in the following (v/v) percentages 0, 10, 20, 30, 40, 50, 60, 70, 80, 90 were taken as calibration standards while restricting the final sample volume to 50 mL in each case. The sample was taken in the conductivity cell and was kept under mild stirring to bring the solution to homogeneous mixture. To each heavy water standard appropriate amount of boric acid followed by mannitol was added in order to bring the overall concentration of boron and mannitol to 10 ppm and 2% w/v respectively. The resulting shift in conductivity due to the generation of boron mannitol complex was noted. Table V.1

shows the measured specific conductances before and after the complexation for each composition.

**Table V.1.** Shift in conductivity due to the formation of boron mannitol complex with increasing concentration of D<sub>2</sub>O in the sample.

%D <sub>2</sub> O (v/v)in H <sub>2</sub> O-D <sub>2</sub> O mixture	Specific conductance ( $\mu\text{S cm}^{-1}$ )		$\Delta k$ ( $\mu\text{S cm}^{-1}$ )
	After mannitol addition	After boric acid addition	
0	2.56	9.46	6.90
9.0	2.37	8.81	6.44
18.0	2.19	8.07	5.88
27.0	2.15	7.36	5.21
36.0	2.09	6.76	4.66
45.0	1.99	6.35	4.36
54.1	1.93	5.98	4.05
63.1	1.82	5.51	3.69
72.1	2.11	5.40	3.30
81.1	1.81	4.92	3.11
90.1	1.62	4.47	2.85

\*Volume taken for each analysis is 50 mL.

Sample conductivities measured at solution temperature.

From the table it is seen that there is a gradual decrease in ‘conductivity shifts’ with increasing percentage of heavy water in the sample. Using a suitable software package a polynomial relationship was established between shift in conductivity and percentage heavy water in the sample. Figure V.3 shows the calibration plot along with the following third degree polynomial relationship existing between the two variables

$$y = 6.97111 - 0.0717 * x + 3.2444e-4 * x^2 - 3.81292e-7 * x^3 \quad (1)$$

Where y is the shift in conductivity in  $\mu\text{Scm}^{-1}$  and x is the volume percent  $\text{D}_2\text{O}$ .

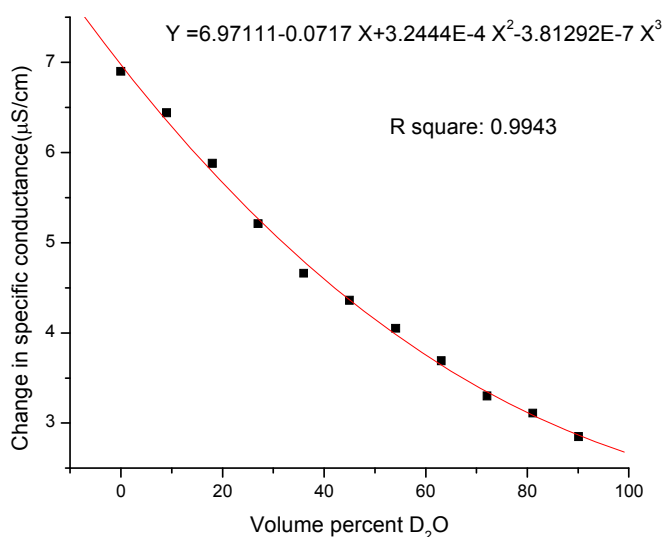


**Fig.V.3.** Shift in specific conductance on complexation as a function of  $\text{D}_2\text{O}$  content in  $\text{H}_2\text{O}$ - $\text{D}_2\text{O}$  mixture.

#### 5.5.4. Effect of temperature on conductivity measurement

In the scoping study described in the above section all the conductivity measurements were carried out at solution temperature. It is a well known fact that the conductivity of an ionic solution gets affected by temperature. In the present work the percentage content of heavy water

in the sample is purely dependent on the small shift in conductivity that is observed before and after the formation of boron- mannitol complex. Hence with minor change in temperature the shift in conductivity gets affected which in turn affects the accuracy of the final analytical result. Therefore in the subsequent stages of work all measurements were carried out at a fixed temperature using a high resolution temperature bath. A temperature of 25°C was chosen although any other temperature would suffice as long as the calibration and analysis of samples of unknown compositions are done at the same temperature. However if a constant temperature bath is not available the conductivity at solution temperature can be converted to a common reference temperature such as 25 °C using the formula shown below

$$k_t = k_{25} ( 1 + ( t - 25 ) * 0.02 ) \quad (2)$$

where t is temperature in °C,  $k_t$  is conductivity at temperature t and  $k_{25}$  is the conductivity at 25°C.

However for accurate work it is advisable to carry out the conductivity measurements using a constant temperature bath as it improves the accuracy of the final result.

#### **5.5.5. Miniaturization of conductivity probe**

As heavy water is highly expensive it is advisable to follow a technique that is either non-destructive or requires minimum sample volume for analysis. With the encouraging results obtained from the initial studies further investigations were carried out to evaluate a methodology that requires as minimum sample as possible for each analysis as the present technique is destructive in nature. Towards this a second conductivity cell requiring 5mL of sample volume was used to measure the solution conductivities (refer section 5.2.1.5). All conductivity measurements were carried out at a fixed temperature of 25°C using a constant

temperature bath (Hakke DC 10 having an accuracy of  $\pm 0.1$  °C). A dedicated GUI, as discussed in section 5.3, was used to record the solution conductivities. The GUI was developed in order to make the method suitable for routine analysis where rapidity and convenience are important factors. With the above modifications experiments were repeated by taking 5mL of sample for each analysis instead of 50mL. Three independent sets of campaigns were carried out and the summary of the results is presented in Table V.2.

**Table V.2.** Summary of results obtained from three independent campaigns.

Experimental campaign	% D <sub>2</sub> O v/v in H <sub>2</sub> O-D <sub>2</sub> O mixture	Conductivity after mannitol addition ( $\mu\text{S cm}^{-1}$ )	Conductivity after boric acid addition ( $\mu\text{S cm}^{-1}$ )	Shift in conductivity ( $\mu\text{S cm}^{-1}$ )
Set-1	0	1.296	10.170	8.874
	19.9	1.578	8.780	7.202
	39.9	1.841	7.328	5.487
	59.8	2.173	6.363	4.190
	79.7	2.674	5.617	2.943
	99.6	2.945	5.048	2.103
Set-2	0	1.238	9.946	8.708
	19.9	1.543	8.686	7.143
	39.9	1.815	7.210	5.395
	59.8	2.218	6.283	4.065
	79.7	2.654	5.541	2.887
	99.6	2.978	5.025	2.047
Set-3	0	1.216	10.072	8.856
	19.9	1.524	8.580	7.056
	39.9	1.832	7.110	5.278
	59.8	2.123	6.268	4.145
	79.7	2.611	5.486	2.875
	99.6	3.003	5.237	2.234

\*Volume taken for each analysis is 5 mL.  
Sample conductivities measured at 25°C.

A relationship between shift in conductivity and percentage composition of heavy water was constructed using the data given in the table. The resulting calibration plot is shown in Figure V.4 along with the following second degree polynomial relationship connecting the two variables

$$\text{Volume\% D}_2\text{O} = 145.33425 - 24.39999 * (\Delta k) + 0.91149 * (\Delta k)^2 \quad (3)$$

Where  $\Delta k$  = shift in conductivity.

Using the above equation few synthetic samples of light water-heavy water mixture taken in various compositions were analyzed in order to test the validity of the equation. The results obtained from the study are reproduced in Table V.3. From the table it is seen that the conductivity based approach produces satisfactory results.

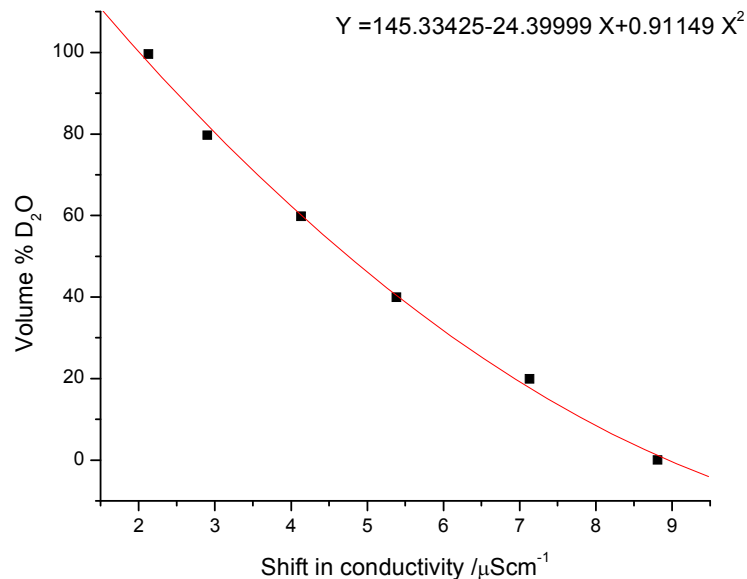


**Fig.V.4.** Relationship between shift in specific conductance and volume percent heavy water.

**Table V.3** Assay of isotopic purity of heavy water in synthetic mixtures of light water and heavy water.

Sl.no	Sample designation	Shift in conductivity ( $\mu\text{Scm}^{-1}$ )	% D <sub>2</sub> O (v/v) in H <sub>2</sub> O-D <sub>2</sub> O sought	% D <sub>2</sub> O (v/v) in H <sub>2</sub> O-D <sub>2</sub> O obtained
1.	Synth-1	4.67	50	51.3
2.	Synth-2	3.25	75	75.6
3.	Synth-3	6.7	20	22.7
4.	Synth-4	2.4	90	92.0
5.	Synth-5	5.5	40	38.7

*\*Volume taken for each analysis is 5 mL.  
Sample conductivities measured at 25°C.*

### 5.5.6. Further miniaturization of conductivity probe

With the satisfactory results obtained using this new method a miniaturized conductivity probe requiring 1mL of sample volume was used in order to reduce the sample consumption. A detailed specification of the conductivity probe is given in section 5.2.1.5. Although the conductivity probe was miniaturized, other experimental parameters as described in section 5.5.5 remained the same. However in this final phase of work the composition of each heavy water standard was expressed in terms of weight% instead of volume% while constructing the calibration plot. This was achieved by knowing the concentration of heavy water and the densities of light water and heavy water at 25°C. The densities of light water and heavy water as reported in the literature [111] are 0.997048 and 1.1044  $\text{gcm}^{-3}$  respectively while the

concentration of heavy water used in this present study was found to be 99.68%(w/w) by IR spectroscopy. Expressing the sample composition in terms of weight % allows for the easy comparison of results with other standard techniques such as IR and refractometry where the isotopic purity is reported in terms of weight %. Further in this phase of work the calibration curve was split into two as shown in Figures V.5a and V.5b.

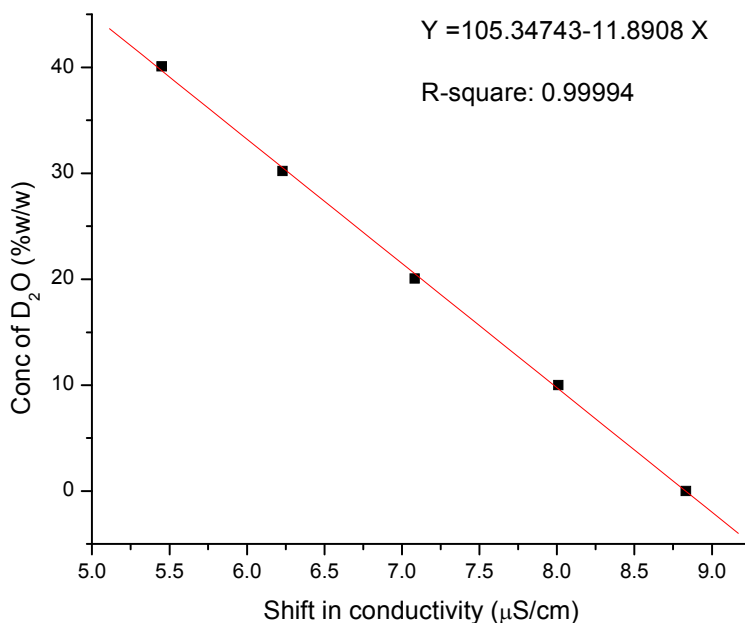


**Fig.V.5a.** Relationship between shift in conductivity and concentration of  $\text{D}_2\text{O}$  in lower range (0-40% concentration of  $\text{D}_2\text{O}$ ).

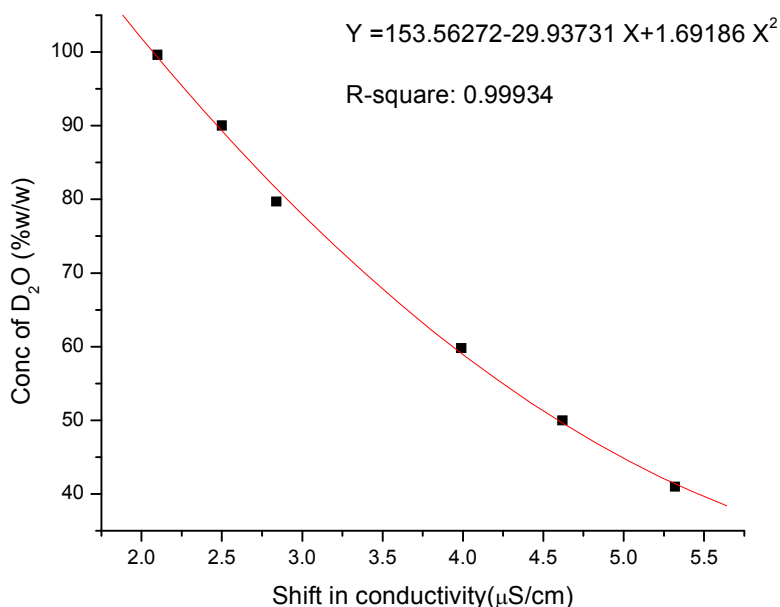


**Fig.V.5b.** Relationship between shift in conductivity and concentration of D<sub>2</sub>O in higher range (40-100% concentration of D<sub>2</sub>O).

One of the calibration plots was used to find the composition of heavy water in the lower range between 0-40% while the other was used to cover the rest of the range between 40- 100%. Though a smooth quadratic equation is followed in the entire range from 0 to 100% D<sub>2</sub>O, it was preferred to divide the plot into two separate ranges in order to achieve better accuracy and reproducibility in analysis. Table V.4 shows the summary of results obtained in four independent experimental runs using the methodology described in section 5.4 while Table V.5 shows the accuracy and precision in measurement for a few synthetic heavy water samples prepared by mixing appropriate quantities of light water and heavy water.

**Table V.4.** Summary of results obtained from four independent measurement campaigns.

Designation of experimental set	% D <sub>2</sub> O v/v in H <sub>2</sub> O-D <sub>2</sub> O mixture	Conductivity after mannitol addition ( $\mu\text{S cm}^{-1}$ )	Conductivity after boric acid addition ( $\mu\text{S cm}^{-1}$ )	Shift in conductivity ( $\mu\text{S cm}^{-1}$ )
Set-1	0	1.116±0.003	10.080±0.005	8.964
	19.9	1.314±0.003	8.465±0.004	7.151
	39.9	1.733±0.004	6.951±0.004	5.218
	59.8	2.040±0.004	6.039±0.004	3.999
	79.7	2.504±0.003	5.346±0.004	2.842
	99.6	2.801±0.003	4.811±0.004	2.010
Set-2	0	1.200±0.003	10.010±0.004	8.81
	19.9	1.424±0.002	8.345±0.005	6.921
	39.9	1.756±0.003	7.083±0.005	5.327
	59.8	2.235±0.003	6.182±0.005	3.947
	79.7	2.573±0.004	5.404±0.004	2.831
	99.6	3.051±0.002	5.142±0.003	2.091
Set-3	0	1.284±0.002	10.090±0.005	8.806
	19.9	1.310±0.003	8.366±0.004	7.056
	39.9	1.614±0.003	6.920±0.004	5.306
	59.8	2.041±0.003	5.975±0.004	3.934
	79.7	2.494±0.005	5.316±0.004	2.822
	99.6	2.861±0.004	4.902±0.003	2.041
Set-4	0	1.235±0.003	10.062±0.004	8.827
	19.9	1.444±0.003	8.557±0.004	7.113
	39.9	1.689±0.004	7.006±0.004	5.317
	59.8	2.125±0.003	6.085±0.004	3.960
	79.7	2.561±0.004	5.393±0.003	2.832
	99.6	3.009±0.003	4.088±0.004	2.047

\*Volume taken for each analysis is 1mL, temperature of measurement is 25°C.

**Table V.5.** Precision and accuracy of the present technique in the assay of heavy water content.

Sample identification number	Actual concentration of D <sub>2</sub> O %(w/w)	Concentration of D <sub>2</sub> O using present technique %(w/w)	Average value with precision %(w/w)	% Deviation
HW-1	62.22	61.76,60.90,61.92,62.56	61.79 SD 0.68 (n=4)	0.69
HW-2	10.92	11.17,10.82,11.41,11.05	11.11 SD 0.25 (n=4)	1.74
HW-3	90.59	90.37,92.55,91.68,89.23	90.96 SD 1.46 (n=4)	0.41
HW-4	99.68	99.37,98.16,97.02,98.61	98.29 SD 0.98 (n=4)	1.39

### 5.5.7. Validation of technique

Finally in order to validate this new technique, samples were tested using the proposed technique and also with well established techniques such as refractive index and IR spectroscopy. Table V.6 shows the comparison of the present technique with the standard techniques.

**Table V.6.** Comparison of the present technique against refractometry and IR spectroscopy.

Sample identification number	Concentration of D <sub>2</sub> O using present technique % (w/w)	Concentration of D <sub>2</sub> O using refractometry %(w/w)	Concentration of D <sub>2</sub> O using IR spectroscopy %(w/w)
S-1	25.4	24.9	-
S-2	40.6	41.7	-
S-3	61.8	61.3	-
S-4	82.2	82.6	-
S-5	47.4	47.9	-
S-6	98.8	-	99.68
S-7	98.5	-	99.23

## **5.6. Conclusion**

In this chapter a novel conductivity based method for the assay of heavy water in samples of light water and heavy water mixtures has been discussed. Probably for the first time a conductivity based measurement approach has been realized for the isotopic assay of heavy water. The method is inexpensive, rapid and requires low sample volumes (1mL) for analysis. The method shows excellent accuracy ( $\leq 1.75\%$ ) and precision ( $\leq 1.5\%$  relative standard deviation) and at the same time it can be used to analyze samples containing a wide range of percentage heavy water composition. The method is standardized such that it can be used routinely in quality control laboratories attached to PHWRs and heavy water production plants.

---

## 6. PARAMETRIC STUDY ON THE RATE OF CARBONATION OF SODIUM AEROSOLS

---

### 6.1. Introduction

A crucial application of conductivity based pulsating sensor is explored in this chapter. This chapter deals with the experimental studies on the carbonation of sodium aerosols. Such safety related studies are needed for hazard evaluation of liquid metal cooled fast breeder reactors, such as Prototype Fast Breeder Test reactor (PFBR), with respect to sodium fires [112]. PFBR is a 500 MWe pool type, mixed oxide fuel, sodium cooled reactor [4]. The heat generated from the reactor core is transferred through two secondary loops. Liquid sodium enters the steam generator at 550°C and returns to the reactor core at 280°C. A sodium leak in the secondary heat transfer loop, inside the steam generator building, results in sodium fires of different kinds such as pool fire, spray fire and column fire. The fire occurs due to the interaction of hot liquid sodium with ambient atmosphere containing oxygen. The resulting fire generates a lot of sodium aerosol that mainly consists of sodium oxide ( $\text{Na}_2\text{O}$ ) and higher oxides of sodium ( $\text{Na}_2\text{O}_2$  and  $\text{NaO}_2$ ) depending on the ratio of sodium and oxygen present during the onset of fire. Since these oxides are highly unstable they immediately react with the ambient carbon dioxide ( $\text{CO}_2$ ) and moisture to form more stable compounds such as sodium hydroxide, sodium carbonate and sodium bicarbonate. The rate of conversion of aerosol from one form to the other depends on many factors such as, (i) size of aerosol, (ii) concentration of aerosol, (iii) physical state of aerosol, (iv) percentage of relative humidity (RH%), (v)  $\text{CO}_2$  level, (vi) stability of product, (vii) rate of diffusion of reactant etc. From safety point of view sodium hydroxide aerosols are not only harmful to humans but also to the equipments placed inside the steam generator building.

These aerosols damage the tissues that come under its contact and produce a burning sensation. Moreover inhalation of these harmful aerosols causes the rapid rupture of the respiratory tract. The inhalation threshold limit for the concentration of sodium hydroxide in atmosphere is  $2 \text{ mg m}^{-3}$  according to American conference of governmental industrial hygienists [113]. With regard to equipments such as gas blowers, heat exchangers, air filters and other electrical components, sodium hydroxide has a highly corrosive effect. Although sodium aerosols in hydroxide form is highly harmful to both humans and equipments it is less harmful if the aerosols are in the carbonate form and not harmful if they are in bicarbonate form. Therefore information on chemical species present in aerosols of sodium fire and the possibility of conversion to harmless bicarbonate form is needed for safety analysis. Further it is of interest to know the conditions that assist in the quick conversion of sodium hydroxide aerosols to sodium bicarbonate form.

Cherdron and Jordan carried out wet chemical analysis to determine the various sodium aerosol species resulting from sodium fire [114]. The experiments were conducted at DEBENE facility. They reported that almost 50% of airborne sodium is converted to sodium carbonate within one minute from the start of the sodium fire. Moreover they found that RH has a strong influence on the rate of conversion and that the entire air borne sodium was completely converted to sodium carbonate within 260 seconds when RH exceeded 50%. Hofmann carried out sodium spray fire experiments in open atmosphere and characterized the chemical form of sodium aerosols [115]. It was observed that sodium oxide aerosols were immediately transformed to NaOH at RH between 40 and 70%, whereas after 30 seconds these particles were converted into sodium carbonate. Clough and Garland theoretically predicted the formation of hydroxide aerosol within minutes even in dense sodium aerosol atmosphere [116]. They also predicted that simultaneous generation of sodium carbonate depends on the particle size and the prevailing RH%. In an

earlier work carried out by our group on the chemical characterization of sodium aerosols, it was found that all the suspended aerosols were converted to carbonate form within 500 seconds from the onset of sodium fire [19]. The experiments were carried out at 50% and 65% RH levels with an initial mass concentration of  $2 \text{ gm}^{-3}$ . In that work a high resolution conductometric titration facility was used in order to characterize and quantify the various sodium aerosol species.

From the above literature survey it is seen that even though work has been done in the area of carbonation of sodium aerosols much information is not yet available. For instance Hoffman et al has not provided information on the mode of sampling, duration of sampling and the technique adopted for characterizing the aerosols. Similarly Cherdrón and Jordan have not specified the quantity sampled, duration of sampling and the technique adopted for chemical characterization. In the case of the earlier work reported by our group the aerosols were sampled only up to 500 seconds and therefore the fate of suspended aerosols beyond 500 seconds is not known. Moreover the experiments were carried out at two different RH% levels only and that too at ambient  $\text{CO}_2$  level. Hence even though the work gave an estimate for the rate of conversion of air borne sodium to sodium carbonate, a systematic parametric study was lacking. In view of the limited information available on the fate of sodium aerosols generated during a sodium fire, the present study was undertaken to investigate the effect of RH% and  $\text{CO}_2$  content on the rate of carbonation of sodium aerosols.

There are many fast reactor facilities around the world. Each of the location housing the fast reactor facility experiences a different RH% depending on the time of the year. For instance Kalpakkam experiences an average RH of 67% between May and July while it experiences above 75% for the rest of the year. However, Cadarache in France which has a number of nuclear facilities experiences a RH ranging from 20% to 80%. Considering this wide variation in

RH values, the experiments were conducted at 20%, 50% and 90% RH. Further experiments were also carried out at 390 ppm CO<sub>2</sub> level and at 280 ppm CO<sub>2</sub> level. While 390 ppm corresponds to the ambient CO<sub>2</sub> concentration at Kalpakkam, 280 ppm corresponds to a reduced CO<sub>2</sub> concentration in the core plume. A reduced CO<sub>2</sub> concentration is expected at the core of the plume as some amount of CO<sub>2</sub> will be consumed by the plume itself.

## **6.2. Experimental**

### **6.2.1. Aerosol Test Facility**

An Aerosol Test Facility (ATF) has been designed and commissioned at Radiological Safety Division at IGCAR. The facility was developed to carryout experimental investigations on sodium aerosols and nuclear aerosols in the context of fast reactor safety. The main components of the ATF are (i) a 1000 liter aerosol chamber made of SS-304, (ii) a plasma torch for the production of aerosols of fuel and fission product equivalent materials, (iii) a sodium combustion cell for the generation of sodium aerosols, (iv) aerosol diagnostic tools such as Anderson sampler, Mastersizer, filtration set up etc., (v) auxiliary systems such as water cooling, gas flow, vacuum pumping system, pneumatic control and material handling system. Figure V1.1 shows the schematic diagram of the ATF.

The aerosol characteristics of sodium, fuel and fission product equivalent materials and their mixtures are studied in the aerosol chamber. The chamber which is 150 cm in diameter and 60 cm in height has a total of twelve different ports of following specifications (i) eight 3" ports, (ii) three 4" ports and (iii) one 6" port. The various other components of the ATF such as sodium combustion cell, vacuum pumping system, plasma torch, filter paper sampler, mastersizer etc., are connected through these ports. The weight of the aerosol chamber is around 1000 kg while that of the top plate is 400 kg. The entire system rests on a sturdy MS bench. A detailed

description of the facility is reported elsewhere [117]. Apart from the above mentioned facilities the following three additional facilities (6.2.2, 6.2.3, and 6.2.4) were integrated with the ATF for the present work on the carbonation of sodium aerosols.

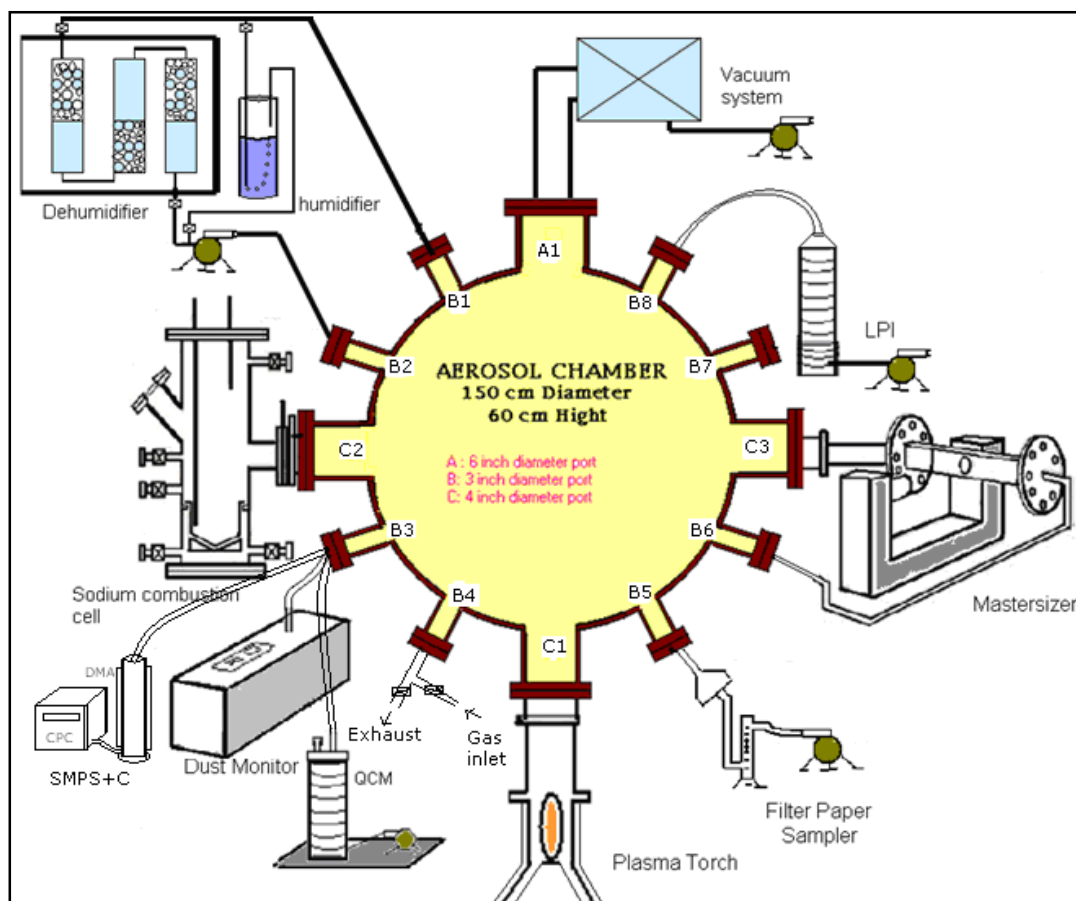


**Fig. VI.1.** Schematic diagram of ATF facility

### **6.2.2. Dual filter paper sampling system**

The existing sampling system is made of stainless steel (SS) and is connected to one of the ports of the aerosol chamber. The sampling system has a filter paper holder to accommodate a filter paper of 25mm diameter. The aerosol from the chamber is sucked on to the filter paper loaded inside the sample holder using a suction pump at the required flow rate. A fresh filter paper is loaded once the sampling is over. Usually it takes about 30-45 seconds to replace a filter paper

and hence the existing system is not suitable when the time interval between successive sampling times is short. In order to circumvent this problem a new dual filter paper sampling system was fabricated and integrated with the ATF. The new setup has two independent sampling systems that are held parallel by two three way connectors as shown in Figure VI.2. A ball valve on the three ways connector attached to the aerosol chamber allows the user to direct the flow of air from the chamber through any one of the two sampling pathways. Using the ball valve the user can select the line which is ready for sampling while the other line can be made ready for the next sampling.



**Fig.VI.2.** Photograph of the dual filter paper sampling system.

### **6.2.3. Humidity adjustment system**

A humidity adjustment system was used to regulate the RH% inside the chamber from 20% to 90% RH. In order to decrease the RH the air inside the chamber was circulated through silica gel granules while the air was purged through a water bath to increase the RH. The circulation of air was achieved using a 50 lpm oil free rotary pump and the circulation was continued till the online humidity meter displayed the attainment of the required RH. Although this set up worked well for establishing high RH values it was not able to achieve RH values below 40%. In order to

attain low RH values the temperature of the chamber was raised using a coil heater wound around the chamber. Using this approach RH value as low as 20% could be achieved very quickly.

#### **6.2.4. Nitrogen flow setup**

The ambient concentration of CO<sub>2</sub> inside the chamber was found to be around 390 ppm. In order to reduce the CO<sub>2</sub> concentration, nitrogen from a cylinder was flushed inside the chamber. The flow of nitrogen was stopped once the required CO<sub>2</sub> level was attained as indicated by the online CO<sub>2</sub> monitoring instrument. In the present work a CO<sub>2</sub> analyzer having model number IR-200 was procured from Ms Endee engineers pvt ltd Mumbai, India.

#### **6.2.5. Conductometric titration facility**

In the current work a high resolution conductometric titration facility described earlier in section 2.7 of chapter 2 was successfully used to quantify the various aerosol species. A conductometric titration plot is composed of different regions with distinct slopes that are characteristic of specific chemical reactions between the individual species present in the titration vessel and the titrant during the course of titration. In order to accurately delineate the various regions a high resolution conductivity meter capable of detecting minor shifts in conductivity must be employed. Moreover the conductivity meter should be capable of recording titration plots even in extremely dilute solutions. Extremely dilute solutions are obtained when the aerosols are sampled after a long duration from the onset of sodium fire. In such cases only a small quantity of aerosol remains in the suspended form as the major portion gets deposited on to the walls and floor of the chamber.

### **6.3. Methodology**

#### **6.3.1. Combustion of sodium and sampling of sodium aerosol**

Before loading the sodium inside the combustion cell the aerosol chamber was adjusted to the desired RH% and CO<sub>2</sub> level by following the procedure detailed in sections 6.2.3 and 6.2.4 respectively. About 10g of sodium was loaded inside the combustion cell and heated to 550°C under an argon atmosphere. 550°C corresponds to the temperature of liquid sodium entering the steam generator building from the reactor core. The hot sodium was ignited by exposing it to compressed air after letting the argon out. The resulting fire generated a lot of sodium oxide aerosol inside the combustion cell and was released into the chamber by opening the valve connecting the chamber and the combustion cell. Excess pressure inside the combustion cell ensured the quick flow of aerosol inside the chamber and its diagnostic ports. Aerosol inside the chamber was sampled successively at predetermined time intervals using the dual filter paper sampling system described in section 6.2.2. The flow rate of sampling was fixed at 5 lpm throughout this work. After sampling the filter paper was weighed immediately using a semi microbalance (model no GR200, from M/s AND limited, Japan). The weighed filter paper was placed inside a beaker containing a few mL (~5mL) of deionized water and properly covered using parafilm in order to protect the sample from environmental impurities. After collecting all the filter papers in a similar fashion the contents of each filter paper were subjected to conductometric titration.

### 6.3.2. Analysis of aerosol samples

For carrying out a conductometric titration the aerosol collected on the filter paper was quantitatively transferred to deionized water. The sample solution was made up to a fixed volume and two aliquots of the sample were titrated against freshly standardized 0.1N HCl using the high resolution conductometric titration setup. Each titration took about 5 minutes for completion and immediately after titration the various end points were obtained using the offline features available in the GUI described in section 2.5 of chapter 2. From the resulting titration end points the various species of sodium aerosol as deposited on the filter paper were computed.

## 6.4. Results and discussion

### 6.4.1. Calculation of various aerosol species from conductometric titration plot

Figure VI.3 shows a typical conductometric titration plot obtained by titrating an aerosol sample in water medium against HCl solution.

The figure shows four distinct regions. Region I is obtained due to the replacement of highly conducting hydroxide ions ( $\lambda_0=197 \text{ S cm}^2 \text{ mol}^{-1}$ ) with less conducting chloride ions ( $\lambda_0=76 \text{ S cm}^2 \text{ mol}^{-1}$ ).



A sharp fall in conductivity is observed due to the large difference in molar ionic conductance existing between  $\text{OH}^-$  and  $\text{Cl}^-$  ions that are involved in the above reaction.

Region II is obtained due to the replacement of  $\text{CO}_3^{2-}$  ions ( $\lambda_0=144 \text{ S cm}^2 \text{ mol}^{-1}$ ) with chloride ( $\lambda_0=76 \text{ S cm}^2 \text{ mol}^{-1}$ ) and bicarbonate ions ( $\lambda_0=45 \text{ S cm}^2 \text{ mol}^{-1}$ ). As the combined molar ionic

conductance of a chloride ion and a bicarbonate ion is less than that of a carbonate ion there is a fall in conductivity. The equation governing this region is shown below

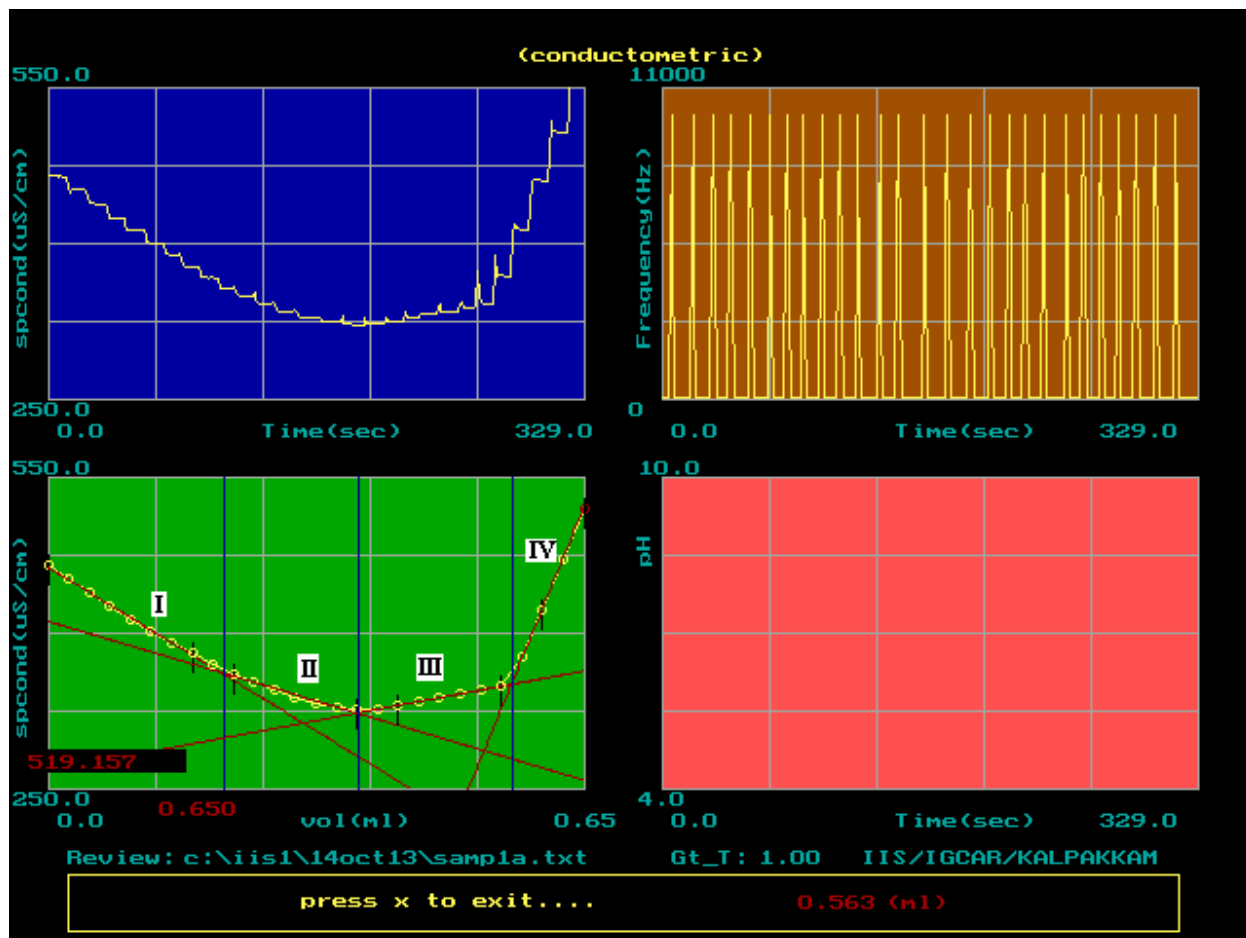


**Fig.VI.3.** A typical conductometric titration plot obtained by titrating an aerosol sample in water medium against HCl solution.

Region III shows a slight positive slope. This is due to the replacement of less conducting bicarbonate ions with slightly more conducting chloride ions.



The final region (region IV) is obtained due to the accumulation of  $\text{H}^+$  and  $\text{Cl}^-$  ions after the end point is crossed. As the combined molar ionic conductance of  $\text{H}^+$  and  $\text{Cl}^-$  ions ( $\lambda_0=426 \text{ S cm}^2 \text{ mol}^{-1}$ ) is very high, a sharp rise in conductivity is observed.

From the above discussion it is clear that the various species present in the sample can be quantified using the below equations

$$[\text{NaOH}]_{\text{aq}} = (V_1 * C_{\text{HCl}}) / V_{\text{Solution}} \quad (4)$$

$$[\text{Na}_2\text{CO}_3]_{\text{aq}} = (2 * (V_2 - V_1) * C_{\text{HCl}}) / V_{\text{Solution}} \quad (5)$$

$$[\text{NaHCO}_3]_{\text{aq}} = [(V_3 - V_2) - (V_2 - V_1) * C_{\text{HCl}}] / V_{\text{Solution}} \quad (6)$$

where  $V_1$ ,  $V_2$ , and  $V_3$  correspond to the first, second and third end points in the titration plot.

However the above set of equations do not take into account the partial hydrolysis of sodium carbonate that takes place when the aerosols deposited on the filter paper are quantitatively transferred to water. The equation representing the partial hydrolysis is given below



Due to hydrolysis of  $\text{Na}_2\text{CO}_3$  the concentration of various species present in the water medium will be different from that deposited on the filter paper. Therefore in order to correctly quantify the various species as deposited on the filter paper the above set of equations (4, 5 & 6) have to be suitably modified. The modified set of equations are given below

Case 1: If  $[\text{NaOH}]_{\text{aq}} > [\text{NaHCO}_3]_{\text{aq}}$

$$[\text{NaOH}]_s = [\text{NaOH}]_{\text{aq}} - [\text{NaHCO}_3]_{\text{aq}} \quad (8)$$

$$[\text{Na}_2\text{CO}_3]_s = [\text{Na}_2\text{CO}_3]_{\text{aq}} + 2*[\text{NaHCO}_3]_{\text{aq}} \quad (9)$$

Case 2: if  $[\text{NaOH}]_{\text{aq}} < [\text{NaHCO}_3]_{\text{aq}}$

$$[\text{NaHCO}_3]_s = [\text{NaHCO}_3]_{\text{aq}} - [\text{NaOH}]_{\text{aq}} \quad (10)$$

$$[\text{Na}_2\text{CO}_3]_s = [\text{Na}_2\text{CO}_3]_{\text{aq}} + 2*[\text{NaOH}]_{\text{aq}} \quad (11)$$

*Where the subscript 'aq' refers to aerosol in aqueous solution while 's' refers to aerosol as deposited on the filter paper.*

The above set of formulas (8 to 11) which take hydrolysis of sodium carbonate into account were used to quantify the various aerosol species as deposited on the filter paper.

#### **6.4.2. Influence of %RH and CO<sub>2</sub> content in the carbonation of sodium aerosols**

All the experiments were conducted in the ATF facility which is a closed facility whose details are described in 6.2.1. The experiments were carried out (i) at ambient air containing ~390 ppm CO<sub>2</sub> and (ii) at a reduced CO<sub>2</sub> atmosphere (~280 ppm) by flushing the chamber with nitrogen. Further in each case experiments were conducted by maintaining RH% at three different levels namely ~20%, ~50%, ~90%. In all the experiments the initial mass concentration of the aerosol was maintained at ~4 g. m<sup>-3</sup>. Experiments in the same test condition were repeated twice and the average result is presented in Table VI.1. Using the data as given in the table the real time plot of conversion of sodium hydroxide to sodium carbonate in most cases, mixture of sodium carbonate and bicarbonate or only bicarbonate species in a few cases for each test atmosphere was generated and shown in Figure VI.4.

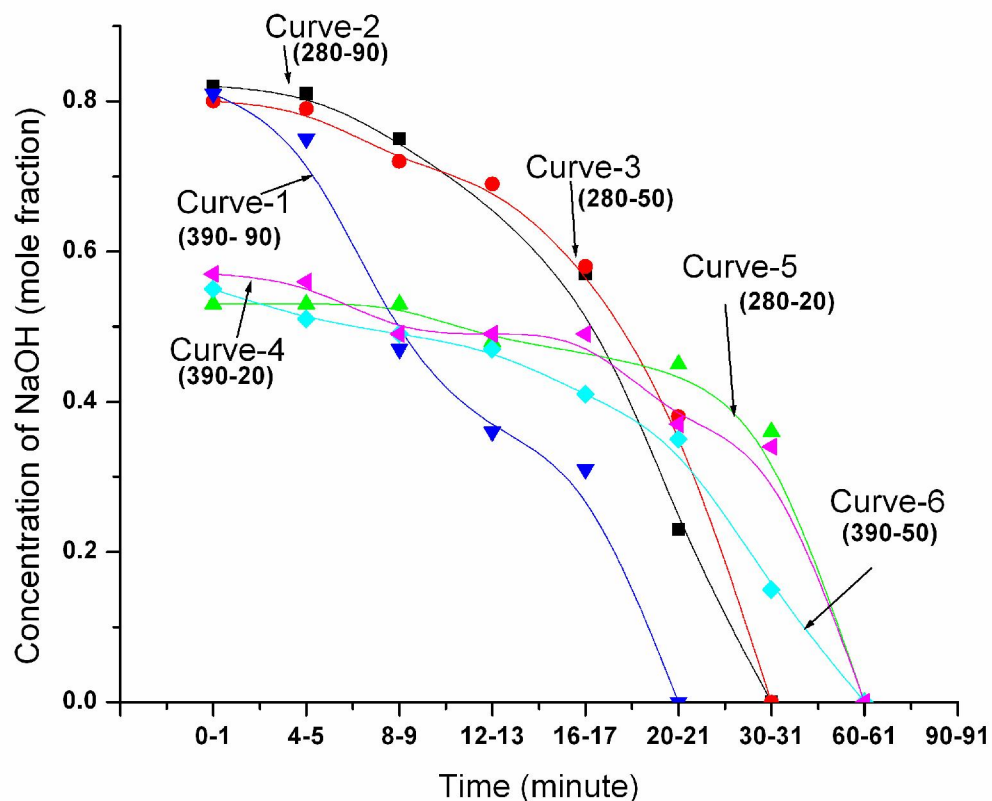


**Fig.VI.4.** Real time change in concentration of NaOH as a function of different %RH and CO<sub>2</sub> concentrations.

From the study it was found that at high humidity and at ambient CO<sub>2</sub> concentration (90% RH & 390 ppm), the sample collected just after 1 minute of sodium fire contains a high percentage of sodium hydroxide (~ 0.8 mole fraction). The sodium hydroxide thus generated undergoes rapid carbonation and it is fully converted to a mixture of Na<sub>2</sub>CO<sub>3</sub> and NaHCO<sub>3</sub> after 20 minutes of sodium fire. This is shown in curve 1 of the Figure VI.4. Due to high humidity the oxide aerosols (Na<sub>2</sub>O) released from sodium fire are immediately converted to NaOH due to reaction with excess moisture content in the surrounding environment as per the following reaction.



NaOH further reacts with  $\text{CO}_2$  and is converted to  $\text{Na}_2\text{CO}_3$ . Some sodium carbonate may further react with  $\text{CO}_2$  and  $\text{H}_2\text{O}$  present in the chamber to form  $\text{NaHCO}_3$ . The reactions responsible for such conversions are given below.



When the same experiment was repeated at a reduced  $\text{CO}_2$  concentration (280 ppm) without changing the %RH (i.e., at 90%), it was found that the initial sample contains almost the same mole fraction of NaOH ( $\sim 0.8$ ) while the rate of carbonation was slightly lowered as compared to the experiments conducted at 90% RH and 390 ppm  $\text{CO}_2$  (refer curve 1). This behavior is on the expected lines as reduced  $\text{CO}_2$  concentration delays the carbonation of sodium hydroxide. This trend is shown in curve 2 of the figure. A similar trend in carbonation is exhibited by curve 3 also. In this case the surrounding atmosphere contains 50% RH and 280 ppm  $\text{CO}_2$ . This implies that even if relative humidity is reduced from 90% to 50% it does not affect the initial formation of NaOH when surrounding atmosphere is depleted by  $\sim 100$  ppm  $\text{CO}_2$  from ambient atmospheric  $\text{CO}_2$  concentration. Both processes, formation of NaOH from  $\text{Na}_2\text{O}$  and carbonation of NaOH to  $\text{Na}_2\text{CO}_3$  are fully governed by the presence of reactants such as water vapour and  $\text{CO}_2$  in the surrounding atmosphere. Hence in this case reduced  $\text{CO}_2$  atmosphere slows down the carbonation process to some extent, thereby maintaining NaOH concentration between 0.7 and 0.8 mole fraction in first 10 minutes of sodium fire.

Curve 4 shows the experimental data obtained at 20% RH and 390 ppm  $\text{CO}_2$  while curve 5 represents the data obtained at 20% RH and 280 ppm  $\text{CO}_2$ . In both the cases the samples

collected in the first minute after sodium fire show almost the same concentration of NaOH (~0.55). Also in both the cases it takes about 30 minutes for the concentration of sodium hydroxide to reduce to 0.35 mole fraction while complete carbonation takes about 1 hour from sodium fire. Hence it can be concluded that a reduction of 100 ppm of CO<sub>2</sub> does not have any significant effect on the carbonation of NaOH at 20 %RH. Curve 6 represents the data obtained at 50% RH and 390 ppm CO<sub>2</sub>. It is seen that the experimental condition does not permit the enhanced formation of NaOH in the initial stages as a considerable part of it is consumed by CO<sub>2</sub> which is sufficiently available in the atmosphere. Both NaOH and Na<sub>2</sub>CO<sub>3</sub> are equally distributed in the aerosol for the first 13 minutes immediately after sodium fire. About 85% carbonation of NaOH occurs after half an hour and for complete carbonation of NaOH it takes about 1 hour. An important observation in this work was that the rate of carbonation of NaOH does not follow either first order or second order kinetics. When initial concentration of a specimen is gradually reduced due its chemical reaction with other reactants with respect to time, it is possible to evaluate the order of reaction. But in this case the real time concentration loss of dispersed aerosol is due to both chemical reaction with other reactants (such as H<sub>2</sub>O and CO<sub>2</sub>) and also due to other physical phenomena such as agglomeration and settling of aerosol particles in the aerosol chamber.

**Table VI.1.** Summary of results obtained on the carbonation of sodium aerosols under different RH% and CO<sub>2</sub> levels.

Sam- pling- Time inte- rval (min.)	~90% RH ~390 ppm CO <sub>2</sub>			~50% RH ~390 ppm CO <sub>2</sub>			~20% RH ~390 ppm CO <sub>2</sub>			~90% RH ~280 ppm CO <sub>2</sub>			~50% RH ~280 ppm CO <sub>2</sub>			~20% RH ~280 ppm CO <sub>2</sub>		
	A	B	C	A	B	C	A	B	C	A	B	C	A	B	C	A	B	C
0-1	0.81	0.19	0	0.55	0.45	0	0.57	0.43	0	0.82	0.18	0	0.80	0.20	0	0.53	0.47	0
4-5	0.75	0.25	0	0.51	0.49	0	0.56	0.44	0	0.81	0.19	0	0.79	0.21	0	0.53	0.47	0
8-9	0.47	0.53	0	0.49	0.51	0	0.49	0.51	0	0.75	0.25	0	0.72	0.28	0	0.53	0.47	0
12-13	0.36	0.64	0	0.47	0.53	0	0.49	0.51	0	-	-	-	0.69	0.31	0	0.48	0.52	0
16-17	0.31	0.69	0	0.41	0.59	0	0.49	0.51	0	0.57	0.43	0	0.58	0.42	0	-	-	-
20-21	0	0.47	0.53	0.35	0.65	0	0.37	0.63	0	0.23	0.77	0	0.38	0.62	0	0.45	0.55	0
30-31	0	0	1	0.15	0.85	0	0.34	0.66	0	0	0.09	0.91	0	0.85	0.15	0.36	0.64	0
60-61	-	-	-	0	0	1	0	0.1	0.9	0	0	1	0	0	1	0	0.40	0.60
90-91							0	0	1							0	0.23	0.77

\* *A* denotes mole fraction of NaOH  
*B* denotes mole fraction of Na<sub>2</sub>CO<sub>3</sub>  
*C* denotes mole fraction of NaHCO<sub>3</sub>

## 6.5. Conclusion

In this work a high performance conductivity based approach was used to quantify the various sodium aerosol species present at different time intervals from the onset of sodium fire. Based on this approach the speciation of NaOH, Na<sub>2</sub>CO<sub>3</sub> and NaHCO<sub>3</sub> as a function of real time was studied. As oxides of sodium get immediately converted to sodium hydroxide in water medium, the oxides could not be identified separately. Hence the oxides of sodium, if any, were reported along with sodium hydroxide. The experiments were carried out by burning about 10g of sodium which produced a mass concentration of 4 g m<sup>-3</sup>. Studies were carried out at two different CO<sub>2</sub> levels namely 390 ppm and 280 ppm. Further at each CO<sub>2</sub> concentration the experiments were conducted at three different RH% levels namely ~20%, ~50% and ~90% RH. From the study it was found that as RH% increases the rate of conversion from hydroxide form to bicarbonate form also increases. Further it was found that as the carbon dioxide level in the chamber decreases the rate of conversion of sodium hydroxide aerosol to sodium bicarbonate form takes much longer time.

---

## 7. CONCLUSION

---

In this thesis deployment of a new class of sensors called pulsating sensors in physico-chemical applications suitable for nuclear facilities has been presented. Out of four different analytical techniques presented as individual chapters in this thesis, two of the techniques are recommended for the assay of species at trace levels. The third technique is used for the determination of isotopic purity of heavy water in mixtures of light water and heavy water while fourth technique was used to characterize the sodium aerosol species in carbonation process. Analysis at trace levels presented in this thesis are based on either conductometric or potentiometric techniques. The results obtained using such techniques are comparable with those obtained from analytical instrumentation techniques using optical instruments or ion chromatography. All these could be possible due to the evolution of such pulsating sensors based instrumentation. These pulsating sensor based instruments have been designed in such a way that, unlike conventional instruments, the primary signal obtained from the sensor head is directly in digital domain which simplifies the instrumentation. Besides simpler instrumentation these sensors have many salient features like (i) high resolution and sensitivity in measurement, (ii) adaptable for remote measurements, (iii) low power consumption with 5V DC in most cases, (iv) handy for field use with battery operated stand alone system, (v) flexible probe design, and (vi) transmission of signal to long distances without loss in quality. In all cases the signal output is pulse frequency which carries information on respective physico-chemical parameter. With minor change in modification of instruments and by making appropriate probes it was possible to develop such powerful, simple and inexpensive analytical techniques suitable for nuclear facility besides general applications. The major findings arising out of this work are listed below

**(i) Development of a potentiometric titration technique for the assay of dissolved oxygen in water down to a few ppb levels.**

A PC based potentiometric titration facility using pulsating sensor based instrumentation was successfully developed to assay dissolved oxygen (DO) down to  $8 \mu\text{gL}^{-1}$ (ppb). The precision in measurement at 10 ppb level of DO was found to be 1.4% relative standard deviation (RSD). Although there are many techniques to assay DO at a few ppb levels, probably this is the only titration technique to achieve such low levels of detection. Moreover being a primary technique it can be used to check the performance of DO meters. Using this technique it was possible to reliably measure the DO content in the steam generator feed waters of Fast Breeder Test Reactor and Madras Atomic Power Station (MAPS). It was found that unambiguous detection of end point, by taking the first derivative of the titration plot, would be achieved even when working with very dilute solutions containing DO at a few ppb levels (8-15 ppb). This was made possible due to the reliable measurement of small jumps in potential occurring at the end point. Kinetic investigations showed that the sample can be preserved even overnight after fixing the DO while it is advisable to titrate the sample immediately once the iodine is liberated by acidifying the sample. It was found that there is a considerable loss of iodine (20%) if samples are titrated after 3 hours from acidification while there is no loss of iodine if samples are titrated within 2 hours from acidification.

**(ii) Development of digital conductometric technique for the trace assay of boron in water and heavy water.**

Two conductivity based approaches were developed to assay boron in light water as well as in heavy water. A conductometric titration approach was followed when the samples contained boron above 0.2 ppm and a direct conductivity approach was followed when samples contained boron below 0.2 ppm.

Although the principle behind the conductometric titration approach is widely followed in volumetric titration using phenolphthalein indicator and by potentiometric titration approaches, it is done either at percentage or at several ppm levels. Probably for the first time an extensive study was carried out to quantify boron in both light water as well as in heavy water matrices at sub-ppm levels using a simple titration approach. Titration plots in light water matrix revealed the presence of three regions while that in heavy water matrix showed only two regions. It was found that boron can be quantified even at elevated background conductivities, caused by the presence of non interfering salts, provided one uses a high resolution conductivity meter. With regard to interfering impurities, a simple methodology was developed to assay boron in the presence of either a trace acid or a trace base. Studies carried out using direct conductivity approach revealed that the shift in frequency due to the formation of boron mannitol complex in light water matrix was almost five times that of the frequency shift observed in heavy water matrix for a given concentration of boron. The precision in measurement using the titration approach was found to be 1% RSD at 1 ppm boron while the precision in measurement using the direct conductivity approach was found to be 4.1% RSD at 20 ppb boron. Using these two methods it was possible to analyze boron in the heavy water moderator of MAPS reactor in a much simpler way.

### **(iii) Assay of isotopic purity of heavy water by conductivity approach**

A conductivity based approach was successfully evolved for the determination of isotopic purity of heavy water in mixtures of light water and heavy water. Generally infrared, refractive index and density measurement techniques are widely followed. Probably for the first time a conductivity based approach has been reported. The method is simple, inexpensive and most importantly covers almost the entire range of heavy water concentration. The principle of the method is based on the observation that the shift in conductivity of a light water-heavy water mixture, due to the generation of a fixed quantity of boron mannitol complex, decreases as the percentage of heavy water in the sample increases. This

property was utilized to establish a relationship between shift in conductivity and % purity of heavy water. A dedicated graphical user interface was developed to make the method suitable for routine analysis in plants such as heavy water enrichment plants where the isotopic purity of heavy water is monitored periodically. Although the technique is destructive, it requires only 1mL of sample volume for each analysis.

#### **(iv) Parametric study on the carbonation of sodium aerosols.**

A parametric study was carried out on the rate of carbonation of sodium aerosols in the context of fast reactor safety. A detailed investigation was carried out on the influence of percentage relative humidity (RH%) and carbon dioxide (CO<sub>2</sub>) content on the rate of carbonation. In all the experiments the initial mass concentration of sodium aerosol was kept at 4 g m<sup>-3</sup>. From the study it was found that a high RH% and an ambient CO<sub>2</sub> concentration ( i.e., 90% RH and 390 ppm CO<sub>2</sub>) helped in the quick carbonation of air borne sodium. Such experimental investigations will be helpful towards environmental safety analysis at fast reactor site in Kalpakkam. Moreover the experimental data are useful for validating core shrinking chemical conversion model of sodium aerosols. Such useful data could be generated by using an in-house developed high resolution digital conductometric titration facility.

#### **FUTURE WORK**

Pulsating sensors, either individually or in combination, offer an extensive scope for developing newer techniques. Based on these novel sensing devices the following future work can be taken up

- ❖ Study of oscillating chemical reactions using pulsation potentiometric instrumentation facility.
- ❖ Third phase detection in PUREX process using pulsating conductivity approach.
- ❖ Carbonation studies on sodium aerosols with different initial mass concentrations.
- ❖ Carrying out analysis by thermometric titrations using pulsating sensor based instrumentation.

- ❖ Constructing an inexpensive homemade ion chromatographic instrument using pulsating conductivity meter.
- ❖ Assay of ethanol in ethanol mixed petrol by dielectric based approach.
- ❖ Online pH and conductivity monitoring in various locations of pressurized heavy water reactors.

## REFERENCES

1. Baldevraj, Mannan, S.L., Vasudeva Rao, P.R., Mathews, M.D., *Sadhana-Acad. P. Eng. S.*, **27** (2002) 527.
2. Vaidyanathan, G., *Indian J. Eng. Mater. Sci.*, **18** (2011) 321.
3. Bhaduri, A.K., Indira, R., Albert, S.K., Rao, B.P.S., Jain, S.C., Ashokkumar, S., *J. Nucl. Mater.*, **334** (2004) 109.
4. Chetal, S.C., Balasubramanian, V., Chellapandi, P., Mohankrishnan, P., Puthiyavinayagam, P., Pillai, C.P., Raghupathy, S., Shanmugam, T.K., Sivathanu Pillai, C., *Nucl. Eng. Des.*, **236** (2006) 852.
5. Electrochemical sensors, Mathews, C.K., *Curr. Sci. India*, **61** (1991) 511.
6. Gnanasekaran, T., Shridharan, R., Mahendran, K.H., Ganesan, V., Periaswami, G., Mathews, C.K., *Nucl. Technol.*, **90** (1990) 408.
7. Sridharan, R., Mahendran, K.H., Nagaraj, S., Gnanasekaran, T., Periaswami, G., *J. Nucl. Mater.*, **312** (2003) 10.
8. [www.dae.nic.in/?q=node/312](http://www.dae.nic.in/?q=node/312).
9. Janawadkar, M.P., Baskara, R., Nagendra, R., Gireesan, K., Harishkumar, N., Rita Saha, Vaidhyathan, L.S., Jayapandian, J., Hariharan, Y., and Radhakrishnan, T.S., *Pramana-J. Phys.*, **58** (2002) 1159
10. Jayakumar, T., Babu Rao, C., John Philip, Mukhopadhyay, C.K., Jayapandian, J., Pandian, C., *Int. J. Smart sens. Intell. Syst.*, **3** (2010) 61.
11. Aggarwal, P.K., Pandey, G.K., Malathi, N., Arun, A.D., Ananthanaraynan, R., Banerjee, I., Sahoo, P., Padmakumar, G., Murali, N., *Ann. Nucl. Energy*, **41**(2012) 87.

12. Embedded pulse processor cum controller for laboratory developed sensors, internal report-IGCAR/EIG/IIS/DN/2005/03.
13. Sahoo, P., Malathi, N., Praveen, K., Ananthanarayanan, R., Arun, A.D., Murali, N., Swaminathan, P., *Rev. Sci. Instrum.*, **81** (2010) 065109.
14. Pulsating sensor based conductivity monitoring device, IGCAR annual report 2006.
15. Bench top type conductivity meter for FBTR, internal report-IGCAR/EIG/RTSD/IIS/RN/2009/02.
16. Electro-analytical measurement facility for reprocessing group, internal report-IGCAR/EIG/RTSD/IIS/RN/2010/02.
17. Conductivity meters for Kakrapar atomic power station, internal report-IGCAR/EIG/RTSD/IIS/RN/2012/01.
18. Ahmed, M.K., Geetha, R., Pandey, N.K., Murugesan, S., Koganti, S.B., Saha, B., Sahoo, P., Sundarajan, M.K., *Talanta*, **52** (2000) 885.
19. Subramanian, V., Sahoo, P., Malathi, N., Ananthanarayanan, R., Baskaran, R., Saha, B., *Nucl. Technol.*, **165** (2009) 257.
20. Acid leak detection system for nitric acid loop, internal report-SEG/USD&TS/DN/2003/02.
21. An intelligent titrator for quick chemical assay of process solutions, IGC annual report 2007.
22. Conductivity monitoring for characterization of aqueous flowing systems, 1999, internal report-SHINE/USDTS/02/99.
23. A pumpless flow injection analysis utility based on pulsating sensors, IGCAR annual report 2008.
24. Praveen, K., Rajiniganth, M.P., Arun, A.D., Ananthanarayanan, R., Malathi, N., Sahoo, P., and Murali, N., *Nucl. Technol.*, **176** (2011) 127.

25. Continuous type oil level sensors for the dashpots of control and safety rod drive mechanisms in prototype fast breeder reactor, IGCAR high impact breakthroughs 2004-2007.
26. Rajan, Babu, V., Veerasamy, R., Sudheer patri, Ignatious sundar raj, S., Kumar Krovvidi, S.C.S.P., Dash, S.K., Meikandamurthy, C., Rajan, K.K., Puthiyavinayagam, P., Chellapandi, P., Vaidyanathan, G., Chetal, S.C., *Nucl. Eng. Des.*, **240** (2010) 1728.
27. An indigenous device for water film thickness monitoring, IGCAR high impact breakthroughs 2004-2007.
28. Ananthanarayanan, R., Sahoo, .P, Murali, N., International conference on vistas in chemistry, Kalpakkam, India, 11-13 Oct 2011.
29. Olander, D., *J. Nucl. Mater.*, **389** (2009) 1.
30. Singh, N.S.B., Mohan, S.V., Balasubramanian, G.R., *Radiochim. Acta*, **72** ( 1996) 93.
31. Biddle, P., Miles, J.M., *J. Inorg. Nucl. Chem.*, **30** (1968) 1291.
32. Sahoo, P., Malathi, N., Ananthanaraynan, R., Praveen, K., Murali, N., *Rev. Sci. Instrum.*, **82** (2011) 114102.
33. Sahoo, P., Mallika, C., Ananthanarayanan, R., Falix Lawrance, Murali, N., Mudali, K., *J. Radioanal. Nucl. Chem.*, **292** (2012) 1401.
34. Davies, W., Gray, W., *Talanta*, **11** (1964) 1203.
35. Principles of corrosion engineering and corrosion control, Ahmed, Z., Butterworth-Heinemann, 1<sup>st</sup> edition (2006).
36. Standard test methods for iron in water, ASTM, D1068-10.
37. Standard test method of silica in water, ASTM, D859-10.
38. Standard test method for hydrazine in water, D1385-07, ASTM.
39. Standard test method for boron in water, D 3082-09, ASTM.

40. Gupta, H.K.L., Boltz, D.F., *Microchim. Acta*, **62** (1974) 415.
41. Standard test method for copper in water, ASTM, D1688-12.
42. Standard test methods for nickel in water, ASTM, D1886-08.
43. Skjoldebrand, R., *Appl. Sci. Res. B-Elec.*, **5** (1956) 401.
44. Kimbrough, R.D. Jr., Askins, R.W., *Anal. Chem.*, **41** (1969) 1147.
45. Han, S., Chung, H., Han, J.W., *Analyst*, **130** (2005) 745.
46. Lappi, S.E., Smith, B., Frazen, S., *Spectrochim. Acta A*, **60** (2004) 2611.
47. Baxter, G.P., Bargess, L.L., Daudt, H.W., *J. Am. Chem. Soc.*, **33** (1911) 893.
48. Ingelstam, E., Djurle, E., Johansson, L., *J. Opt. Soc. Am.*, **44** (1954) 472.
49. Dhole, K., Roy, M., Ghosh, S., Datta, K., Tripathy, M.K., Bose, H., *Ann. Nucl. Energy*, **55** (2013) 116.
50. [www.thermo.com/eThermo/CMA/PDFs/Articles/articlesFile\\_11377.pdf](http://www.thermo.com/eThermo/CMA/PDFs/Articles/articlesFile_11377.pdf).
51. da Rocha, R.T., Gutz, I.G.R., Lago, C.L., *J. Chem. Educ.*, **74** (1997) 572.
52. Munoz, D.R., Berga, S.C., *Measurement*, **38** (2005) 181.
53. Physical chemistry, Atkins, P.W., Oxford University press, 4<sup>th</sup> edition (1990).
54. Lange's handbook of chemistry, Dean, J.A., McGraw-Hill, 14<sup>th</sup> edition (1992).
55. Development of GUI for PC-based measurement facility using pulsating sensors, internal report-EIRSG/ICG/RTSD/IIS/2012/02.
56. Analytical Chemistry, Christian, G.D., Wiley-India, 6<sup>th</sup> edition (2004).
57. Instrumental methods of chemical analysis, Ewing, G.W., McGraw-Hill book company, 4<sup>th</sup> edition (1975).
58. Duckworth, J.H., in 'Applied spectroscopy: A compact reference for practitioners', edited by Workman Jr, J., Springsteen, A., Academic press 1<sup>st</sup> edition (1998), Chapter 4.

59. Fundamentals of analytical chemistry, Skoog, West, Holler, Crouch, Cengage Learning, 8<sup>th</sup> edition (2004).
60. Infrared spectral interpretation: A systematic approach, Smith, B.C., CRC press, 1<sup>st</sup> edition (1999).
61. Fritz, J.S., Gjerde, D.T., Ion chromatography, Wiley-VCH, 4<sup>th</sup> edition (2009).
62. The practice of ion chromatography, Smith, F.C., Chang, R.C., Krieger publishing company, 1<sup>st</sup> edition (1983).
63. Ion chromatography applications, Smith, R.E., CRC press, 1<sup>st</sup> edition (1988).
64. Ananthanarayanan, R., Sahoo, P., Murali, N., *Indian J. Chem. Techn.*, **19** (2012) 278.
65. Longhurst, R.S., Geometrical and physical optics, Orient longman limited, 3<sup>rd</sup> edition (1973).
66. Boyes, W., in 'Instrumentation reference book', edited by Boyes, W., Butterworth-Heinemann, 3<sup>rd</sup> edition (2003) chapter 21.
67. Environmental pollution and control, Peirce, J.J., Weiner, R.F., Vesilind, P.A., Butterworth-Heinemann, 4<sup>th</sup> edition (1998).
68. Hansen, H.P., in 'Methods of sea water analysis', edited by Grasshoff, K., Kermling, K., Ehrhardt, M., Wiley-VCH, 3<sup>rd</sup> edition (1999) chapter 4.
69. Hobbs, J.P.A., McDonalds, C.A., *J. Fish Biol.*, **77** (2010) 1219.
70. Kemp, P.J., Peers, C., in 'Oxygen sensing: Methods in Enzymology', edited by Sen, C.K., Semenza, G.L., Elsevier Academic press, 1<sup>st</sup> edition (2004) chapter 1.
71. Power plant water chemistry: A practical guide, Buecker, B., PennWell publishing company, 1<sup>st</sup> edition (1997).
72. Tan, X., Capar, G., Li, K., *J. Membrane Sci.*, **251** (2005) 111.
73. Basson, W.D., Staden, J.F.V., *Analyst*, **103** (1978) 998.

74. Amstrong, F.E., Heemstra, R.J., Kincheloe, G.W., *Anal. Chem*, **27** (1955) 1296.
75. Nei, L., Compton, R.G., *Sensor Actuat. B-Chem.*, **30** (1996) 83.
76. Mancy, K.H., Okun, D.A., Rilley, C.N., *J. Electroanal. Chem.*, **4** (1962) 65.
77. Buchhoff, L.S., Ingber, N.M., Brady, J.H., *Anal. Chem*, **27** (1955) 1401.
78. White, A.F., Peterson, M.L., Solbau, R.D., *Ground Water*, **28** (1990) 584.
79. Winkler, L.W., *Ber. Deut. Chem. Ges.*, **21** (1888) 2843.
80. Labasque, T., Chaumery, C., Aminot, A., Kergoat, G., *Mar. Chem.*, **88** (2004) 53.
81. Sakai, T., Takio, H., Teshima, N., Nishikawa, H., *Anal. Chim. Acta*, **438** (2001) 117.
82. Martinez, A.S., Rios, A., Valcarcel, M., *Anal. Chim. Acta*, **284** (1993) 189.
83. [www.hach.com/fmmimghach?/CODE%3A](http://www.hach.com/fmmimghach?/CODE%3A)
84. Smith, R.A., *J. Non-Cryst. Solids*, **84** (1986) 421.
85. Economou, A., Thermils, D.J., Bikou, H., Tzanavaras, P.D., Rigas, P.G., *Anal. Chim. Acta*, **510** (2004) 219.
86. Ramanjaneyulu, P.S., Sayi, Y.S., Raman, V.A., Ramkumar, K.L., *J. Radioanal. Nucl. Chem.*, **274** (2007) 109.
87. Staden, J.F.V., Van der Merwe, T.A., *Analyst*, **125** (2000) 2094
88. Magara, Y., Tabata, A., Kohki, M., Kawasaki, M., Hirose, M., *Desalination*, **118** (1998) 25.
89. Gladney, E.S., Jurney, E.T., Curtis, D.B., *Anal. Chem.*, **48** (1976) 2139.
90. G Geffen, N., Semiat, R., Eisen, M.S., Balazs, Y., Katz, I., Dosoretz., *J. Membrane Sci.*, **286** (2006) 45.
91. Taniguchi, M., Fusaoka, Y., Nishikawa, T., Kurihara, M., *Desalination*, **167** (2004) 419.
92. Kilroy, W.P., Moynihan, C.T., *Anal. Chim. Acta*, **83** (1976) 389.
93. Ball, J.W., Thomson, J.M., Jenne, A.E., *Anal. Chim. Acta.*, **98** (1978) 67.

94. Rao, R.M., Parab, A.K., Bhusan, K.S., Aggarwal, S.K., *Microchim. Acta*, **169** (2010) 227.
95. Gregoire, D.C., *J. Anal. Atom. Spectrom.*, **5** (1990) 623.
96. Hill, C.J., Lash, R.P., *Anal. Chem.*, **52** (1980) 24.
97. Spicer, G.S., Strickland, J.D.H., *Anal. Chim. Acta*, **18** (1958) 231.
98. Alfassi, Z.B., Sellschop, J.P.F., *J. Radioanal. Nucl. Chem.*, **135** (1989) 341.
99. Ramanjaneyulu, P.S., Sayi, Y.S., Nathaneil, T.N., Reddy, A.V.R., Ramkumar, K.L., *J. Radioanal. Nucl. Chem.*, **273** (2007) 411
100. Kumar, S.D., Maiti, B., Mathur, P.K., *Anal. Chem.*, **71** (1999) 2551.
101. Sarica, D.Y., Ertas, N., *Turk. J. Chem.*, **25** (2001) 305.
102. Tapparo, A., Bombi, G.G., *Analyst*, **123** (1998) 1771.
103. Vogel, A.I., A text book of quantitative inorganic analysis, John Wiley and sons, 3<sup>rd</sup> edition (1961).
104. Arnikar, A.J., Essentials of nuclear chemistry, Wiley eastern limited, 3<sup>rd</sup> edition (1990).
105. Applied Chemistry, A text book for Engineers and Technologists, Roussak, O.V., Gesser, H.D., Springer, 2<sup>nd</sup> edition (2013).
106. Advances in chemical physics, Lawley, K.P., John Wiley and sons, 1<sup>st</sup> edition (1985).
107. Thurston, W.M., James, M.W.D., *Anal. Chem.*, **56** (1984) 386.
108. Thomas, B.W., *Anal. Chem.*, **22** (1950) 1476.
109. Ananthanarayanan, R., Sahoo, P., Murali, N., *J. Radioanal. Nucl. Chem.*, **299** (2014) 293.
110. Inoue, Y., Tanaka, K., Kasida, Y., *Analyst*, **106** (1981) 609.
111. In CRC handbook of chemistry and physics, edited by Lide, D.R., 84<sup>th</sup> edition (2003) Section 6.
112. Jordan, S., Cherdron, W., Malet, J.C., Rzekieki, R., and Himeno, Y., *Nucl. Technol.*, **81** (1988) 183.

113. [www.osha.gov/dts/chemicalsampling/data/CH\\_267700.html](http://www.osha.gov/dts/chemicalsampling/data/CH_267700.html).
114. Cherdron, W., Jordan, S., International topical meeting on LMFBR safety, Lyon, France, 19-23 July 1982.
115. CH.Hofmann, S.Jordan and W.Lindner, Jahrestagung der Gesellschaft Fur Aerosolforschung, Wien, September 1978.
116. Clough, W.S., and Garland, J.A., *J. Nucl. Energy*, **25** (1971) 425.
117. Baskaran, R., Selvakumaran T.S., and Subramanian, V., *Indian J. Pure Appl. Phys.*, **42**, (2004) 873.